SYNTHESIS AND APPLICATION OF
THIOUREA AND AMIDE BASED CHEMOSENSORS FOR
RECOGNITION OF ANIONS

SENSÖR ÖZELLİKLİ TİYOÜRE
VE AMİT BİLEŞİKLERİNİN SENTEZİ
VE ANYON TAYİNİNDE KULLANILMASI

DENİZ TÖZENDEMİR

Prof.Dr. NAZAN TUNOĞLU

Advisor

Prepared as a THESIS of MASTER of SCIENCE

Proposed by the Regulations of the

Institute for Graduate Studies in Pure and Applied Sciences

For the Department of CHEMISTRY

of Hacettepe University

2013

This study named **"Synthesis And Application of Thiourea and Amide Based Chemosensors for Recognition of Anions"** by **DENİZ TÖZENDEMİR** has been accepted as a **THESIS of MASTER of SCIENCE** in **CHEMISTRY** by the Examining Committee Members below.

Head

Prof.Dr. Hatice Beytiye ÖZGÜN

Advisor

Prof.Dr. Nazan Tunoğlu

Member

Prof.Dr. Canan Ünaleroğlu

Member

Doç.Dr. Hülya Şenöz

Member

Yrd.Doç.Dr. Fatma Aydın

This thesis has been certified as **A THESIS FOR THE DEGREE OF MASTER OF SCIENCE** by the Examining Committee Members above.

Prof.Dr. Fatma Sevin Düz

Director of the Graduate School of
Natural and Applied Sciences

ETHICS

In this thesis study, prepared in accordance with the guidelines of Institute of Graduate Studies in Science of Hacettepe University,

I declare that

- all the information and documents in the thesis were obtained within the academic rules and regulations

- all audio-visual and written information and results were presented according to the rules of scientific ethics

- when referring to other works, the related works were cited in accordance with the scientific standards

- all cited studies were fully referenced

- I did not do any alterations in the data sets

- and no part of this thesis have not been presented as another thesis study in any university.

--- / --- / 2013

Deniz Tözendemir

ABSTRACT

SYNTHESIS AND APPLICATION OF THIOUREA AND AMIDE BASED

CHEMOSENSORS FOR RECOGNITION OF ANIONS

DENİZ TÖZENDEMİR

Master of Science, Department of Chemistry

Supervisor: Prof.Dr. NAZAN TUNOĞLU

June 2013

Because of the importance of anions in biological and chemical processes, studies based on anion recognition are increasingly popular. The common property of the compounds synthesized and used as anion receptors is their ability to form complexes by hydrogen bonding with the anions in solution. The presence of anions in the solution can be determined by examining the changes on the sensor molecules by spectroscopic techniques. In addition to this, the development of "colorimetric" sensors that changes their colors upon complexation with anions is preferred because of the ease of use.

In this study, six thiourea (five are new) and two amide (one is new) are synthesized and characterized by FT-IR, ^{1}H NMR, ^{13}C NMR and for four chosen compounds by COSY and HETCOR techniques. After that, the interactions and selectivities of those compounds with several anions were investigated by ^{1}H NMR spectroscopy, UV-Vis titrations and by naked-eye observations.

Keywords: thiourea, amide, anion sensor, hydrogen bonding, UV-Vis titrations

ÖZET

SENSÖR ÖZELLİKLİ TİYOÜRE VE AMİT BİLEŞİKLERİNİN SENTEZİ VE ANYON TAYİNİNDE KULLANILMASI

DENİZ TÖZENDEMİR

Yüksek Lisans, Kimya Bölümü

Tez Danışmanı: Prof.Dr. NAZAN TUNOĞLU

Haziran 2013

Anyonların biyolojik ve kimyasal proseslerdeki öneminden dolayı, son yıllarda anyon tayinine yönelik çalışmalar artmaktadır. Anyon reseptörü olarak sentezlenen bileşiklerin ortak özellikleri, çözeltideki anyonla hidrojen bağı yaparak kompleks oluşturmalarıdır. Bu komplekslerin oluşumunun reseptör yapıları üzerindeki değişimleri spektroskopik olarak incelenerek, çözeltideki anyon varlığı tespit edilebilir. Bunun yanı sıra, son yıllarda anyon etkileşimi sonucu kompleks oluşumuyla çıplak gözle görülebilir renk değişimi gösteren "kolorimetrik" sensörlerin geliştirilmesi, kullanım kolaylığı açısından tercih edilmektedir.

Bu çalışmada sensör olarak kullanılmak üzere altı tiyoüre türevi (beşi yeni) ve iki amit türevi (biri yeni) sentezlenip FT-IR, ^{1}H NMR, ^{13}C NMR ve seçilen dört bileşik için COSY ve HETCOR teknikleriyle karakterize edilmiştir. Daha sonra bu bileşiklerin çeşitli anyonlarla etkileşimleri ^{1}H NMR spektroskopisiyle, UV-Vis titrasyonlarıyla ve çıplak gözle izlenerek sensör özellikleri ve seçicilikleri incelenmiştir.

Anahtar kelimeler: tiyoüre, amit, anyon sensörü, hidrojen bağı, UV-Vis titrasyonu

ACKNOWLEDGEMENTS

CONTENTS

LIST OF ABBREVIATIONS

NMR: Nuclear Magnetic Resonance

COSY: Correlation Spectroscopy

HETCOR: Heteronuclear Correlation Spectroscopy

FT-IR: Fourier Transform Infrared Spectroscopy

UV-Vis: Ultraviolet-Visible

DMSO: Dimethyl sulfoxide

DMF: Dimethyl formamide

PEG: Polyethylene glycol

mL: Milliliter

mmol: Milimole

ppm: Parts-per-million

eq: Equivalent

INDEX OF FIGURES

INDEX OF SCHEMES

1. INTRODUCTION

1.1. Thioureas

1.1.1. Applications

Thioureas attract a lot of interest due to their biological and industrial uses, as well as synthetic purposes. One of the important uses of thioureas is as antimicrobial and antifungal agents. Developing new anti-infective drugs have become an important area of research due to the increasing tolerance of well-known and used antibiotics in the past decades and due to the emergence of new diseases [1]. Thioureas are known to possess antimicrobial activity for over 50 years [2]. 1-(Fluorobenzoyl)-3-(fluorophenyl)thioureas were synthesized by Saeed et al. [3] and their antimicrobial activities against Gram-positive and Gram-negative bacteria, and several fungi were screened and they were proven to be effective as both antibacterial and antifungal agents. The most effective ones were found to be the fluorine-substituted compounds.

R' = 2-Cl   R = 3-Cl
    3-Cl   2-F
    2-F   3-F
    3-F   4-F
    4-F
    3,4,5-tri-OCH$_3$
R'Ph = t-butyl

1
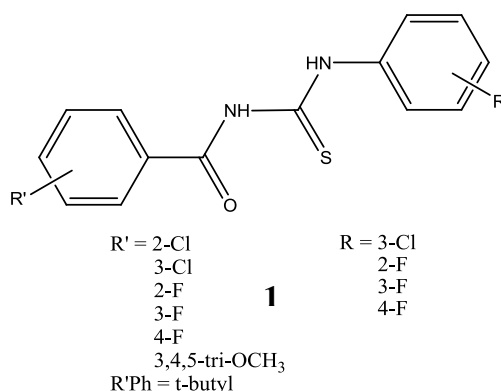
Figure 1: Novel 1-(fluorobenzoyl)-3-(fluorophenyl)thiourea derivatives used as antibacterial agents.

Another class of thioureas, 2-(4-R-phenoxymethyl)benzoic acid thioureides were synthesized by Müller et al. [4]. Their activities against several parasites that live in gastrointestinal track were investigated and found to be potential anti-parasitic agents against G. Lamblia, T. Gondii and E. multilocularis metacestodes. Their mechanism of action was thought to be due to the capacity of the thioureide group to chelate metal ions, which lead to the inhibition of the metal-dependent enzymes of the parasites. The experiments showed that there was a strong structure-function relationship and the highest antibacterial activity was reached with halogen substituents on the aromatic ring at the end of the thiourea moiety. Their experiments showed that compound **2** was the most active compound that was synthesized in that research.

2
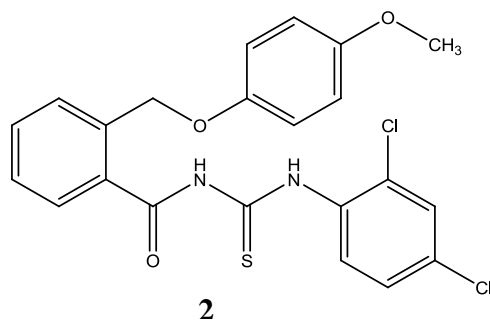
Figure 2: Substituted thioureide of 2-(phenoxymethyl)benzoic acid as antimicrobial agent.

However, the low solubility of thioureas in water limits their effectiveness in biologic systems, thus their antimicrobial activities. To overcome this, thioureas with moieties that enhance water solubilities are synthesized and employed as antimicrobial agents. Abbas et al. [5] have synthesized thiourea derivatives with hippuric acid moieties and tested their effectiveness as broad-spectrum antibiotics on several Gram-positive and Gram-negative bacteria. They showed that antimicrobial activity is strongly dependent on the substituent on the thiourea nitrogens and is increased or reduced depending on whether a matching or mismatching interaction exist between the pathogen and thiourea, which proved compounds 3,4,5 and 6 were the most effective among the synthesized thioureas.

3   **4**

5

6
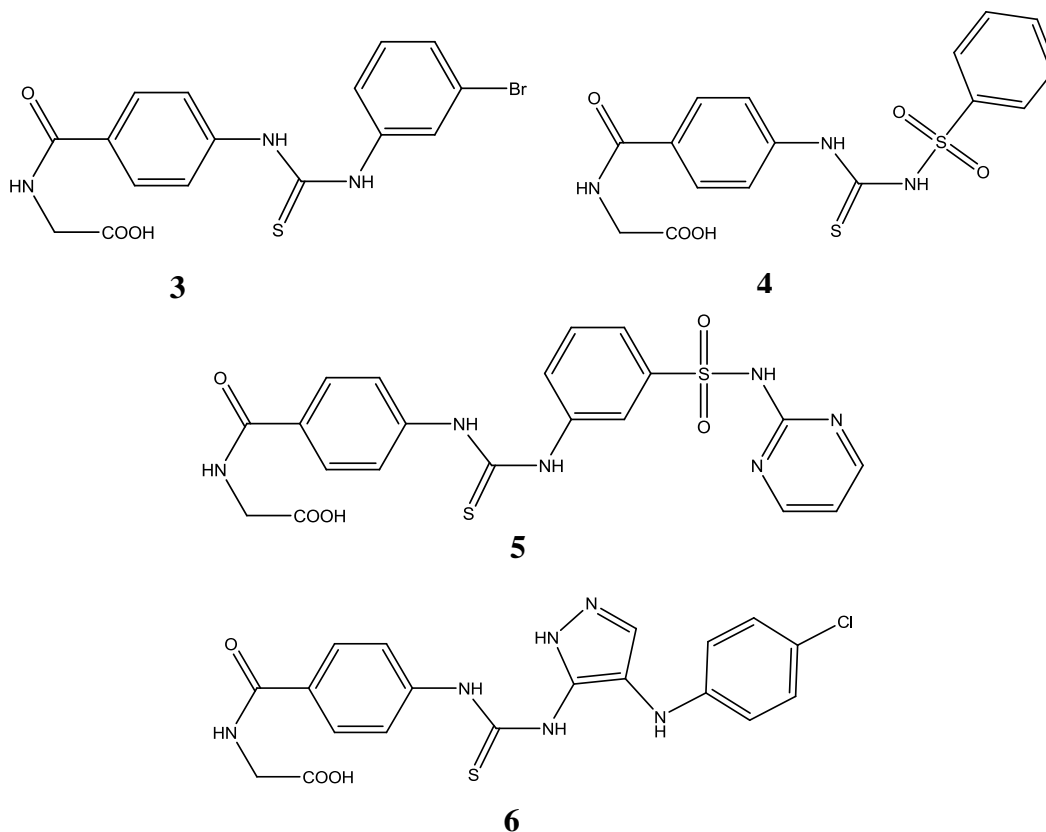
Figure 3: Thiourea derivatives that contain hippuric acid moieties.

Thioureas are also designed and used as anticancer and antitumor agents due to their cytotoxic and DNA altering properties [6]. Jianwen Yao et al. [7] have synthesized diaryl thiourea derivatives (**7**) as potent antitumor agents against human colorectal carcinoma (HCT116) and human breast cancer cell (MDA-MB-231).

Ar = 4-Chlorophenyl
(3-Trifluoromethyl)phenyl
3,5-bis(Trifluoromethyl)phenyl
(3-trifluoromethyl-4-chloro)phenyl
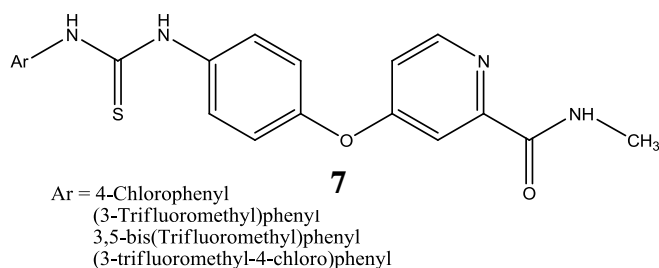
Figure 4: Diaryl thiourea derivatives as antitumor agents.

Another study on antitumor effects of thioureas was carried out by Liu et al. [8] using thiourea derivatives containing benzo[5,6]cyclohepta[1,2-b]pyridine moieties against mammary and colon carcinoma cells. The results showed that the synthesized thioureas showed cell growth inhibitory effects that are close to 5-fluorouracil, which is a widely used anticancer drug. The same compounds also showed excellent anti-inflammatory activities that are stronger than ibuprofen.

R = CH$_3$NH–
C$_6$H$_{11}$NH–
C$_6$H$_5$NH–
2-CH$_3$C$_6$H$_5$NH–
2-OCH$_3$C$_6$H$_5$NH–

8
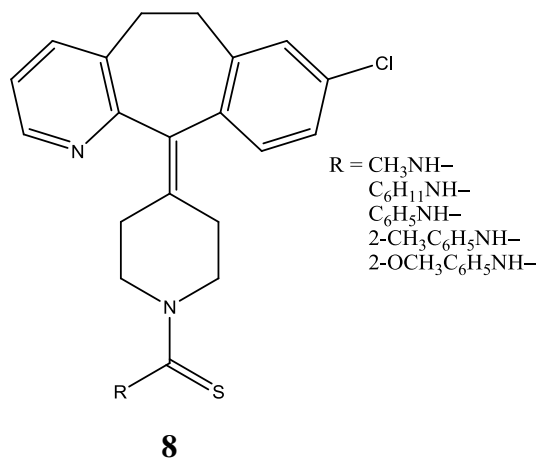
Figure 5: Thiourea derivatives containing benzo[5,6]cyclohepta[1,2-b]pyridine moieties as anticancer and anti-inflammatory drugs.

In addition to antimicrobial and antitumor activities, thioureas are proven to be powerful radical scavengers [9]. Azam et al. [10] have shown that thioureas could be employed to treat neurodegenerative diseases such as Parkinson's in the future because of their ability to scavenge the reactive oxygen species in the body. In the study, urea and thiourea

derivatives of 3-phenyl/ethyl-2-thioxo-2,3-dihydrothiazolo[4,5-*d*]pyrimidine were synthesized and tested to treat induced catalepsy in mice. The results have proven that the thiourea compound **9** showed better activity than the standard antiparkinsonian drug Levadopa.
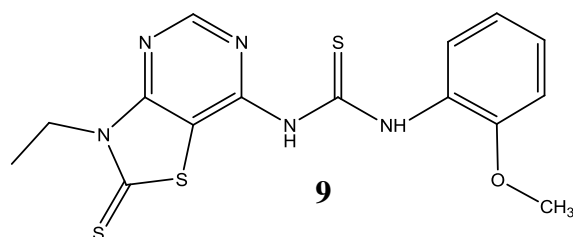
Figure 6: Thiourea derivative of 3-phenyl/ethyl-2-thioxo-2,3-dihydrothiazolo[4,5-*d*]pyrimidine used as a potent antiparkinsonian drug.

Thioureas are known to be efficient organocatalysts in asymmetric syntheses due to their ability to form hydrogen bonds [11]. Bis(thioureas) **10** are used to catalyze Morita–Baylis–Hillman reactions of 2-cyclohexen-1-one with up to 96% ee [12].
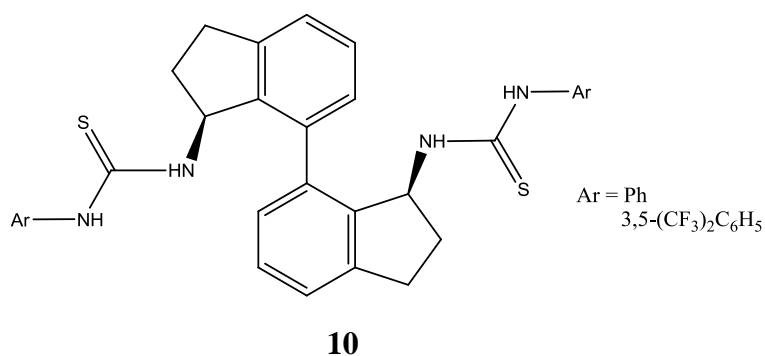
Figure 7: Bis(thiourea) catalysts for Morita–Baylis–Hillman reactions

Cinchona alkaloid thioureas were used to catalyze asymmetric Mannich reactions to synthesize β-aminoester derivatives with high yields and high ee [11]. The most efficient catalyst was **11** which has powerful electron withdrawing −CF$_3$ groups that enhances hydrogen bonding.

11
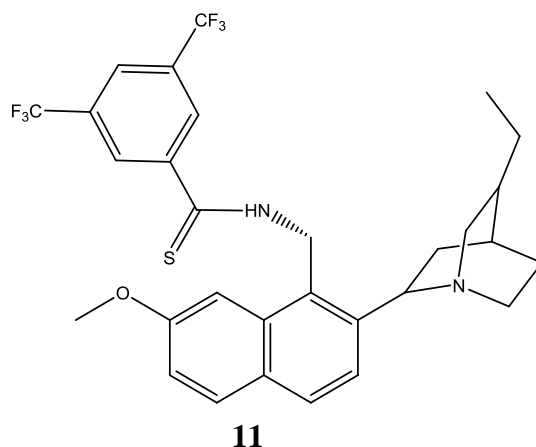
Figure 8: Cinchona alkaloid thioureas for Mannich reactions

To catalyze Michael reactions of 1,3-dicarbonyls to nitroalkanes, bifunctional thioureas are used with up to 92% ee [13]. The most efficient catalyst was **12**.

12
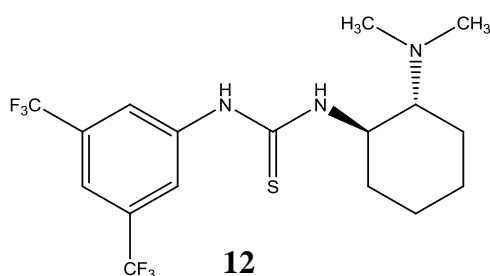
Figure 9: Bifunctional thiourea for Michael reactions

Thioureas have long been known to form stable complexes with metal cations, and specifically, platinum group metals [14]. Since then, many new thioureas have been synthesized for metal coordination and this phenomena has been applied to various areas such as ion selective membranes [15]. Berhe and co-workers designed and synthesized a N,N-diethyl-N'-camphanyl thiourea and used is as a liquid membrane to selectively transport Ag(I).

13
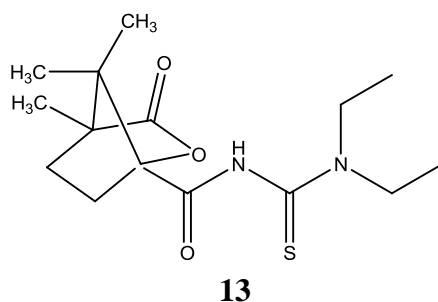
Figure 10: Thiourea derivative as bulk liquid membrane for transport of Ag(I)

The concept of ion selective thiourea membranes are also used in the design of thiourea based ion selective electrodes [16]. Cubillana-Aguilera et al. [17] have designed 1-furoylthiourea-Sonogel-Carbon electrodes for Cd(II) determination. Electrodes modified with compound **14** showed appreciable detection limit and gave good electrochemical response. Also the presence of thiourea on the electrode caused to decrease the erosion on the electrode surface.

14
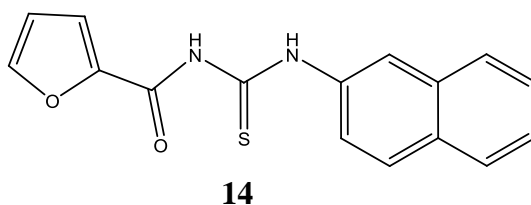
Figure 11: 1-(2-Furoyl)-3-(1-naphthyl)thiourea used to modify Sonogel-Carbon electrodes

The ability of thioureas to coordinate with metals has made thioureas to be employed as transition metal sensors [18]. Luckay et al. [19] have designed various acyl(aroyl)thioureas to extract Ag(III) from aqueous media. Compound **15** was the most efficient sensor among the others.

15
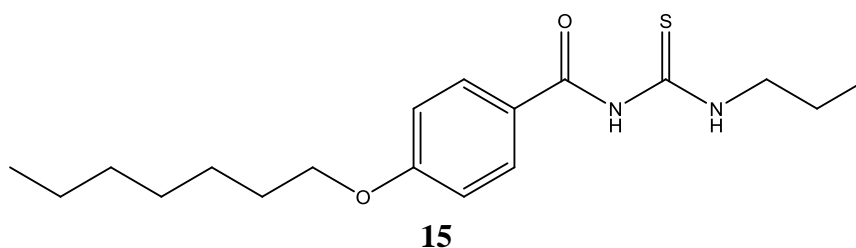
Figure 12: Acyl(aroyl)thiourea derivative as gold(III) ligand

Another very important area that thioureas are employed is anion sensing. A naphthalene based receptor was designed by Seo et al. [20] and immobilized on silica. The experiments showed that the compound sensed the presence of fluoride ion selevtively in aqueous media.
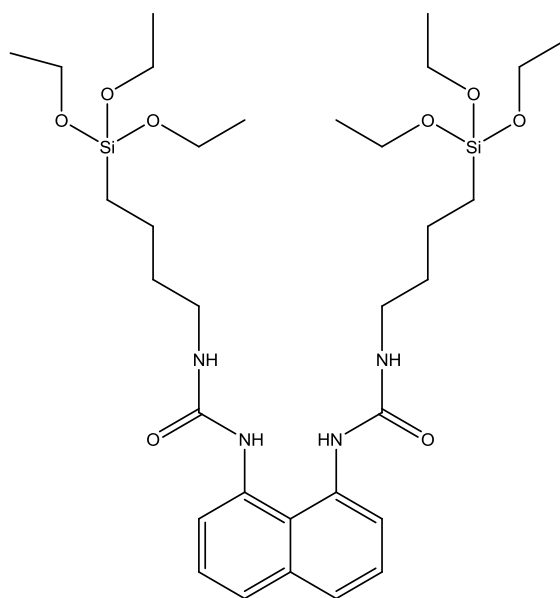
16

Figure 13: Naphthalene based receptor on silica for the detection of F⁻ in water.

This subject will be covered in detail in the following topics in the anion recognition chemistry section.

1.1.2. Methods of Synthesis

The most frequently employed synthesis of thioureas is from the direct reaction of isothiocyanates with amines [21].

R_1 = 4-nitrophenyl
    2-thiophene
    phenyl
    n-butyl
    4-morpholine

R = H
    NO_2
    NH_2
    Br
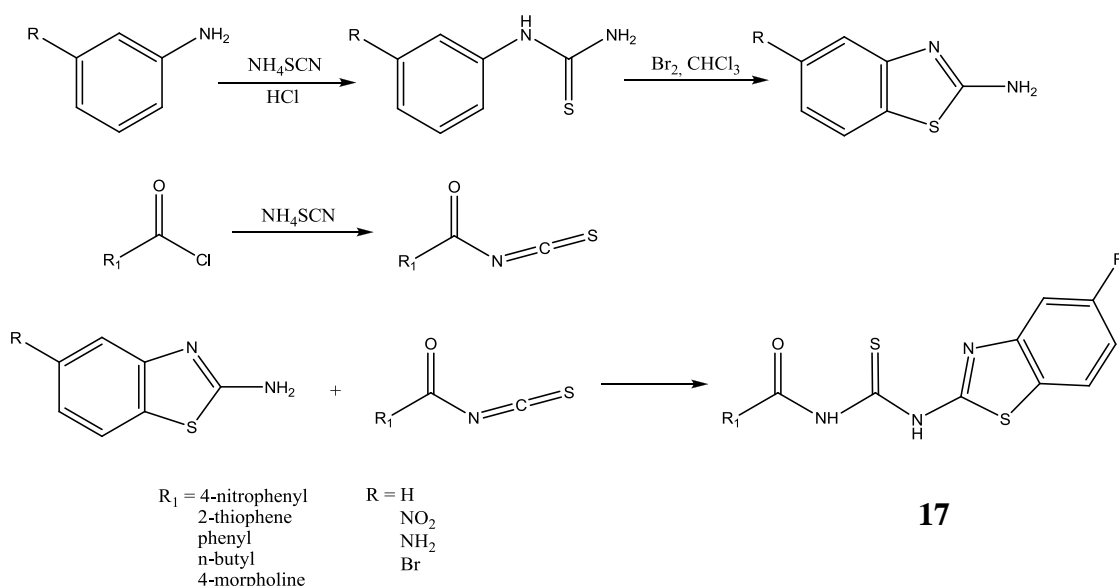
17

Figure 14: Direct thiourea synthesis from isothiocyanates and amines

To improve the yields of these reactions, phase transfer catalysts can be employed, which homogenizes the reaction medium by transferring the water soluble reactant to the organic phase, when mutually immiscible reactants are the case [22]. One of the most widely used phase transfer catalyst is PEG-400 [23] because of its good solubility in many organic solvents and water. Ke et al. [24] have carried out thiourea synthesis in the presence of PEG-400 as phase transfer catalyst and with ultrasonic irradiation. PEG-400 transferred KSCN to the organic reaction medium and let it react with the acyl chloride.
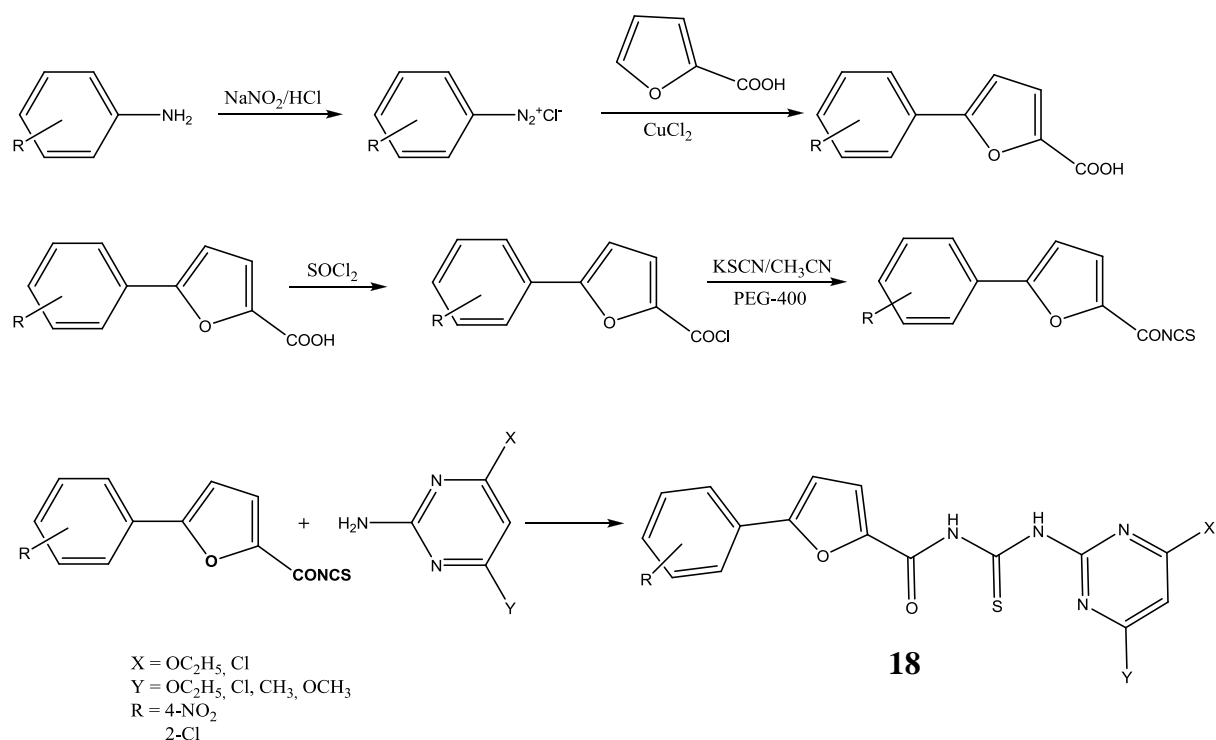
Figure 15: Synthesis of *N'*-(disubstituted-pyrimidin-2-yl)-*N*-(5-aryl-2-furoyl)thiourea derivatives in the presence of PEG-400

Another synthesis route for thioureas is the use of peptide coupling reagents, which allows the synthesis to be carried out in solid state. Boas et al. [25] have synthesized aliphatic thioureas using DIPEA (*N,N'*-diisopropylethylamine) and HFIP (1,1,1,3,3,3-hexafluoro-2-propanol) in solid phase.
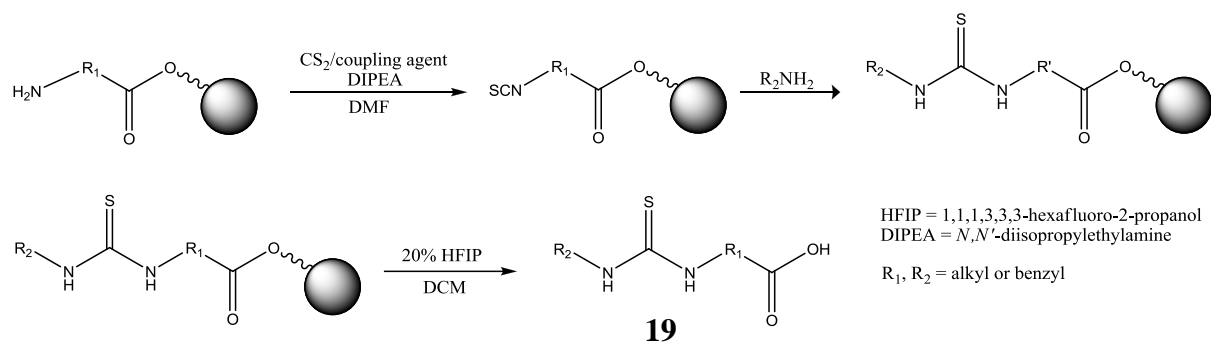
Figure 16: Synthesis of thioureas in solid phase using peptide coupling reagents

The reaction of thiourea formation can be accelerated by microwave irradiation. Thanh et al. [26] have synthesized *N*-tetra-*O*-acetyl-β-D-glucopyranosyl-*N'*-(4',6'-diarylpyrimidin-2'-yl)thioureas in two steps, using a household microwave oven.
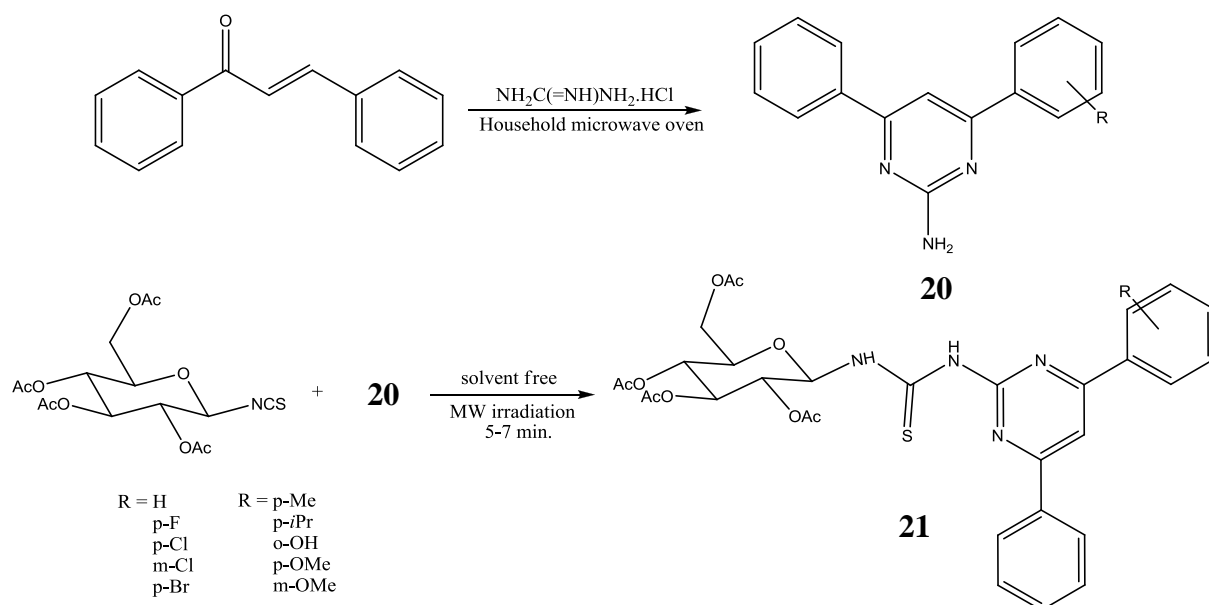
Figure 17: Microwave assisted synthesis of thioureas

1.2. Anion Recognition Chemistry

In the 1970's, coordination chemistry of group 1 and 2 metals were very popular and since then, recognition of cations are a well-developed area of supramolecular chemistry whereas anion recognition chemistry has been attracting interest for the past 20 years [27]. The reasons of this sudden interest is the realization of the importance of anions. The most widely used anion receptors are the compounds with amide, thiourea, urea and pyrrole moieties. The geometries of the anions also affect the recognition process. For instance it is

known that thioureas are good receptors for Y-shaped anions such as acetate and nitrate anions [28]

1.2.1. Importance of Anions and Anion Sensing

Anions play many roles in biological systems as enzyme substrates and cofactors [29]; phosphate anion is known to take part in many biological processes such as gene regulation, metabolism, antibiotic resistance and signal transduction [30]. Fluorine is widely used in dental care and for the treatment of osteoporosis, on the other hand, over exposure causes fluorosis [31]. Acetate anion is one of the biologically important anions, since it is known to be an indicator of organic decomposition in marine sediments [32]. Also, the design of new anion sensors are important because of their potential use as membrane transport carriers [33] and as reaction catalysts [34].

1.2.2. How Do Anions Bind to Hosts
1.2.2.1. By Electrostatic Interactions

Protonation of amines to their polyammonium forms increases the positive charge density of the amines and also increases their affinity for anions. Schmidtchen et al. [35] have worked on ammonium based anion receptors and found that compounds **21** and **22** have showed selectivity for Br^-. In the later studies, **21** and **22** turned out to catalyze reactions that have anionic transition states [36].

21   **22**   n = 4
                                    n = 6
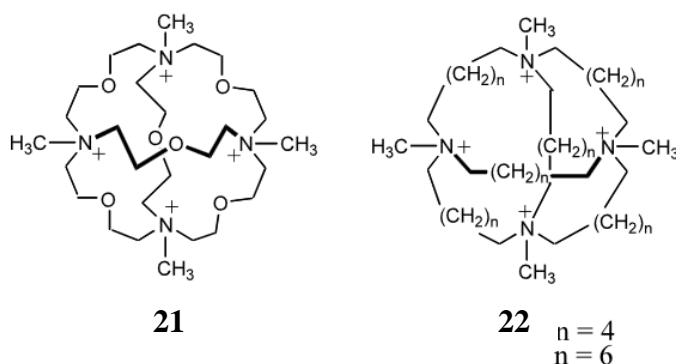
Figure 18: Ammonium based receptors based on recongition with electrostatic interactions

These receptors were modified and two quarternary ammonium polycycles were clicked together to obtain the zwitterionic receptor **23** for dianionic guests [35].
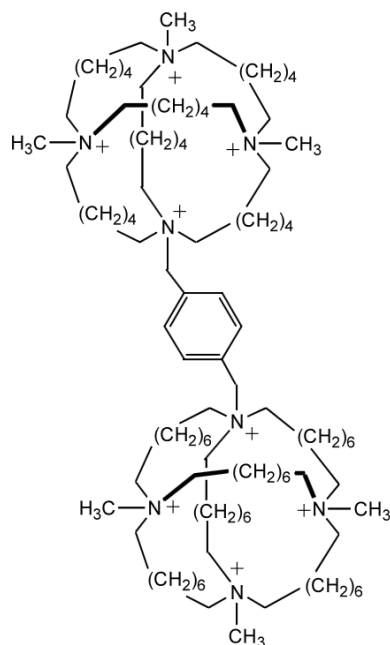
23

Figure 19: Ditopic receptor for dianionic guests

1.2.2.2. By Hydrogen Bonding

Amide, thiourea, urea and pyrrole derivatives can form hydrogen bonds with anions using their N-bonded hydrogens, thus are used frequently as anion sensors. Since hydrogen bonds are directional, it is possible to synthesize receptors that are capable of selectively binding anions with specific geometries [27]. Bisson et al. [37] have designed a rigid cyclophane derivative with a trigonal box geometry (**24**), which selectively recognizes nitrate anion.
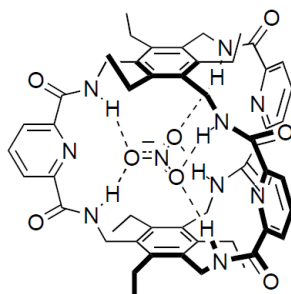
24

Figure 20: Rigid cyclophane derivative as a selective nitrate anion sensor

Since the amide NH groups of compound **24** are arranged to form a trigonal prismatic cavity at the center of the molecule, they are able to coordinate well by forming hydrogen

bonds with the π-electron systems of Y-shaped anions such as carboxylates and nitrates [27]. Yan et al. [38] have synthesized organic urea-type nanoparticles (**25**) that selectively bind carboxylates in water via hydrogen bonding.

25
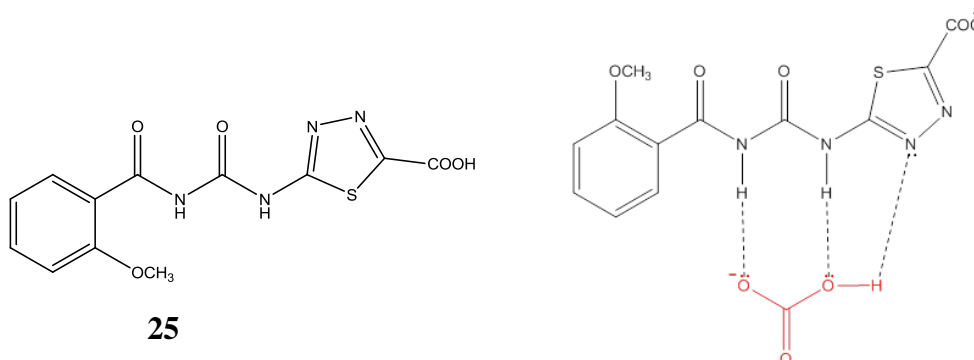
Figure 21: Urea type sensor for selective recognition of acetete anion via hydogen bonding

Pyrrole derivatives are also used as successful anion receptors due to their ability to form hydrogen bonds with their NH groups. Andrievski et al. [39] have synthesized a bipyrrole-based [2]catenane (**26**) that forms very stable complexes with anions, especially with $H_2PO_4^-$. This extremely strong binding ability arises from the tetrahedral cavity between the rings and the cavity favors the binding of anions that have tetrahedral geometries.

26
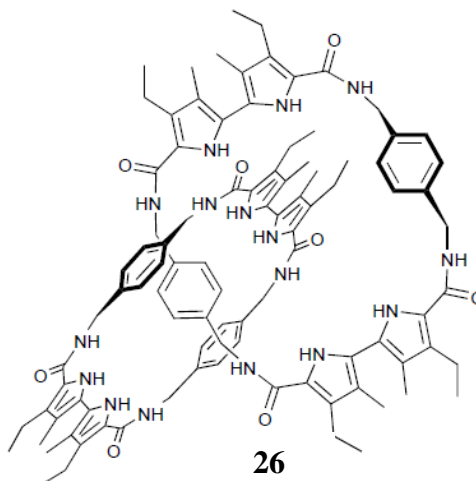
Figure 22: Bipyrrole-based [2]catenane as dihydrogen phosphate receptor.

1.2.2.3. Coordination with Lewis Acid Centers

Metal or Lewis-acid centers are able to coordinate with anions by chelation due to their electron deficiencies [27]. Panda et al. [40] have proposed new selenaza macrocycles and employed them in the recognition of various anions. The study showed that the macrocycle **27** displayed the highest binding affinity towards sulfate anion. The presence of selenium

in the macrocycle provides the center for secondary interactions with heteroatoms as well as providing the somewhat bent structure due to the V-shaped arrangement around selenium, which enhances the anion binding affinity.

27
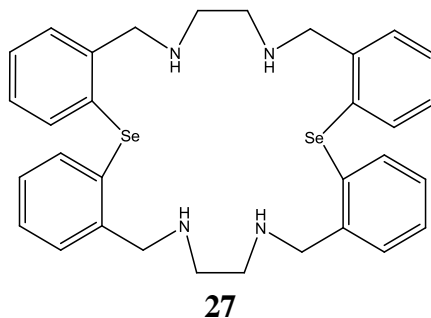
Figure 23: Selenaza macrocycle for recognition of SO_4^{2-}

1.2.3. How to Detect the Recognition Process

The complex formation via hydrogen bonding, electrostatic interactions or Lewis acid coordination can be detected with various methods or analysis or inspection.

1.2.3.1. Colorimetric Sensors

Colorimetric sensors are compounds which show a color change that is visible to the naked eye upon interaction with ligands, due to their change in absorbance. They are advantageous because of eliminating the need to resort to any spectroscopic device [41]. Ghosh et al. [42] have designed a receptor with triphenyleneamine moiety for the recognition of dicarboxylates.

28
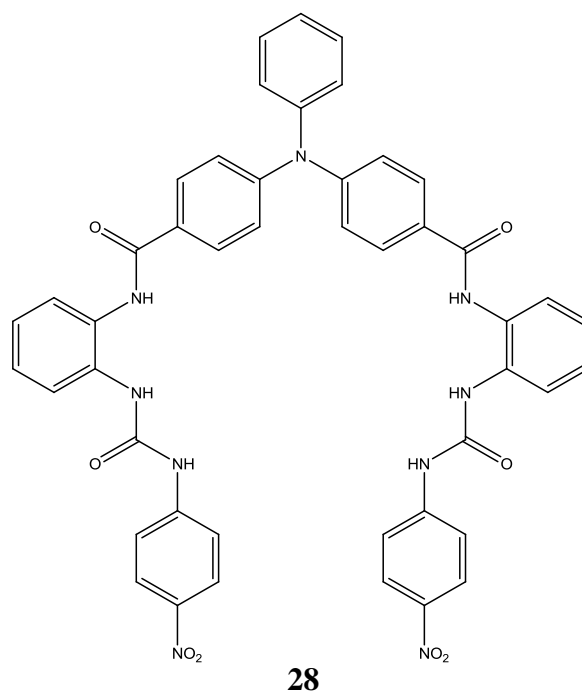
Figure 24: Triphenyleneamine based colorimetric sensor for carboxylates

In the study, DMSO solutions of host molecule **28** were prepared, and then various dicarboxylates were added to those solutions. Addition of malonate anion showed the most striking color change from light yellow to blood red.

1.2.3.2. UV-Vis Titrations

Coordination of the host molecules with anions may lead to a change in the molecules' own absorbance, thus in their UV-Vis spectra. By slowly increasing the amount of anion added, it is possible to inspect the sensor properties of the host molecule by watching the absorbance pattern of the compound. In many cases, a new absorption band appears for the newly formed complex, while the original absorption band of the host gradually shifts or shrinks [43]. Also Job plots are constructed by plotting the λ_{max} values at a specific wavelength against mole fractions to determine the stoichiometry of the complex formation [41]. Kim et al. [44] have reported a thiourea-based host that is sensitive to fluorine.

29
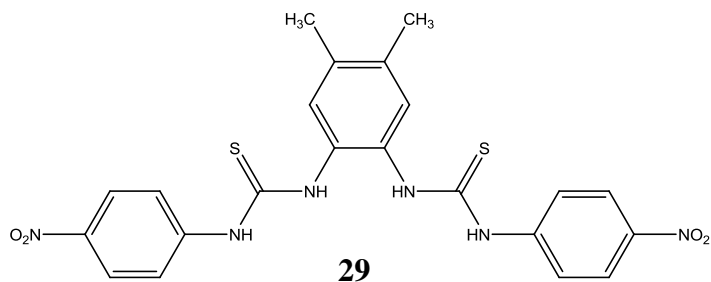
Figure 25: A thiourea-based host that is sensitive to F⁻

UV-Vis titration was performed by gradually increasing the amount of fluorine added to the DMSO solutions of **29**. Upon addition of fluorine, a new peak at λ_{max}=488 nm and two isosbestic points 374 nm and 409 nm at were observed, which indicate the formation of the host-anion complex.

1.2.3.3. ^{1}H NMR Titrations

It is known that intra- or intermolecular hydrogen bonding of a H-bond donor group to a H-bond acceptor decreases in the magnetic shielding around that hydrogen, thus results in a shift of the resonance of the concerned proton to low field [45]. In some cases, the hydrogen bonding interaction is then followed by deprotonation of the donor with fully transferring its proton to the acceptor [46]. In this case the ^{1}H NMR peak of the donated proton completely disappears [47]. Bao et al. [48] have reported the synthesis of an amide based and hydroxyl containing sensor molecule (**30**) which was tested against various anions.

30
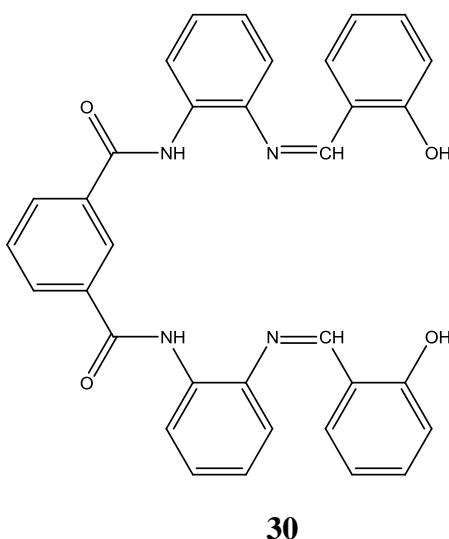
Figure 26: Amide and hydroxyl containing anion sensor

The host-guest solutions were analyzed by ^{1}H NMR titrations by adding 1 equivalent of anions. The addition of H_2PO_4 caused the disappearance of the OH signal in the spectrum which means that the anion deprotonates only the OH proton. Upon addition of F^-, both OH and NH signals were disappeared which indicates the binding occurs both from hydroxyl and amide moieties, and results in deprotonation of both groups.

1.2.3.4. Recognition by Changes in Luminescence

The existence or degree of complexation can also be detected by monitoring the changes in the luminescence intensity of the sensor if the molecule is luminescent [49]. Zhang et al. [50] have reported the synthesis of a heterobimetallic Ru(II)–Cu(II) complex (**31**) for selective sensing of sulfide anion.
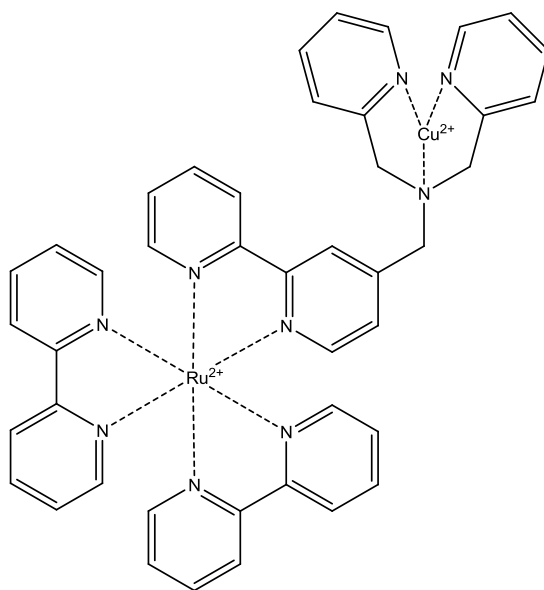
31

Figure 27: Heterobimetallic Ru(II)–Cu(II) sensor for S^{2-}

The ruthenium complex was found to be a strong luminescent. After the complex reacts with Cu^{2+}, the luminescence of the complex was quenched. However, addition of sulfide anion restores the luminescence of the ruthenium complex.

1.2.3.5. Recognition by Changes in Fluorescence

Another way to analyze anion-receptor complexes is by monitoring the changes in fluorescence of the receptor upon addition of anions. Lee et al. [51] have synthesized a fluorescent receptor with an o-(carboxamido)trifluoroacetophenone moiety (**32**) for detection of anions.

32
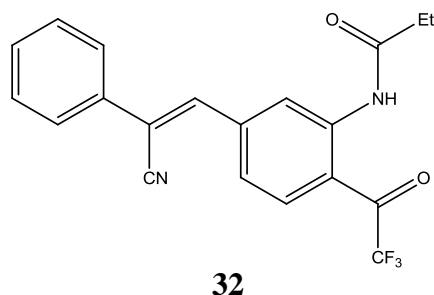
Figure 28: Fluorescent receptor based on o-(carboxamido)trifluoroacetophenone

The results showed that the addition of CN⁻ significantly decreases the fluorescence intensity of the receptor.

1.2.3.6. Electrochemical Recognition

The electrochemical recognition of anion-receptor complexes were known to be applied mainly in three ways [27]; by the extraction of the anion through a membrane by a neutral host and the detection of the changes in the membrane potential [52], by the detection of the changes in potential or current of a redox-active receptor upon complex formation [53] and by chemically modified electrodes that have an anion binding moiety.

2. EXPERIMENTAL SECTION

2.1. General Procedures

All chemicals were purchased from Sigma-Aldrich and Acros Organics. The solvents used in the experiments were reagent or tecnical grade and were purified by the appropriate technique when needed.

The progress of all reactions were monitored by Thin Layer Chromatography (TLC) using silica plates manifactured by Merck (Kiesel Gel 60, F254) and visualised by UV light or by anisaldehyde stain. Purifications by column chromatography were performed using silica gel with 70-230 mesh, manifactured by Merck.

All melting points were measured in capillary tubes using Gallenkamp electrothermal digital melting point apparatus.

UV-Vis titrations were performed using T80+ UV-Vis Spectrometer by PG Instruments LTD. Infrared spectra were obtained using the Mattson 1000 Moswl FT-IR Spectrometer.

^{1}H NMR and ^{13}C NMR spectra were obtained using Bruker WH-400 NMR spectrometer with tetrametylsilane as the internal standard.

2.2. Syntheses

2.2.1. Syntheses of Thioureas

2.2.1.1. *N,N*-(2-Methylpentane-1,5-diyl)-*N',N'*-benzoyldithiourea (33)
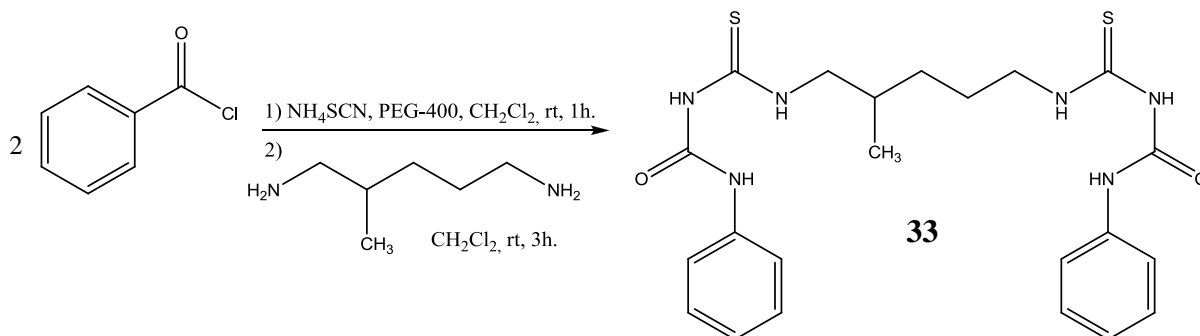
10 mmol (1.16 mL) of benzoyl chloride, 8 drops of PEG-400 (as a phase transfer catalyst) were added to a solution of 10 mmol of NH_4SCN in 25 mL of dichloromethane to a roundbottom flask with stirring. The mixture was stirred for 1 h at room temperature. Then to this mixture, a solution of 5 mmol (0.68 mL) of 2-methyl-1,5-diaminopentane was added dropwise with stirring. The resulting mixture was stirred for 3 h and the contents of the flask was poured into a beaker containing ice-water mixture to quench the reaction. Two separate layers were observed and those layers were separated by extraction. The organic phase was dried with anhydrous $CaCl_2$. The solvent was evaporated and a waxy product was obtained. After treating the product with ethanol, a white solid was obtained. The solid was then purified by column chromatography (silica gel, 3:7 EtOAc-hexane) to yield white crystals of **33**.

White powder, 48% yield; m.p.: 101.7°C; IR (v_{max}/cm^{-1}): 3224, 3016, 2986, 2930, 2845, 1749, 1678, 1519, 1489, 1436, 1363, 1310, 1246, 1217, 1189, 1142, 1068, 1036, 997, 772, 720 (Scheme: 12); ^{1}H NMR: (400 MHz, DMSO-d6) δ (ppm) 0.97 (d, 3H, CH_3), 1.26 (m, 2H, CH_2), 1.44 (m, 2H, CH_2), 1.96 (m, 1H, CH), 3.48 (m, 2H, CH_2), 3.62 (m, 2H, CH_2), 7.50 (t, 4H, ArH), 7.63 (t, 2H, ArH), 7.91 (t, 4H, ArH) 10.90 (s, 1H, NH), 10.99 (s, 1H, NH), 11.27 (s, 1H, NH), 11.32 (s, 1H, NH) (Scheme: 8); ^{13}C NMR: (100 MHz, DMSO-d6) δ (ppm): 18.0 (*C*H), 25.5 (*C*H$_2$), 31.6 (*C*H$_3$), 31.9 (*C*H$_2$), 45.3 (*C*H$_2$), 51.0 (*C*H$_2$), 128.8 (*C*H=C, Ar), 129.0 (*C*H=C, Ar), 132.7 (*C*H=C, Ar), 133.4 (*C*=C, Ar), 168.6 (*C*=O), 180.7 (*C*=S) (Scheme: 9).

Reaction of p-nitrobenzoyl chloride with NH₄SCN, and then with 2-methyl-1,5-diaminopentane to form the corresponding thiourea:
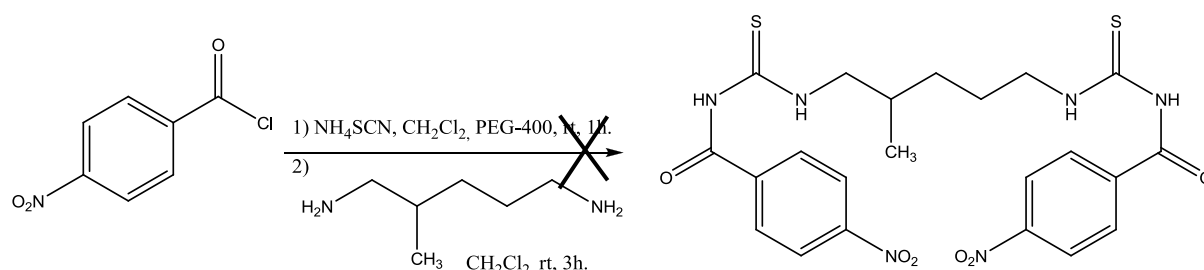
Two different compounds were present in the solid product mixture which ran too close on silica, hence it was not possible to separate them even though many different eluent compositions were employed.

2.2.1.2. *N*-(5-Chloro-2-phenoxyphenyl)-*N'*-benzoylthiourea (34)
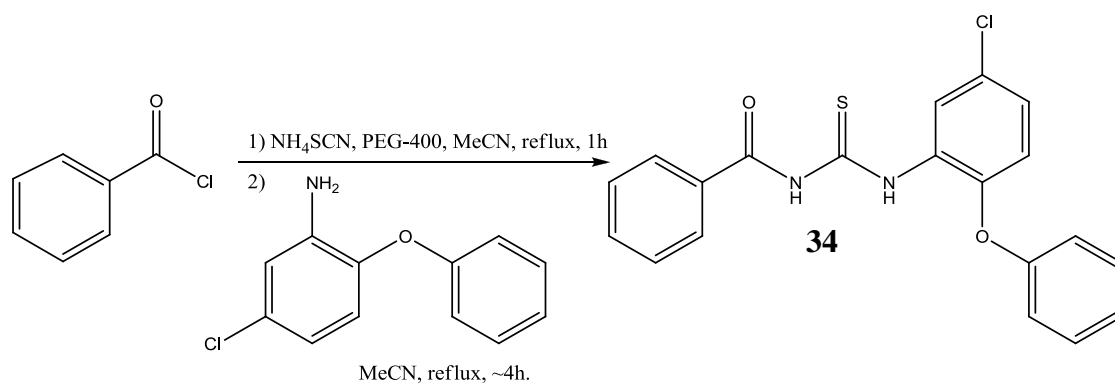
A solution of 5 mmol of benzoyl chloride in 5 mL of acetonitrile, and 4 drops of PEG-400 (as a phase transfer catalyst) were added to a solution of 5 mmol of NH$_4$SCN in 5 mL acetonitrile in a roundbottom flask with stirring. The mixture was refluxed for 1 h, then a solution of 2-amino-4-chlorophenyl phenyl ether in 10 mL of acetonitrile was added to this mixture dropwise with stirring. The mixture was refluxed for about 4 more hours, then the reaction was quenched by pouring the contents of the flask into a beaker containing ice-water mixture. White fuzz like precipitates that formed was filtered off, washed with distilled water and dried. The crude product was purified by recrysrallization from EtOH to yield white needle crystals.

White needles, 61% yield; m.p.: 168.1 °C; IR (v_{max}/cm^{-1}): 3422, 3089, 3024, 1672, 1592, 1513, 1474, 1342, 1282, 1282, 1209, 1192, 1139, 1101, 1068, 1021, 1003, 875, 858, 804, 776, 750, 681(Scheme: 17); ^{1}H NMR: (400 MHz, DMSO-d6) δ (ppm) 6.99 (d, 1H, Ar*H*), 7.12 (d, 2H, Ar*H*), 7.20 (t, 1H, Ar*H*), 7.33 (d, 1H, Ar*H*), 7.43 (t, 2H, Ar*H*), 7.52 (t, 2H, Ar*H*), 7.66 (t, 1H, Ar*H*), 7.93 (d, 2H, Ar*H*), 8.77 (s, 1H, Ar*H*), 11.79 (s, 1H, N*H*), 13.18 (s, 1H, N*H*) (Scheme: 13); ^{13}C NMR: (100 MHz, DMSO-d6) δ (ppm): 119.2 (*C*H=C, Ar), 120.1 (*C*H=C, Ar), 124.5 (*C*H=C, Ar), 124.8 (*C*H=C, Ar), 126.9 (*C*H=C, Ar), 127.1 (*C*H=C, Ar), 128.9 (*C*H=C, Ar), 129.3 (*C*H=C, Ar), 130.7 (*C*H=C, Ar), 131.0 (*C*=C, Ar), 132.3 (*C*=C, Ar), 133.7 (*C*=C, Ar), 148.1 (*C*=C, Ar), 156.3 (*C*=C, Ar), 169.2 (*C*=O), 179.5 (*C*=S) (Scheme: 14).

2.2.1.3. *N*-(5-Chloro-2-phenoxyphenyl)-*N'*-(4-nitrobenzoyl)thiourea (35)
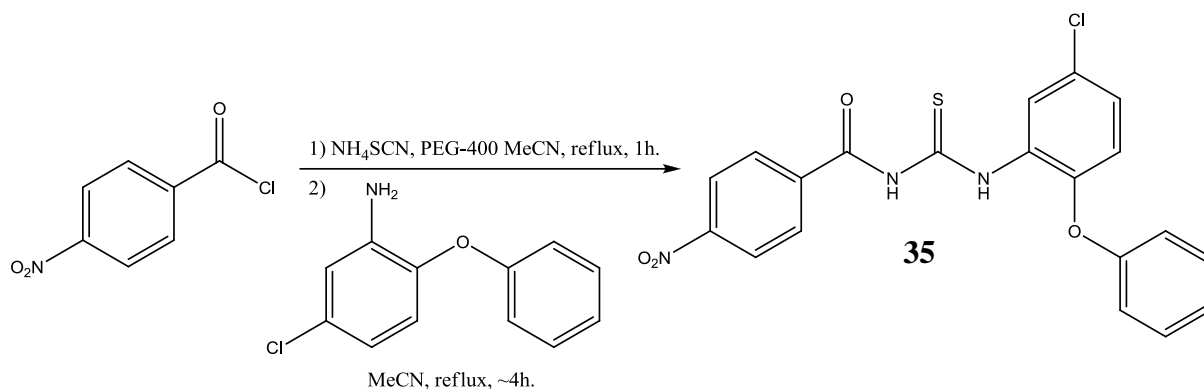
A solution of 5 mmol of 3,5-dinitrobenzoyl chloride in 5 mL of acetonitrile, and 4 drops of PEG-400 (as a phase transfer catalyst) were added to a solution of 5 mmol of NH_4SCN in 5 mL acetonitrile in a roundbottom flask with stirring. The mixture was refluxed for 1 h, then a solution of 2-amino-4-chlorophenyl phenyl ether in 10 mL of acetonitrile was added to this mixture dropwise with stirring. The mixture was refluxed for about 4 more hours, then the reaction was quenched by pouring the contents of the flask into a beaker containing ice-water mixture. Yellow fuzz like precipitates that formed was filtered off, washed with distilled water and dried. The crude product was purified by recrystallization from EtOH to yield bright yellow needle crystals of novel **35**.

Bright yellow needles, 55% yield; m.p.: 186.7 °C; IR (v_{max}/cm^{-1}): 3207, 3101, 3024, 1749, 1687, 1590, 1545, 1421, 1357, 1342, 1288, 1268, 1250, 1224, 1190, 1147, 1118, 1070, 1024, 1012, 963, 859, 850, 817, 748, 708, 691 (Scheme: 20); ^{1}H NMR (400 MHz, DMSO-d6) δ (ppm): 6.99 (d, 2H, Ar*H*), 7.12 (d, 2H, Ar*H*), 7.20 (t, 1H, Ar*H*), 7.34 (d, 1H, Ar*H*), 7.43 (t, 2H, Ar*H*), 8.12 (d, 2H, Ar*H*), 8.32 (d, 2H, Ar*H*), 8.75 (s, 1H, Ar*H*), 12.18 (s, 1H, N*H*), 12.98 (s, 1H, N*H*) (Scheme: 18); ^{13}C NMR: (100 MHz, DMSO-d6) δ (ppm): 119.3 (*C*H=C, Ar), 120.0 (*C*H=C, Ar), 123.7 (*C*H=C, Ar), 124.4 (*C*H=C, Ar), 124.8 (*C*H=C, Ar), 126.9 (*C*H=C, Ar), 127.3 (*C*=C, Ar), 130.7 (*C*H=C, Ar), 130.8 (*C*=C, Ar), 130.9 (*C*H=C, Ar), 138.2 (*C*=C, Ar), 148.2 (*C*=C, Ar), 150.3 (*C*=C, Ar), 156.2 (*C*=C, Ar), 167.7 (*C*=O), 179.1 (*C*=S) (Scheme: 19).

Reaction of oxalyl chloride with NH₄SCN, and then with 2-amino-4-chlorophenyl phenyl ether to form the corresponding thiourea:
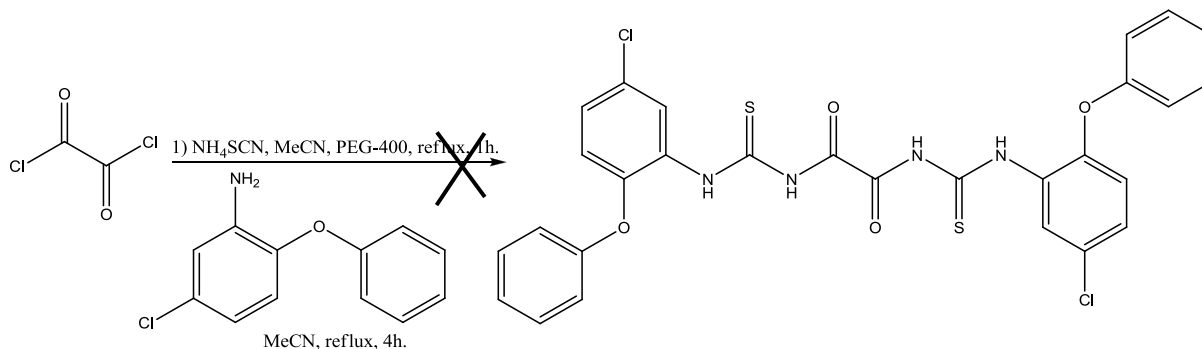
The resulting product was a waxy compound that decomposes with heat and air overtime.

3.2.1.4. *N*-(5-Chloro-2-phenoxyphenyl)-*N'*-(3,5-dinitrobenzoyl)thiourea (36)

A solution of 5 mmol of 3,5-dinitrobenzoyl chloride in 5 mL of acetonitrile, and 4 drops of PEG-400 (as a phase transfer catalyst) were added to a solution of 5 mmol of NH₄SCN in 5 mL acetonitrile in a roundbottom flask with stirring. The mixture was refluxed for 1 h, then a solution of 2-amino-4-chlorophenyl phenyl ether in 10 mL of acetonitrile was added to this mixture dropwise with stirring. The mixture was refluxed for about 4 more hours, then the reaction was quenched by pouring the contents of the flask into a beaker containing ice-water mixture. Dark yellow precipitates that formed was filtered off, washed with distilled water and dried. The crude product was purified by column chromatography (silica gel, 1:4 EtOAc-hexane) to yield bright yellow needle crystals of novel **36**.

Bright yellow needles, 19% yield; m.p.: 204.9 °C; IR (v_{max}/cm⁻¹): 3228, 3095, 3033, 1751, 1678, 1631, 1581, 1525, 1478, 1417, 1333, 1269, 1234, 1206, 1189, 1156, 1129, 1074, 1015, 1003, 815, 791, 749, 725i 714, 693 (Scheme: 23); ¹H NMR: (400 MHz, DMSO-d6)

δ (ppm) 6.99 (d, 1H, Ar*H*), 7.13 (d, 2H, Ar*H*), 7.21 (t, 1H, Ar*H*), 7.34 (d, 1H, Ar*H*), 7.43 (t, 2H, Ar*H*), 8.76 (s, 1H, Ar*H*), 9.03 (s, 1H, Ar*H*), 9.06 (s, 2H, Ar*H*), 12.51 (s, 1H, N*H*), 12.90 (s, 1H, N*H*) (Scheme: 21); ^{13}C NMR: (100 MHz, DMSO-d6) δ (ppm): 109.9 (*C*H=C, Ar), 119.4 (*C*H=C, Ar), 120.0 (*C*H=C, Ar), 122.6 (*C*H=C, Ar), 124.3 (*C*=C, Ar), 124.9 (*C*H=C, Ar), 126.9 (*C*=C, Ar), 127.3 (*C*=C, Ar), 129.9 (*C*H=C, Ar), 130.7 (*C*H=C, Ar), 133.1 (*C*=C, Ar), 133.7 (*C*=C, Ar), 135.5 (*C*=C, Ar), 148.1 (*C*H=C, Ar), 148.2 (*C*=O), 156.2 (*C*=S) (Scheme: 22).

Reaction of 3,5-dinitrobenzoyl chloride with NH₄SCN, and then with 5-Amino-1,4-benzodioxane to form the corresponding thiourea:
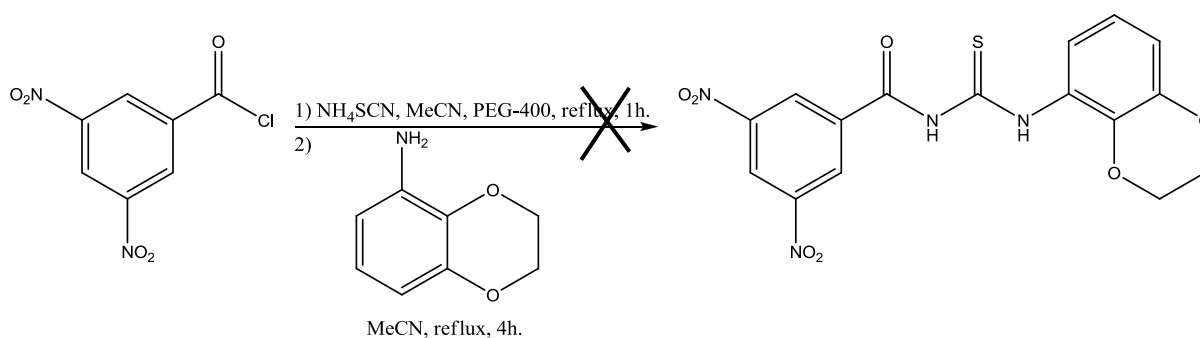
No product was obtained.

Reaction of 3,5-dinitrobenzoyl chloride with NH₄SCN, and then with 2,4-diamino-6-phenyl-1,3,5-triazine to form the corresponding thiourea:
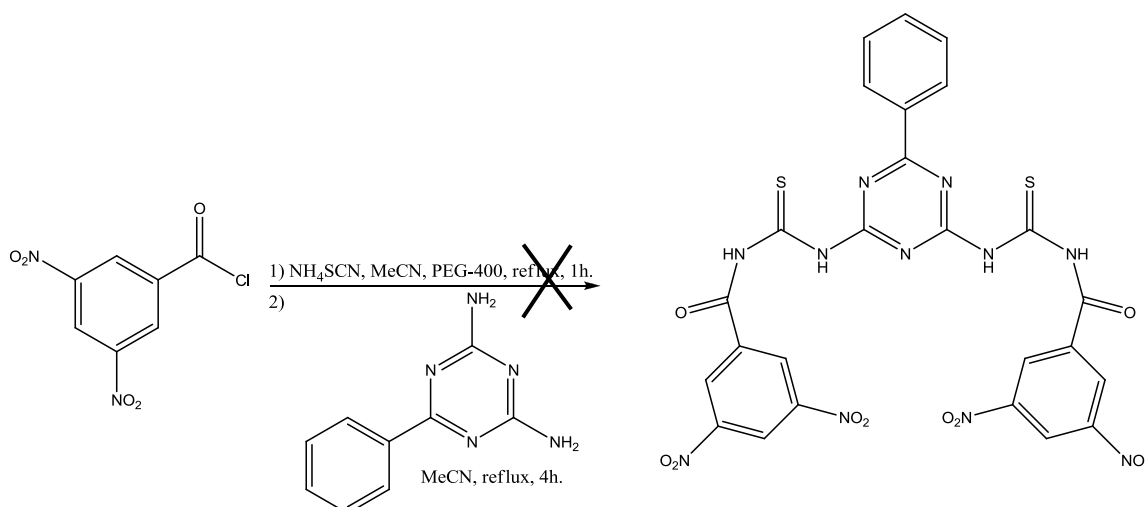
The reaction yielded a small amount of product mixture, which contained excessive impurities. It was not possible to isolate the product from the starting material because of low solubilities.

2.2.1.5. *N*-(4-Biphenyl)-*N'*-(3,5-dinitrobenzoyl)thiourea (37)
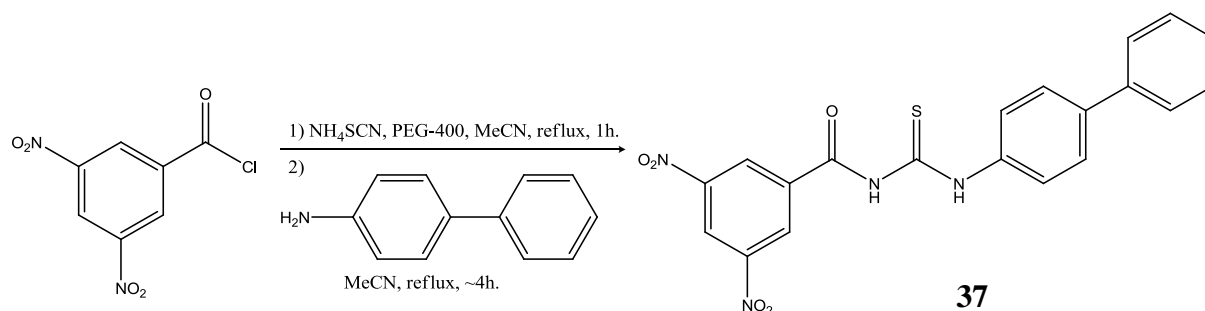
A solution of 5 mmol of benzoyl chloride in 5 mL of acetonitrile, and 4 drops of PEG-400 (as a phase transfer catalyst) were added to a solution of 5 mmol of NH_4SCN in 5 mL acetonitrile in a roundbottom flask with stirring. The mixture was refluxed for 1 h, then a solution of 4-aminobiphenyl in 10 mL of acetonitrile was added to this mixture dropwise with stirring. The mixture was refluxed for about 4 more hours, then the reaction was quenched by pouring the contents of the flask into a beaker containing ice-water mixture. Yellow precipitates that formed were filtered off, washed with distilled water and dried. The crude product was purified by column chromatography (silica gel, 1:5 EtOAc-hexane) to yield bright yellow needle crystals of novel **37**.

Bright yellow needles, 43% yield; m.p.: 213.7 °C; IR (v_{max}/cm^{-1}): 3384, 3104, 3027, 1675, 1604, 1578, 1540, 1516, 1483, 1336, 1251, 1216, 1156, 1121, 1094, 1001, 842, 767, 699 (Scheme: 28); ^{1}H NMR: (400 MHz, DMSO-d6) δ (ppm) 7.40 (t, 1H, Ar*H*), 7.50 (t, 2H, Ar*H*), 7.72 (d, 2H, Ar*H*), 7.76 (d, 2H, Ar*H*), 7.83 (d, 2H, Ar*H*), 9.05 (s, 1H, Ar*H*), 9.14 (s, 2H, Ar*H*), 12.35 (s, 1H, N*H*), 12.39 (s, 1H, N*H*) (Scheme: 24); ^{13}C NMR: (100 MHz, DMSO-d6) δ (ppm): 122.6 (*C*H=C, Ar), 125.1 (*C*H=C, Ar), 127.1 (*C*H=C, Ar), 127.4 (*C*H=C, Ar), 128.1 (*C*=C, Ar), 129.5 (*C*H=C, Ar), 129.7 (*C*H=C, Ar), 148.2 (*C*H=C, Ar), 164.8 (*C*=O), 178.8 (*C*=S) (Scheme: 25).

Reaction of nitrobenzoyl chloride with NH₄SCN, and then with 1,3-cyclohexanebis(methylamine) to form the corresponding thiourea:
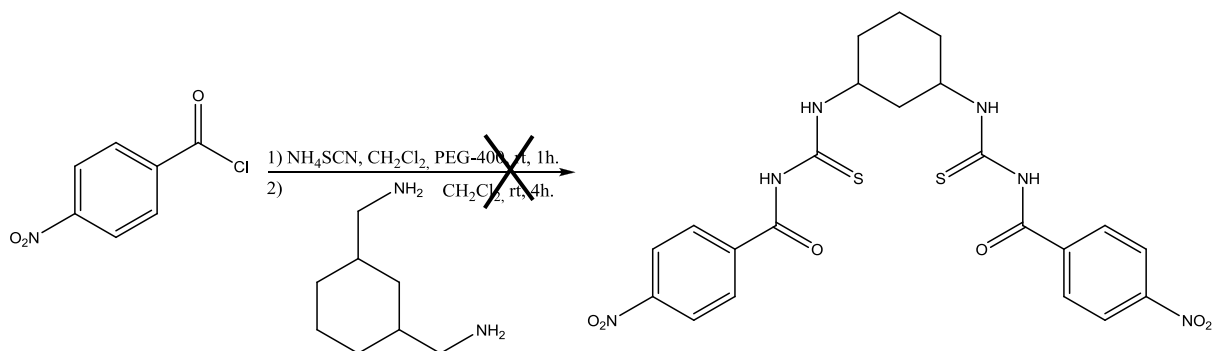
The reaction yielded a waxy product which contained impurities. It was not possible to purify and solidify the compound.

2.2.1.6. *N*-(5-Chloro-2-phenoxyphenyl)-*N'*-[4-(5-chloro-2-phenoxyphenyl)benzamido] thiourea (38)

A solution of 5 mmol of terephthtaloyl chloride in 5 mL of acetonitrile, and 4 drops of PEG-400 (as a phase transfer catalyst) were added to a solution of 5 mmol of NH₄SCN in 5 mL acetonitrile in a roundbottom flask with stirring. The mixture was refluxed for 1 h, then a solution of 2-amino-4-chlorophenyl phenyl ether in 10 mL of acetonitrile was added to this mixture dropwise with stirring. The mixture was refluxed for about 4 more hours, then the reaction was quenched by pouring the contents of the flask into a beaker containing ice-water mixture. Dark yellow precipitates that formed were filtered off, washed with distilled water and dried. The crude product was purified by washing with acetone until the unreacted amine was removed completely to yield the novel **38**. LC or crystallization

techniques were not performed for purification, since the solubility of the product was too low.

Yellow powder, 65 % yield; m.p.: 243.5 °C. IR (v_{max}/cm^{-1}): 3393, 3104, 3048, 1675, 1604, 1516, 1490, 1480, 1455, 1419, 1348, 1286, 1242, 1215, 1185, 1148, 1109, 1087, 1056, 1009, 970, 880, 862, 799, 752, 714, 692 (Scheme: 31); ^{1}H NMR: (400 MHz, DMSO-d6) δ (ppm) 6.63 (d, 1H, Ar*H*), 6.83 (d, 1H, Ar*H*), 6.91 (d, 1H, Ar*H*), 6.98 (d, 2H, Ar*H*), 7.05 (d, 1H, Ar*H*), 7.13 (t, 1H, Ar*H*), 7.17 (d, 2H, Ar*H*), 7.26 (t, 2H, Ar*H*), 7.40 (t, 2H, Ar*H*), 7.48 (t, 2H, Ar*H*), 8.04 (d, 1H, Ar*H*), 8.07 (d, 2H, Ar*H*), 8.11 (s, 2H, Ar*H*), 8.81 (s, 1H, N*H*), 12.06 (d, 1H, N*H*), 13.14 (s, 1H, N*H*) (Scheme: 29); ^{13}C NMR: (100 MHz, DMSO-d6) δ (ppm): 115.2 (*C*H=C, Ar), 116.3 (*C*H=C, Ar), 116.2, 118.8 (*C*H=C, Ar), 119.6 (*C*H=C, Ar), 121.4 (*C*H=C, Ar), 122.7 (*C*H=C, Ar), 124.0 (*C*H=C, Ar), 124.3 (*C*H=C, Ar), 126.4 (*C*H=C, Ar), 126.7 (*C*H=C, Ar), 127.3 (*C*H=C, Ar), 128.7 (*C*H=C, Ar), 129.0 (*C*H=C, Ar), 129.5 (*C*=C, Ar), 129.8 (*C*H=C, Ar), 130.2 (*C*H=C, Ar), 130.4 (*C*=C, Ar), 134.5 (*C*=C, Ar), 135.7 (*C*=C, Ar), 141.0 (*C*=C, Ar), 147.7 (*C*=C, Ar), 155.8 (*C*=C, Ar), 157.0 (*C*=C, Ar), 166.5 (*C*=C, Ar), 168.1 (*C*=O), 178.8 (*C*=S) (Scheme: 30).

After interpreting the ^{1}H NMR data, it turned out that the product was not a dithiourea as expected, but a compound with amide functionality on one side, and thiourea on other.

Reaction of terephthaloyl chloride with NH$_4$SCN, and then with 4-aminobiphenyl to form the corresponding thiourea:

No product was obtained.

Reaction of terephthaloyl chloride with NH₄SCN, and then with 2-Amino-4-chlorophenyl phenyl ether to form the corresponding thiourea:
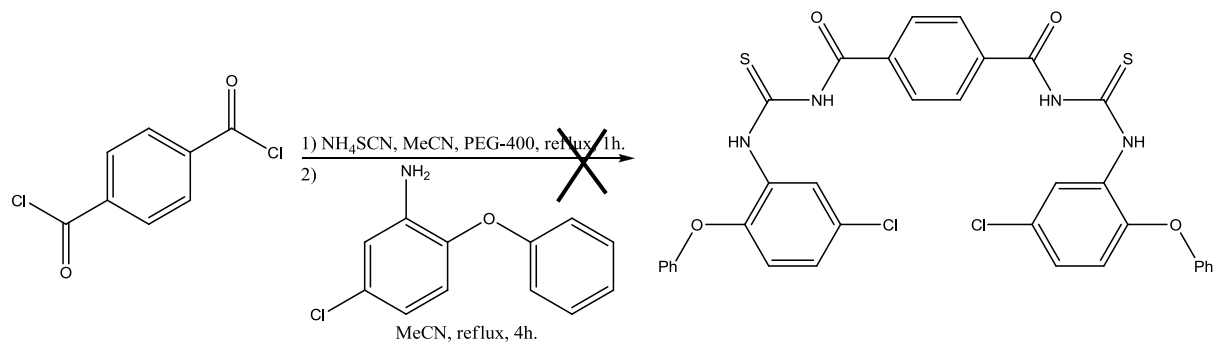
No product was obtained.

2.2.2. Syntheses of Amides

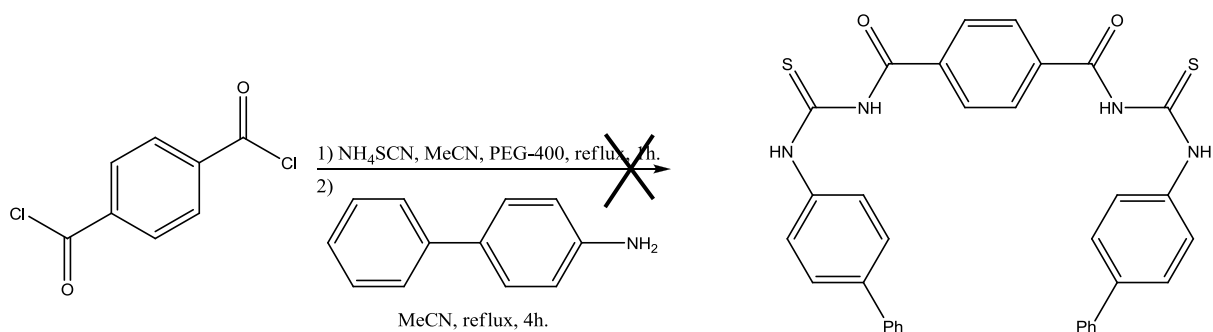### 2.2.2.1. *N*-[5-(4-Methoxyphenyl)-1,3,4-thiadiazol-2-yl]benzamide (39)
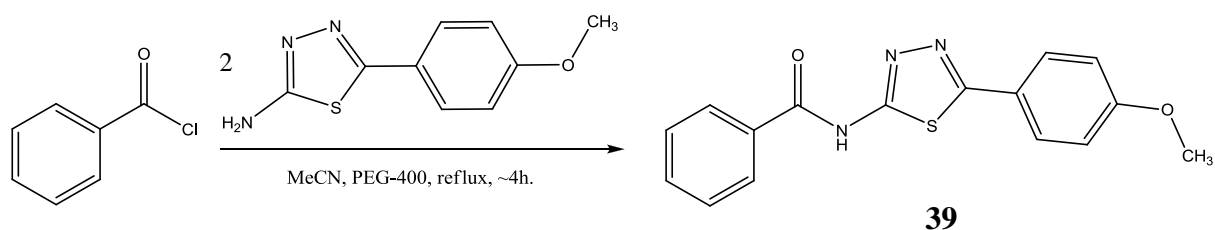
A solution of 5 mmol of benzoyl chloride in 5 mL of acetonitrile, and 4 drops of PEG-400 (as a phase transfer catalyst) were added to a solution of 5 mmol of NH₄SCN in 5 mL acetonitrile in a roundbottom flask with stirring. The mixture was refluxed for 1 h, then a solution of 2-amino-5-(4-methoxyphenyl)-1,3,4-thiadiazole in 10 mL of acetonitrile was added to this mixture dropwise with stirring. The mixture was refluxed for 4 more hours, then the reaction was quenched by pouring the contents of the flask into a beaker containing ice-water mixture. Yellow precipitates that formed was filtered off, washed with distilled water and dried. The crude product was purified by recrystallization from EtOH to yield white crystals.

White needle crystals, 40% yield; m.p.: 269.6°C. IR (v_{max}/cm⁻¹): 3127, 3018, 1760, 1666, 1610, 1569, 1513, 1457, 1419, 1265, 1230, 1209, 1162, 1107, 1044, 1010, 838, 703, 679 (Scheme: 36); ¹H NMR: (400 MHz, DMSO-d6) δ (ppm) 3.79 (s, 3H, C*H*₃), 7.05 (d, 2H, Ar*H*), 7.53 (t, 2H, Ar*H*), 7.62 (t, 1H, Ar*H*), 7.87 (d, 2H, Ar*H*), 8.09 (d, 2H, Ar*H*), 13.04 (s, 1H, N*H*) (Scheme: 32); ¹³C NMR: (100 MHz, DMSO-d6) δ (ppm): 55.8 (*C*H₃), 115.2

(*CH*=C, Ar), 123.2 (*C*=C, Ar), 128.9 (*CH*=C, Ar), 128.9 (*CH*=C, Ar), 129.1 (*CH*=C, Ar), 132.0 (*CH*=C, Ar), 133.4 (*C*=C, Ar), 133.4 (*CH*=C, Ar), 159.2 (*C*=N), 161.5 (*C*=C, Ar), 162.4 (*C*=O), 165.6 (*C*=N) (Scheme: 33).

After interpreting the ^{1}H NMR data, the product turned out to be an amide, instead of the expected thiourea.

Reaction of p-nitrobenzoyl chloride with NH$_4$SCN, and then with 2-Amino-5-(4-methoxyphenyl)-1,3,4-thiadiazole to form the corresponding thiourea:
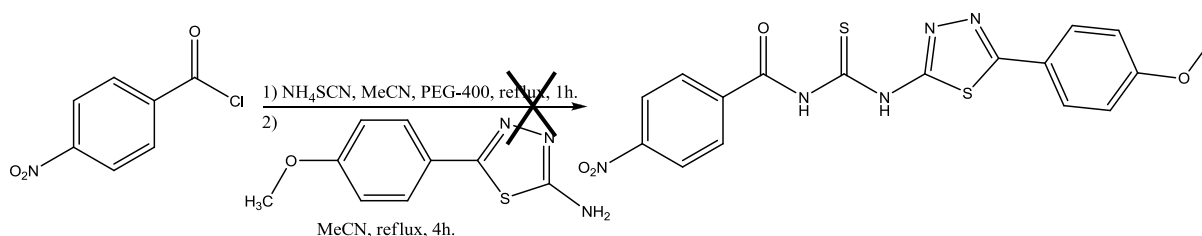
It was not possible to purifiy the product mixture because of its very low solubility in common solvents to perform LC or crystallization.

2.2.2.2. *N,N'*-bis(5-Chloro-2-phenoxyphenyl)benzene-1,4-dicarboxamide (40)
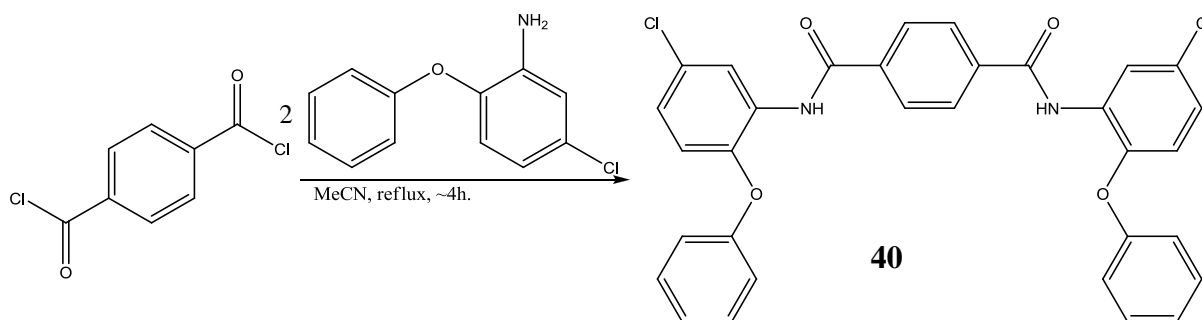
A solution of 2-amino-4-chlorophenyl phenyl ether in 10 mL of acetonitrile, was added dropwise to a solution of 5 mmol of terephthaloyl chloride in 10 mL of acetonitrile, in a roundbottom flask with stirring. The mixture was refluxed for 4 hours, then the reaction was quenched by pouring the contents of the flask into a beaker containing ice-water mixture. White precipitates that formed was filtered off, washed with distilled water and dried. The crude product was purified by recrystallization from EtOH to yield the novel **40**.

White powder, 71% yield; m.p.: 200.4°C; IR (v_{max}/cm^{-1}): 3446, 3357, 3074, 1684, 1595, 1528, 1395, 1312, 1292, 1251, 1215, 1127, 1117, 1103, 1072, 1029, 1009, 893, 859, 837,

744,725, 700 (Scheme: 39); ^{1}H NMR: (400 MHz, DMSO-d6) δ (ppm) 7.01 (d, 4H, ArH), 7.03 (d, 2H, ArH), 7.12 (t, 2H, ArH), 7.31 (d, 2H, ArH), 7.37 (t, 4H, ArH), 7.84 (s, 4H, ArH), 7.89 (d, 2H, ArH), 10.12 (s, 2H, NH) (Scheme: 37); ^{13}C NMR: (100 MHz, DMSO-d6) δ (ppm): 118.6 (*C*H=C, Ar), 121.2 (*C*H=C, Ar), 124.1 (*C*H=C, Ar), 126.2 (*C*H=C, Ar), 126.6 (*C*H=C, Ar), 127.7 (*C*=C, Ar), 128.2 (*C*H=C, Ar), 130.4 (*C*H=C, Ar), 131.0 (*C*=C, Ar), 137.2 (*C*=C, Ar), 148.6 (*C*=C, Ar), 156.8 (*C*=C, Ar), 165.4 (*C*=O) (Scheme: 38).

2.3. Anion Interactions

Tetrabutylammonium salts of Cl$^-$, Br$^-$, I$^-$, CN$^-$, OAc$^-$, H$_2$PO$_4^-$, HSO$_4^-$ and NO$_3^-$; tetramethylammonium salts of F$^-$ and OH$^-$ were used as anion sources and the complexations were performed in DMSO.

For UV-Vis analyses, 1×10^{-3} M solutions of host-anion mixtures of changing mole ratios (3:1, 1:1 and 1:3) in DMSO were prepared. Each mixture was let to stand for 15 min for the complexes to form and then diluted to 5×10^{-5} M prior to introducing the samples in UV-Vis device. The changes in the absorption pattern of the pure hosts with increasing anion concentration were recorded.

For ^{1}H NMR analyses, 20 mg of each host were let to interact with 1:1 molar equivalent of each of the 10 anions in DMSO-d6.

3. RESULTS AND DISCUSSION

3.1. Syntheses

Six thiourea derivatives **33**, **34**, **35**, **36**, **37** and **38** (all except **34** are novel) and two amide derivatives **39** and **40** (**40** is novel) were synthesized in the study. Thioureas were synthesized first by reacting the corresponding acyl chlorides and ammonium thiocyanate in the presence of PEG-400 as a phase transfer catalyst, followed by the tandem addition of corresponding amines with moderate yields. PEG-400 was first used for the synthesis of **33** in this study to imporve the solubility of NH$_4$SCN in dichloromethane. Use of the phase transfer catalyst increased the conversion rate of the reactants significantly, such that almost no product was obtained in the absence of the catalyst. Thus, all thiourea syntheses were carried out in the presence of PEG-400. Also the yield of the reaction to obtain **38** increased from 12.2% to 64.9% when the phase transfer catalyst was employed. Amides

were obtained by the reaction of corresponding acyl chloride with corresponding amine; with moderate yields. The structures of the compounds were elucidated by FT-IR spectroscopy and by ^{1}H and ^{13}C NMR spectroscopy. The spectral data was consistent with the predicted structures.

In the ^{1}H NMR spectrum of **33**, the aliphatic protons were observed between 0.97-3.62 ppm, the aromatic protons between 7.50-7.91 ppm. The NH protons were observed as four singlets. The small chemical shift difference between each of the two pairs at 10.90 & 10.99 and 11.27 & 11.32 ppm arises from their slightly different electron densities created by the methyl group on the aliphatic chain. In the ^{13}C NMR spectrum, the aliphatic carbons were observed between 18.0-51.0 ppm, the aromatic carbons between 128.8-133.4 ppm, and the carbonyl carbons at 168.6 and 180.7 ppm. COSY and HETCOR spectra of **33** verified the deductions made from ^{1}H and ^{13}C NMR spectra.

In the ^{1}H NMR spectrum of **34**, aromatic signals were observed in the 6.99-8.77 ppm interval and the NH signals were observed at 11.79 and 13.17 ppm. In the ^{13}C NMR spectra, the aromatic signals were observed in the 119.2-156.3 ppm interval and the carbonyl signals at 169.2 and 179.5 ppm. COSY and HETCOR spectra of **34** verified the deductions made from ^{1}H and ^{13}C NMR spectra.

In the ^{1}H NMR spectrum of **35**, the aromatic protons were observed between 6.99-8.75 ppm and the NH protons were observed at 12.18 and 12.98 ppm. In the ^{13}C NMR spectrum, the aromatic carbons were observed between 119.3-156.2 ppm and the carbonyl carbons at 167.7 and 179.2 ppm.

In the ^{1}H NMR spectrum of **36**, aromatic signals were observed in the 6.99-9.06 ppm interval and the NH signals were observed at 12.51 and 12.90 ppm. In the ^{13}C NMR spectra, the aromatic signals were observed in the 109.9-148.1 ppm interval and the carbonyl signals at 148.2 and 156.2 ppm.

In the ^{1}H NMR spectrum of **37**, the aromatic protons were observed between 7.40-9.14 ppm and the NH protons were observed at 12.35 and 12.39 ppm. In the ^{13}C NMR spectrum, the aromatic carbons were observed between 122.6-148.2 ppm and the carbonyl carbons at 164.8and 178.8 ppm.

In the ^{1}H NMR spectrum of **38**, aromatic signals were observed in the 6.63-8.11 ppm interval and the NH signals were observed at 8.81, 12.06 and 13.14 ppm. In the ^{13}C NMR

spectra, the aromatic signals were observed in the 115.2-166.5 ppm interval and the carbonyl signals at 168.1 and 178.8 ppm.

In the ^{1}H NMR spectrum of **39**, the methyl proton was observed at 3.79 ppm, the aromatic protons were observed between 7.05-8.09 ppm and the NH proton was observed at 13.04 ppm. In the ^{13}C NMR spectrum, the methyl carbon was observed at 55.8 ppm, the aromatic carbons were observed between 115.2-161.5 ppm, the carbonyl carbon at 162.4 ppm and the C=N carbon at 165.5 ppm. COSY and HETCOR spectra of **39** verified the deductions made from ^{1}H and ^{13}C NMR spectra.

In the ^{1}H NMR spectrum of **40**, aromatic signals were observed in the 7.01-7.89 ppm interval and the two equivalent NH protons were observed at 10.21 ppm as a single peak. In the ^{13}C NMR spectra, the aromatic signals were observed in the 118.6-156.8 ppm interval and a single carbonyl signal was observed for the two equivalent carbonyl groups at 165.4 ppm.

3.2. Anion Interactions

For many host-anion pairs, complex formation led to a distinct change in colour visible to the naked eye, which were photographed using $1x10^{-3}$ M solutions of the host-anion mixtures for better observation.

The purpose of preparing solutions with fixed mole fractions was to construct Job plots with the obtained data to find the stoichiometry of the complexes formed. However, for the majority of host-anion pairs, complexation through hydrogen bonds only caused a change in the absorption pattern of the host molecule. Only some vague deductions can be made by the changes in those patterns. The proportional decrease in absorptions during UV-Vis titrationsis an effect of dilution even though there was no complexation. Another reason for not making a quantitative analysis with the data obtained is that the absorptions of host molecules were too high to begin with, because of the many functional groups they possess, and working with those high values might have compromised the confidence of the quantitative analysis. On the other hand, further dilution of the solutions caused the hydrogen bonds to distrupt. The shifts of the original bands and/or the formation of new bands arise from the delocalization of the lone pairs that result from the deprotonation of NH moieties of hosts by strongly basic anions.

All analyses showed that strongly basic or high-electron-density anions form complexes better with NH moieties of the hosts through hydrogen bonding. In the cases that the hydrogen bonds were too strong, deprotonation occurs, which shows itself by the disappearance of NH peaks in ^{1}H NMR spectra of the complexes. ^{1}H NMR analyses were only performed to 1:1 mixtures of hosts and anions mainly because of financial concerns.

The changes in the color, UV-Vis spectra and ^{1}H NMR spectra of the host molecules are as follows:

3.2.1 *N,N*-(2-Methylpentane-1,5-diyl)-*N',N'*-benzoyldithiourea (33)

Compound **33** didn't show any color change upon addition of anions at any chosen amount. Similarly no change in the spectrum of the compound was observed during UV-Vis titrations. The lack of change in the colors and UV-Vis spectra of **33** can be attributed to the lack of a complete conjugation throughout the compound.
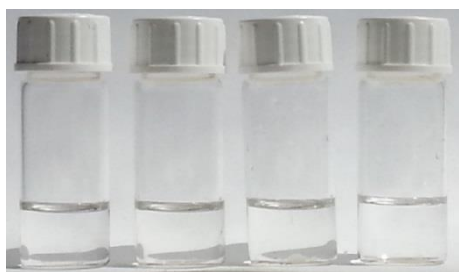
Figure 29: Colors of DMSO solutions of pure **33** and upon addition of 3:1, 1:1 and 1:3 mole ratios of F⁻ from left to right
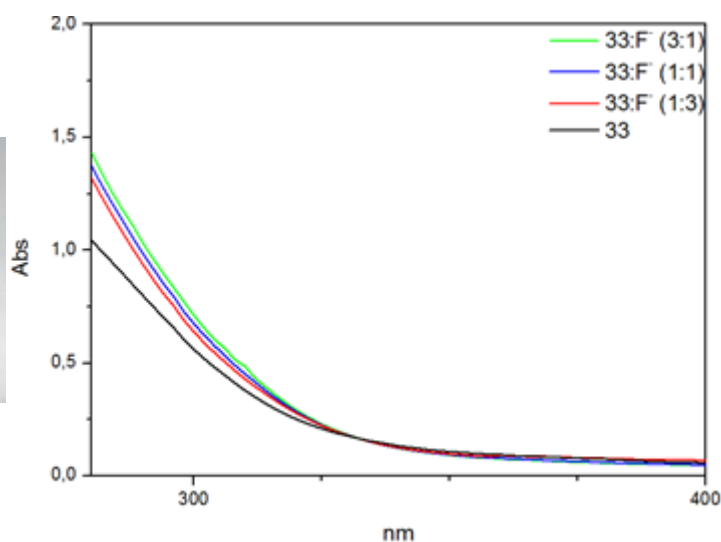
33 + F⁻

Figure 30: Colors of DMSO solutions of pure **33** and upon addition of 3:1, 1:1 and 1:3 mole ratios of Cl⁻ from left to right
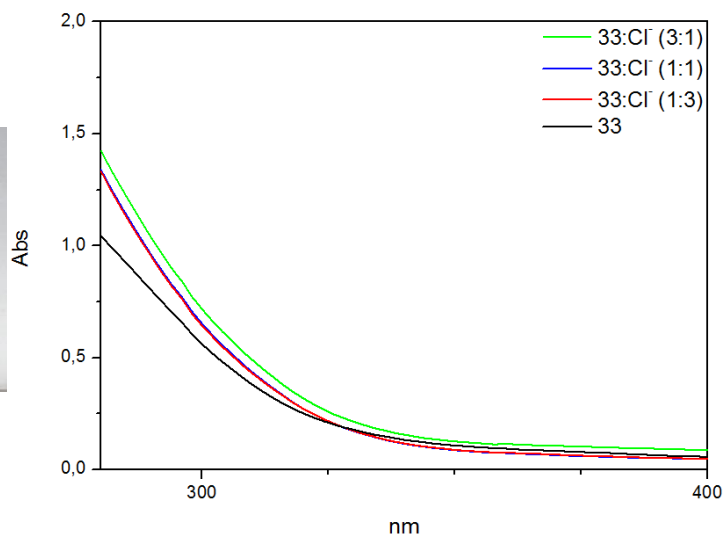
33 + Cl⁻

Figure 31: Colors of DMSO solutions of pure **33** and upon addition of 3:1, 1:1 and 1:3 mole ratios of Br⁻ from left to right
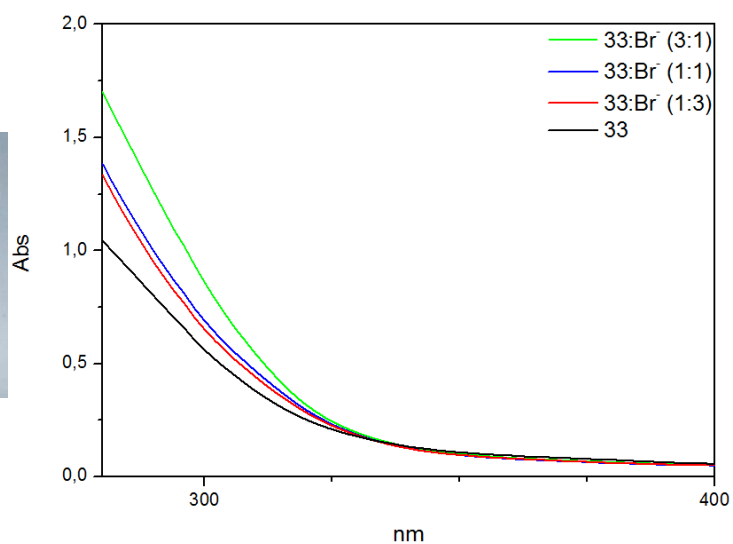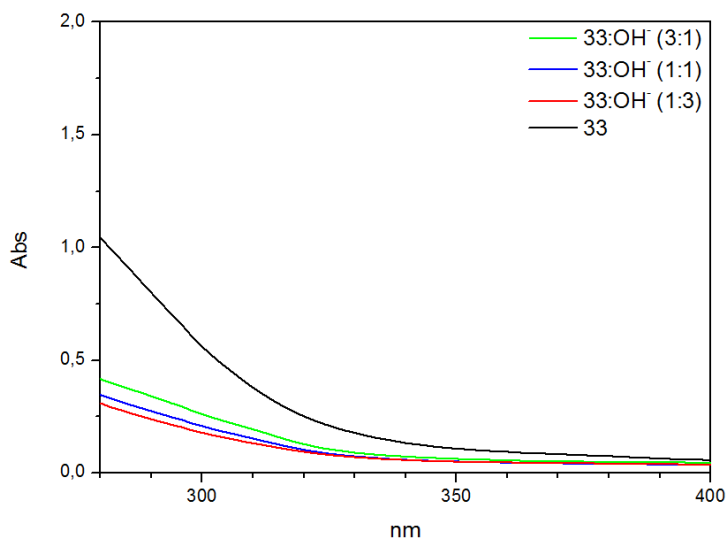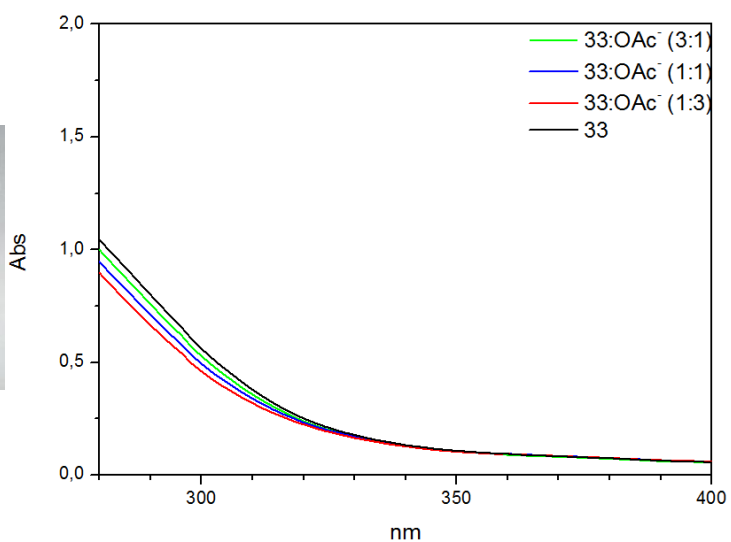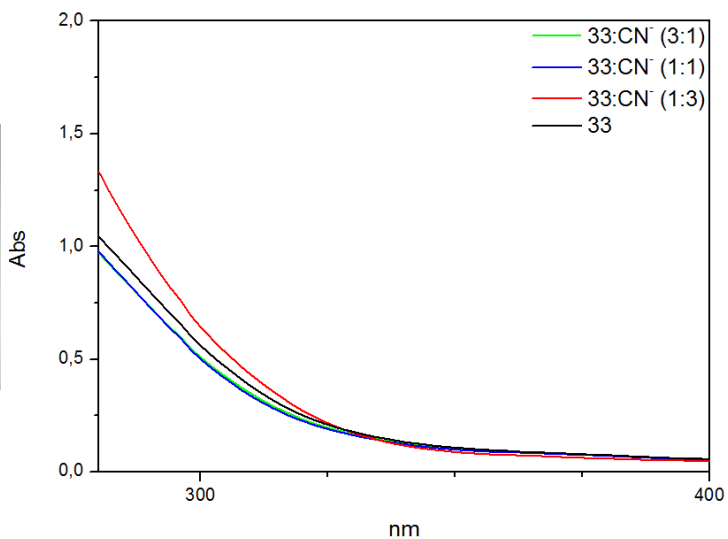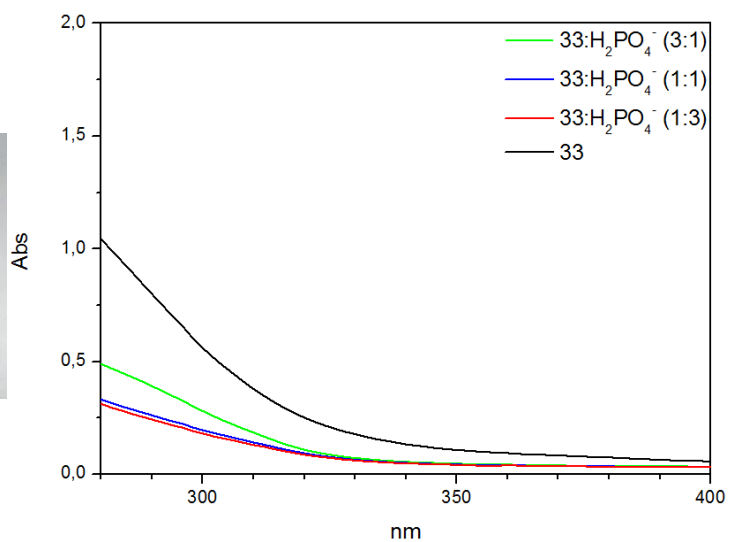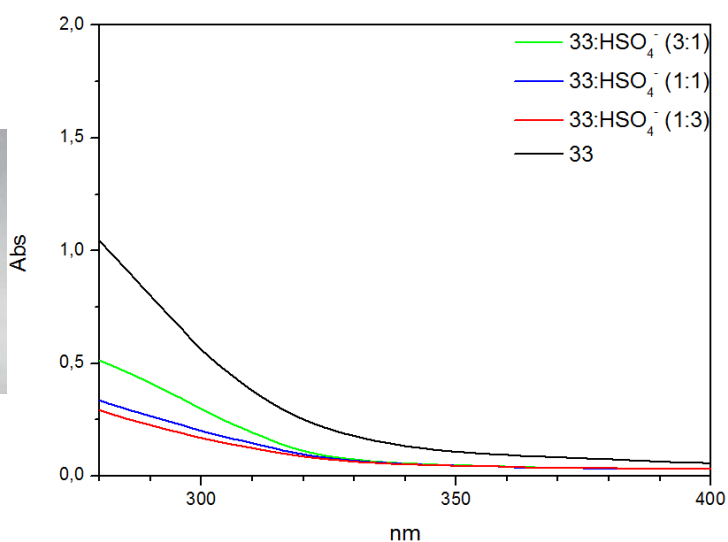
33 + Br⁻

Figure 32: Colors of DMSO solutions of pure **33** and upon addition of 3:1, 1:1 and 1:3 mole ratios of I⁻ from left to right
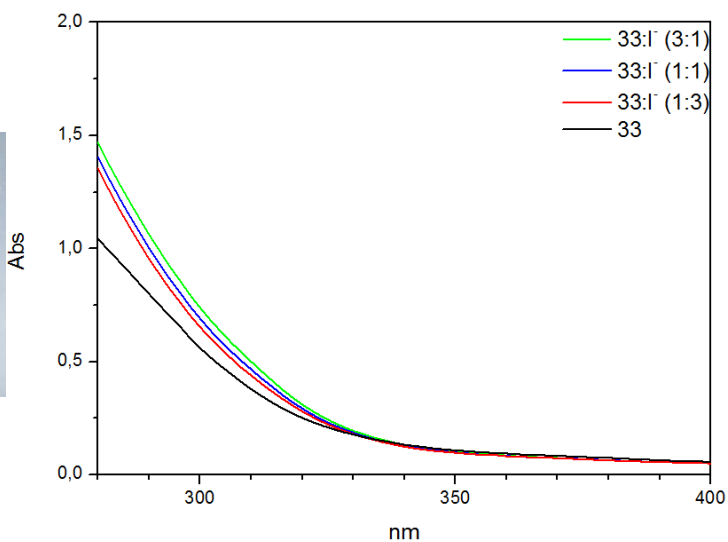
33 + I⁻

Figure 33: Colors of DMSO solutions of pure **33** and upon addition of 3:1, 1:1 and 1:3 mole ratios of OH⁻ from left to right

33 + OH⁻

Figure 34: Colors of DMSO solutions of pure **33** and upon addition of 3:1, 1:1 and 1:3 mole ratios of OAc⁻ from left to right

33 + OAc⁻

Figure 35: Colors of DMSO solutions of pure **33** and upon addition of 3:1, 1:1 and 1:3 mole ratios of CN⁻ from left to right

33 + CN⁻

Figure 36: Colors of DMSO solutions of pure **33** and upon addition of 3:1, 1:1 and 1:3 mole ratios of $H_2PO_4^-$ from left to right

33 + $H_2PO_4^-$

Figure 37: Colors of DMSO solutions of pure **33** and upon addition of 3:1, 1:1 and 1:3 mole ratios of HSO_4^- from left to right

33 + HSO_4^-

Figure 38: Colors of DMSO solutions of pure **33** and upon addition of 3:1, 1:1 and 1:3 mole ratios of NO_3^- from left to right

33 + NO_3^-

35
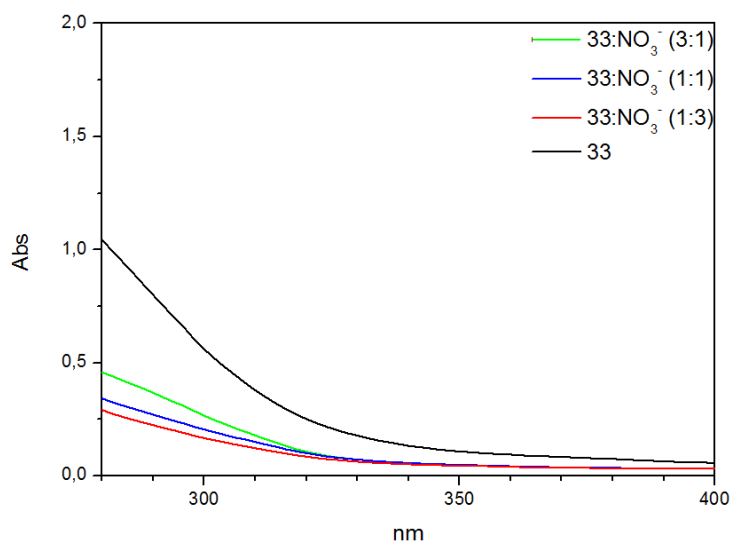
However, the ^{1}H NMR analysis (Scheme 1) showed changes in the spectra of host-anion mixtures. The addition of 1:1 mole ratios of F$^-$ caused the first NH peak (CONH proton) to disappear, and the second to shrink, which shows that the anion was hydrogen bonded to both protons, but the NH proton next to the carbonyl was deprotonated by the anion. Addition of OAc$^-$ had the same effect. Addition of CN$^-$ also had a similar effect, but the second NH peak was broadened to almost disappearance in that case. Upon the addition of OH$^-$, both NH peaks were disappeared, which indicates complete deprotonation of NH groups because of the strong basicity of hydroxyl anion. H$_2$PO$_4$$^-$ seems to form hydrogen bonds with both NH groups, indicated by the decreases in the peak intensities of both. I$^-$ also seems to form a weak hydrogen bond with the thiourea proton of **33**, judging from the slight decrease of its peak intensity. The reason for this preference of H-bond donor can be attributed to the size of the anion. The rest of the anions Cl$^-$, Br$^-$ and HSO$_4$$^-$ didn't cause any changes in the ^{1}H NMR spectrum of **33**, mainly because of their low basicities of all three anions and because of the mismatching geometry in the case of hydrogen sulphate anion.

The studies showed that compound **33** didn't show any particular selectivity to any of the anions. **33** formed complexes with F$^-$, OH$^-$, OAc$^-$, CN$^-$ and H$_2$PO$_4$$^-$ which were only detectable by ^{1}H NMR analysis. The reason may be the dependancy of hydrogen bonding to concentration (concentration of ^{1}H NMR analytes are around 0.1 M, while 5×10^{-5} M solutions of host-anion mixtures were used for UV-Vis titrations). The need for an instrument to detect the recognition is not preferred because of the running costs and the time it needs.

33
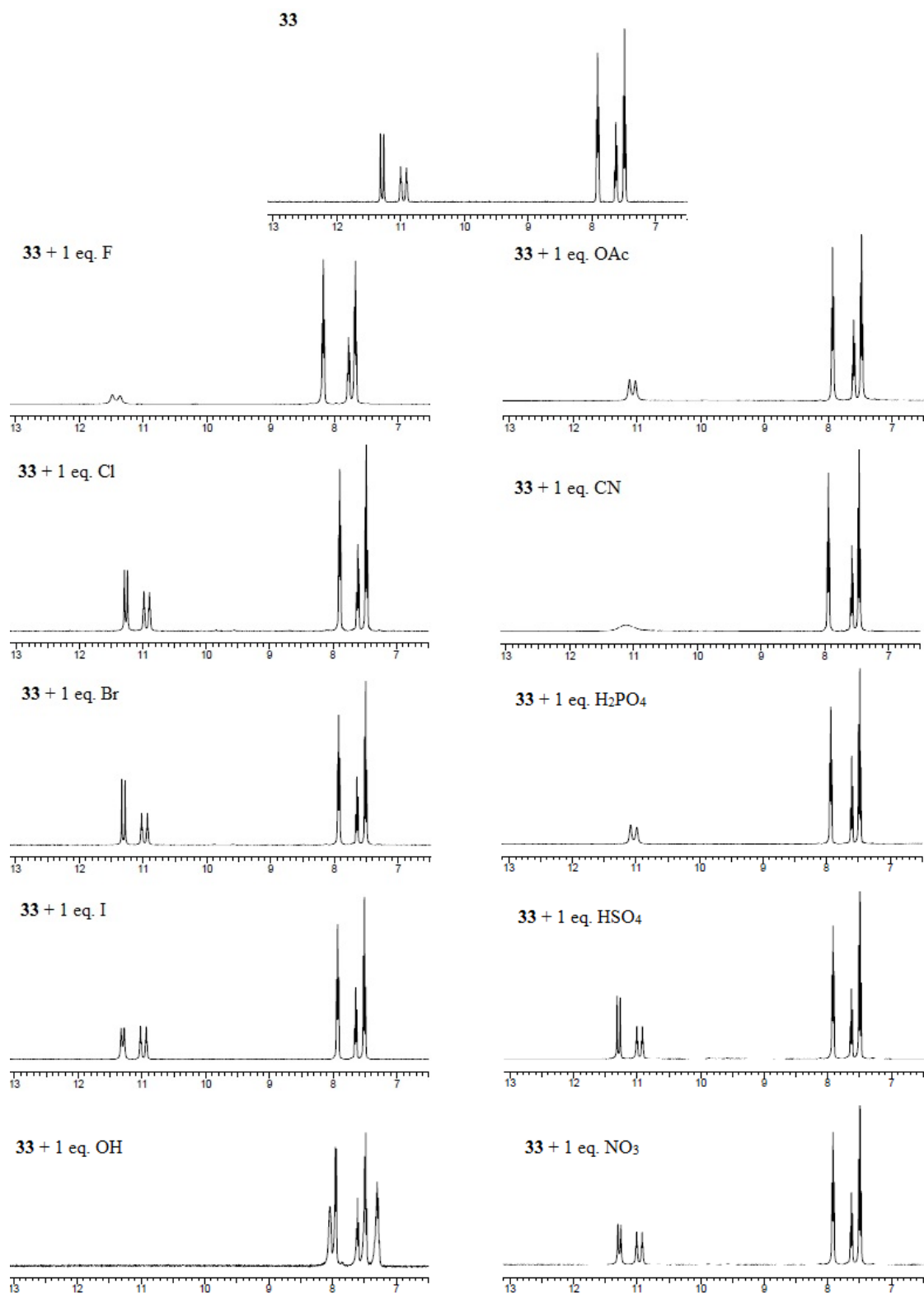
Scheme 1: Partial ^{1}H NMR spectra of **33** upon interaction with 1:1 ratios of anions

3.2.2. *N*-(5-Chloro-2-phenoxyphenyl)-*N'*-benzoylthiourea (34)

Compound **34** turned to yellow from colorless upon addition of OH^-, OAc^- and CN^-. The color change was the most prominent in 1:1 interaction with OH^-; and in 3:1 interactions with OAc^- and CN^-. Addition of both OAc^- and CN^- caused a decrease in the first absorption band below 300 nm. But CN^- caused an increase in the band at 319 nm possibly because of its stronger basicity. There wasn't any change in the UV-Vis spectrum of **34** with OH^- despite the color change it shows. The rest of the anions F^-, Cl^-, Br^-, I^-, $H_2PO_4^-$, HSO_4^- and NO_3^- didn't cause any changes in either color or UV-Vis spectra of **34**.

Figure 39: Colors of DMSO solutions of pure **34** and upon addition of 3:1, 1:1 and 1:3 mole ratios of F^- from left to right
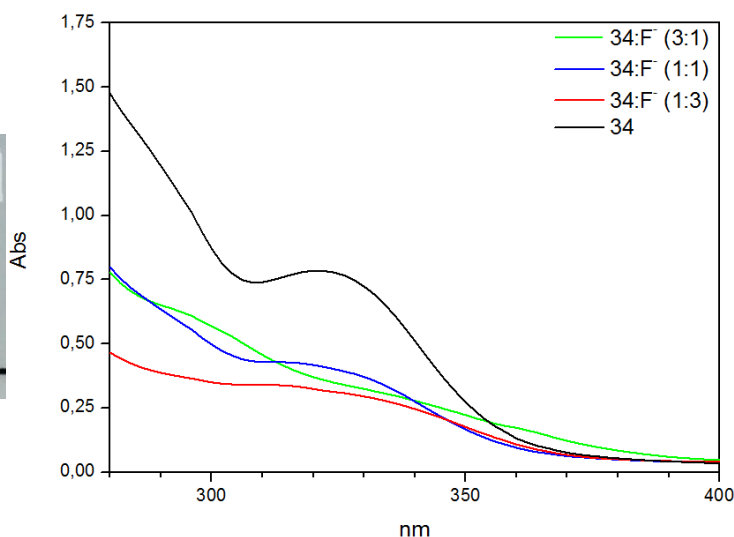
34 + F^-

Figure 40: Colors of DMSO solutions of pure **34** and upon addition 3:1, 1:1 and 1:3 mole ratios of Cl^- from left to right
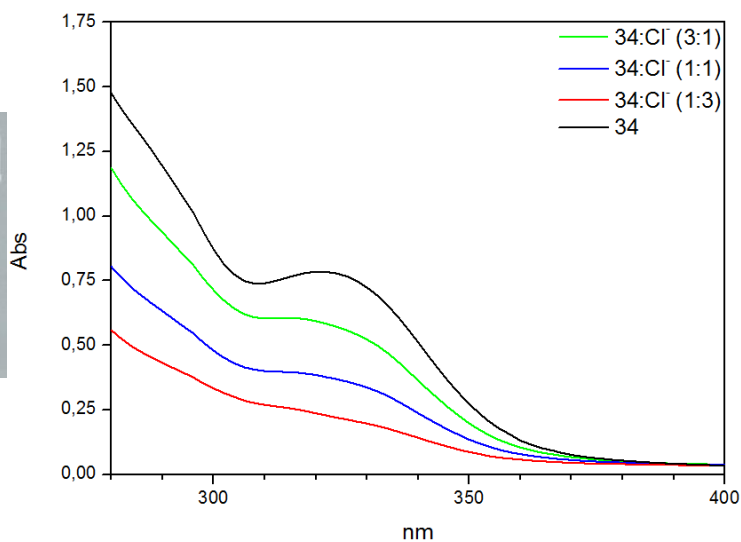
34 + Cl^-
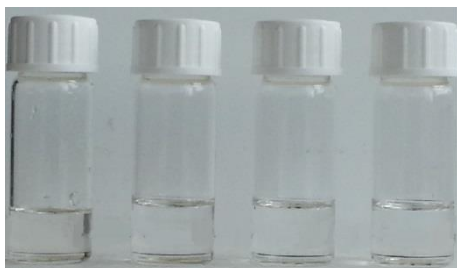
Figure 41: Colors of DMSO solutions of pure **34** and upon addition of 3:1, 1:1 and 1:3 mole ratios of Br⁻ from left to right
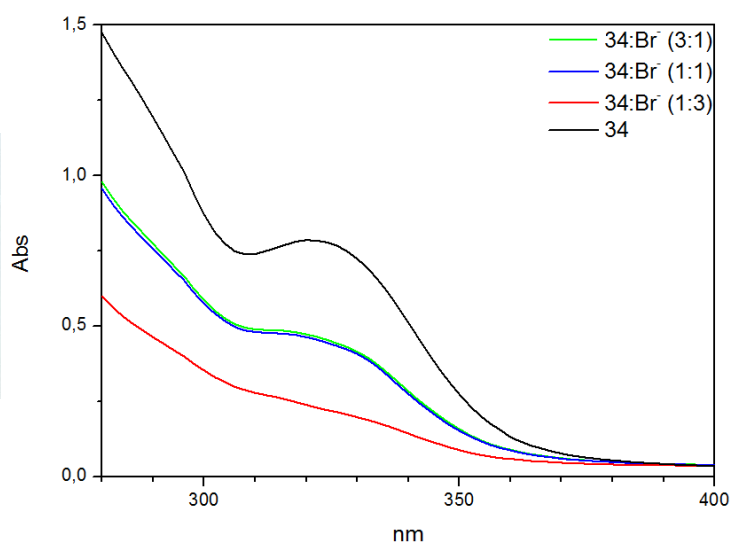
34 + Br⁻
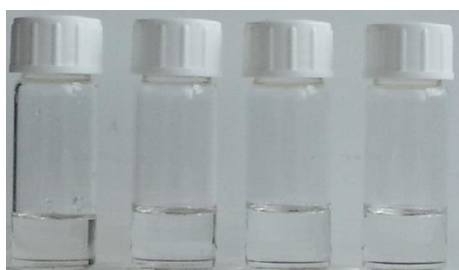
Figure 42: Colors of DMSO solutions of pure **34** and upon addition of 3:1, 1:1 and 1:3 mole ratios of I⁻ from left to right
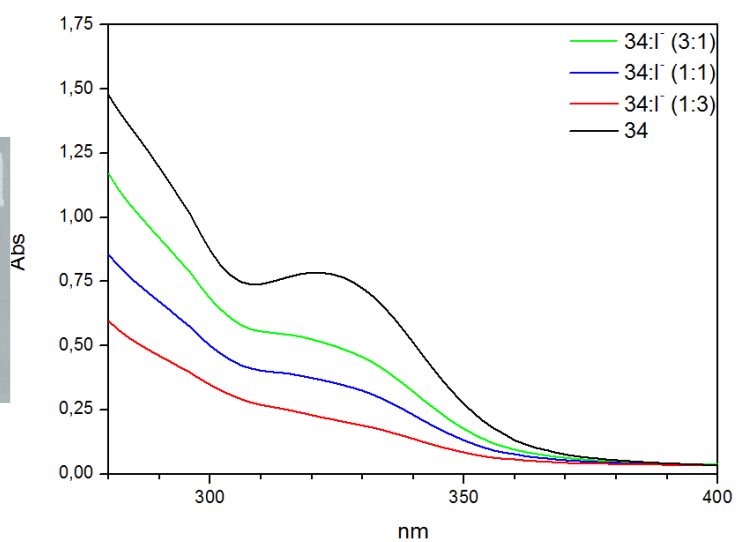
34 + I⁻

Figure 43: Colors of DMSO solutions of pure **34** and upon addition of 3:1, 1:1 and 1:3 mole ratios of OH⁻ from left to right
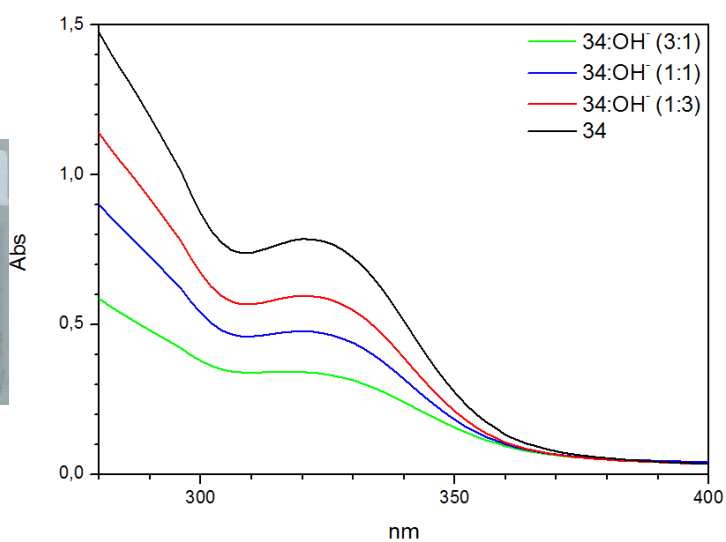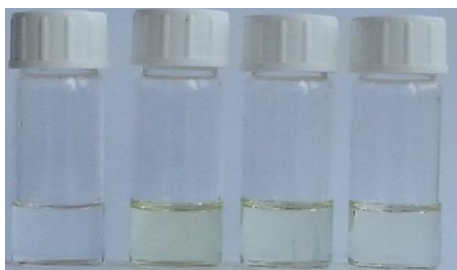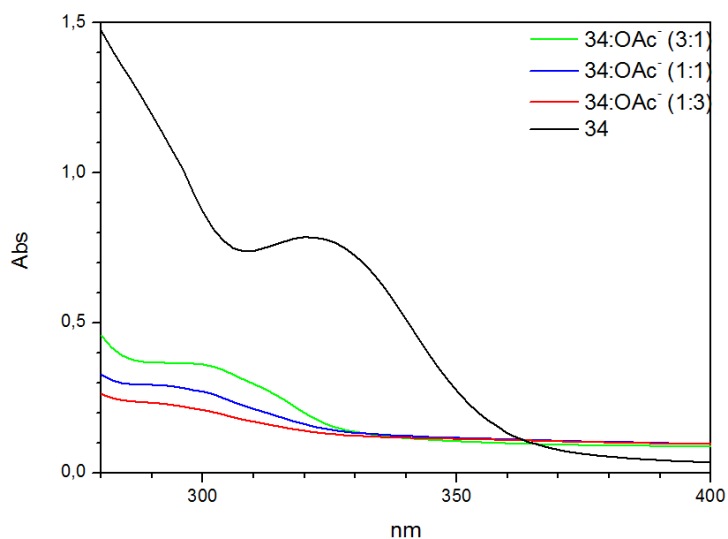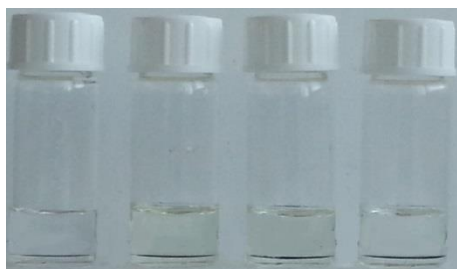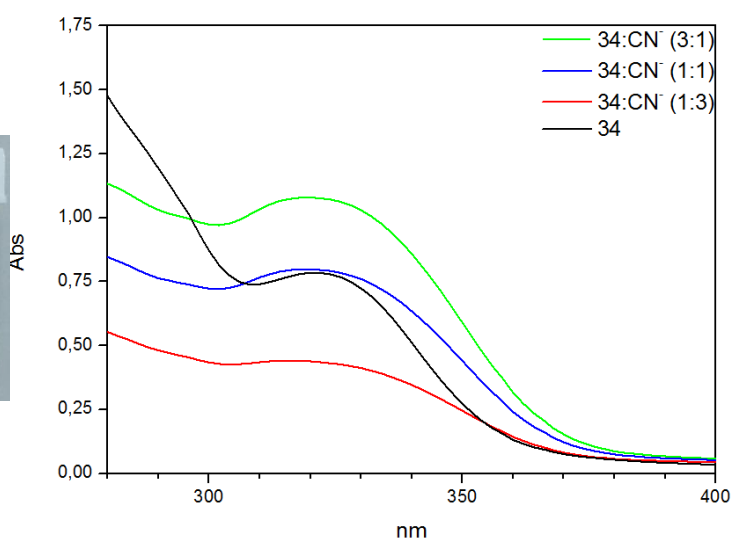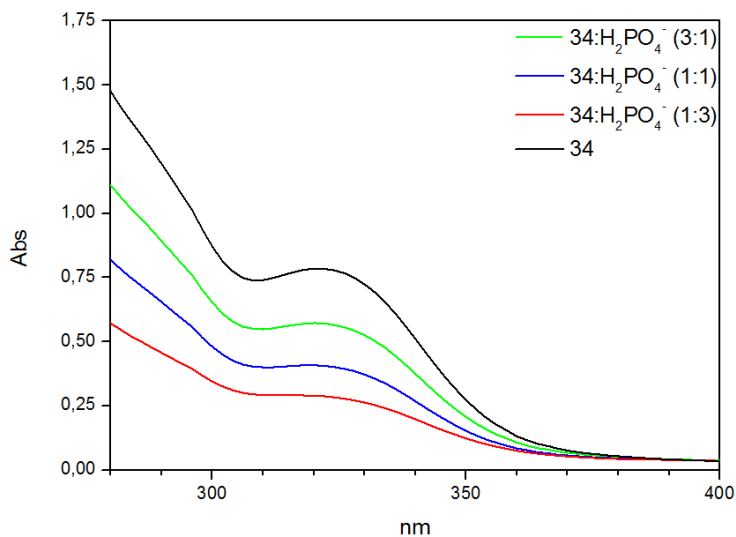
34 + OH⁻

Figure 44: Colors of DMSO solutions of pure **34** and upon addition of 3:1, 1:1 and 1:3 mole ratios of OAc⁻ from left to right

34 + OAc⁻

Figure 45: Colors of DMSO solutions of pure **34** and upon addition of 3:1, 1:1 and 1:3 mole ratios of CN⁻ from left to right

34 + CN⁻

Figure 46: Colors of DMSO solutions of pure **34** and upon addition of 3:1, 1:1 and 1:3 mole ratios of $H_2PO_4^-$ from left to right
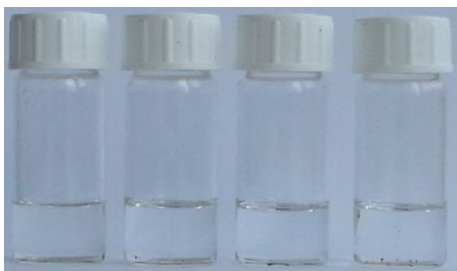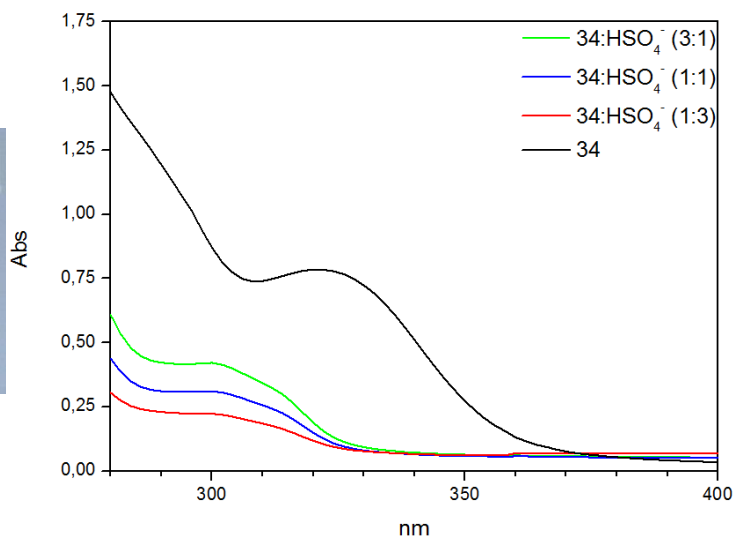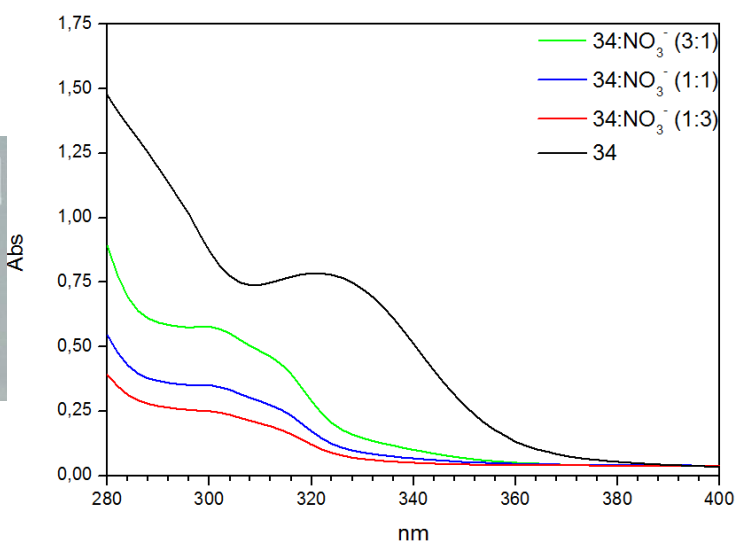
34 + $H_2PO_4^-$

Figure 47: Colors of DMSO solutions of pure **34** and upon addition of 3+1 eq., 1+1 eq.,1+3 eq. of HSO_4^- from left to right


34 + HSO_4^-

Figure 48: Colors of DMSO solutions of pure **34** and upon addition of 3:1, 1:1 and 1:3 mole ratios of NO_3^- from left to right

34 + NO_3^-

Results of ^{1}H NMR studies of **34** were somewhat different than color observations and UV-Vis titrations. The additions of OH^- and OAc^- caused both NH peaks of the sensor to disappear, which indicates deprotonation. Additions of F^-, CN^- and $H_2PO_4^-$ caused the peaks to flatten to almost disappearance, which shows strong hydrogen bonding with the sensor. Upon the addition of Cl^- and I^-, the intensities of both NH peaks of **34** slightly decreased. The decrease was more prominent for I^-, possibly becasue of its greater size that matches the geometry of the sensor better. The remaining anions Br^-, HSO_4^- and NO_3^- didn't cause any changes in the ^{1}H NMR spectrum of **34**.
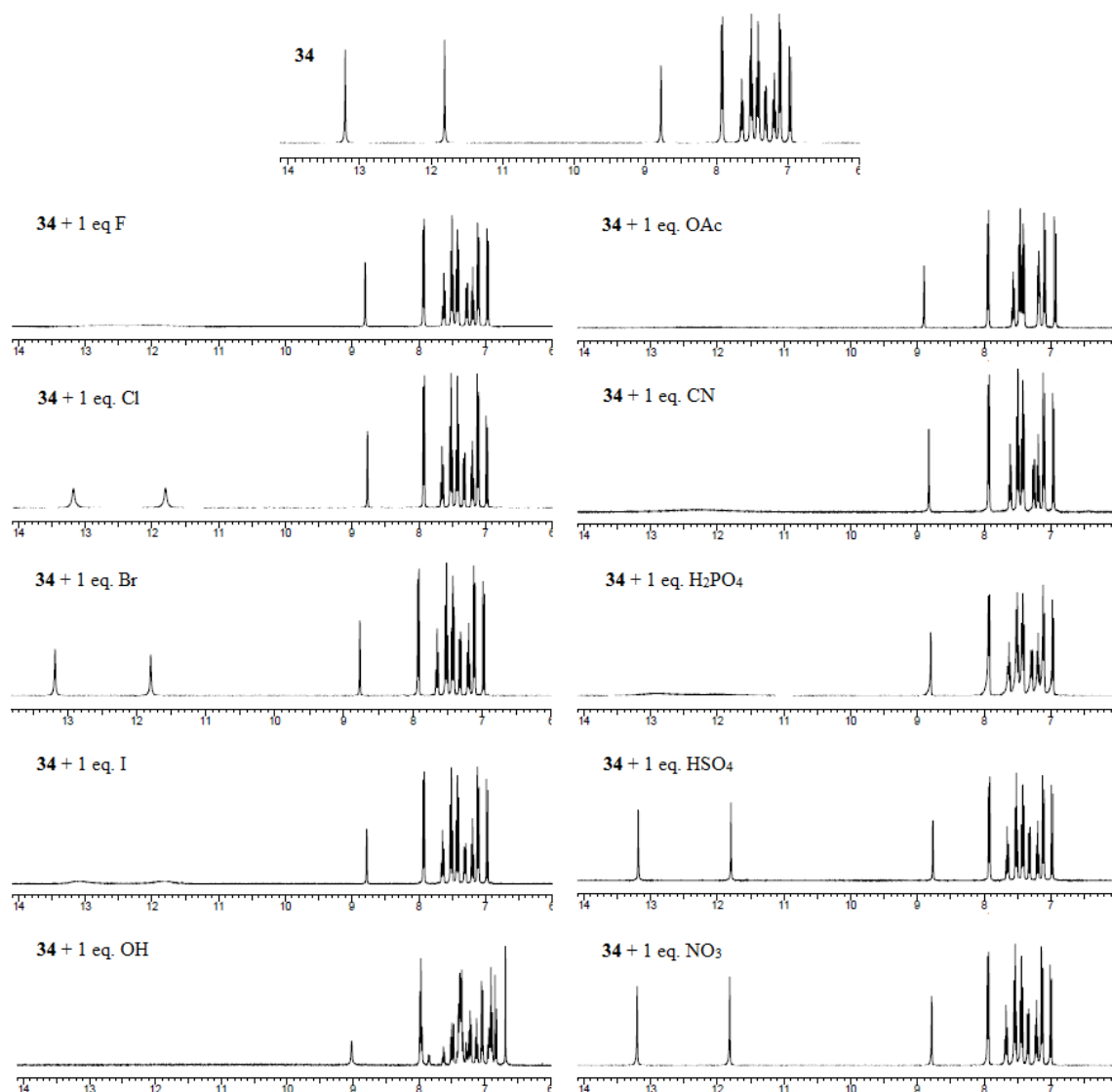
Scheme 2: Partial ^{1}H NMR spectra of **34** upon interaction with 1:1 ratio of anions

Overall, **34** showed no selectivity towards any anion that is monitored by ^{1}H NMR analysis or color changes. The unique change of the UV-Vis absorption pattern of of the sensor towards acetate anion was not suitable for quantitative analysis, so it cannot be used as a practical sensor for acetate. Other anions didn't yield any changes in the sensor's absorption spectra.

3.2.3. *N*-(5-Chloro-2-phenoxyphenyl)-*N'*-(4-nitrobenzoyl)thiourea (35)

In the case of compound **35**, addition of each of the chosen anions caused a new absorption maxima in UV-Vis spectra at 290 nm. The addition of F^-, OAc^-, CN^- and $H_2PO_4^-$ caused the color of the solution of **35** from colorless to a very light yellow which accompanied the appearance of a new absorption band at around 360 nm. The color change was the most prominent for 1:3 interaction, and the new absorption band was first seen with 1:1 interaction in the case of fluoride anion. For OAc^-, CN^- and $H_2PO_4^-$, the most prominent color change and the new absorption band in UV-Vis spectra were observed for 3:1 interactions of host and anion. The rest of the anions Cl^-, Br^-, I^-, OH^-, HSO_4^- and NO_3^- didn't cause any changes in either color or UV-Vis spectra of **35**.

Figure 49: Colors of DMSO solutions of pure **35** and upon addition of 3:1, 1:1 and 1:3 mole ratios of F^- from left to right
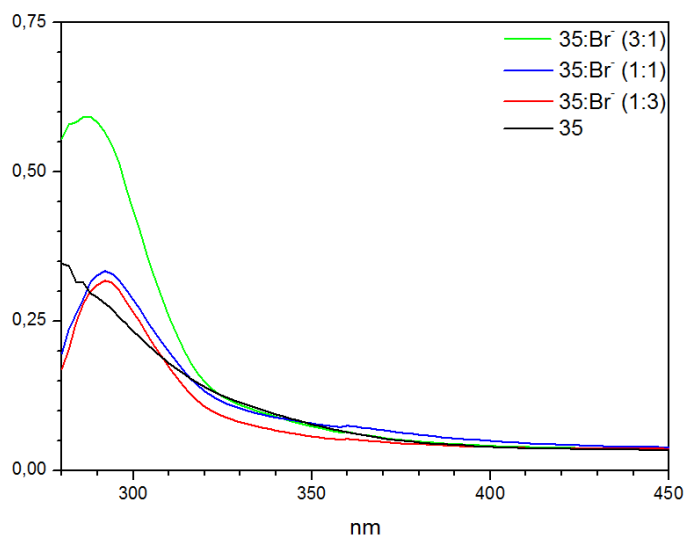

35 + F^-
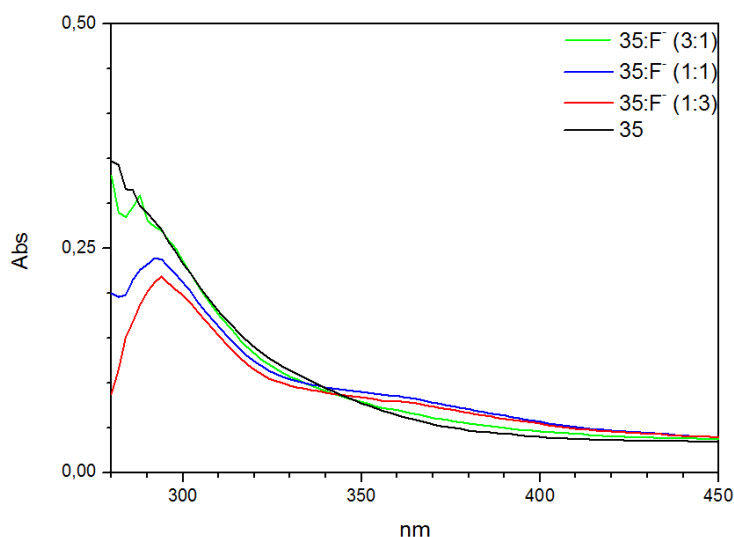
Figure 50: Colors of DMSO solutions of pure **35** and upon addition of 3:1, 1:1 and 1:3 mole ratios of Cl^- from left to right
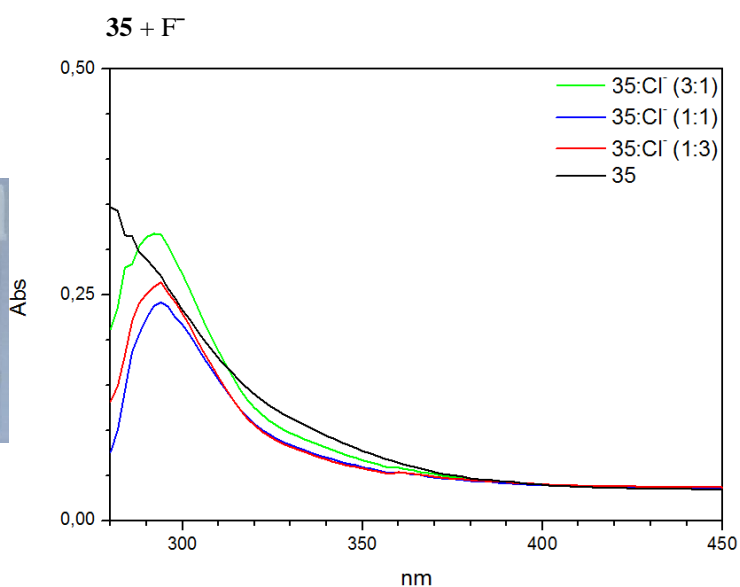
35 + Cl^-

Figure 51: Colors of DMSO solutions of pure **35** and upon addition of 3:1, 1:1 and 1:3 mole ratios of Br⁻ from left to right
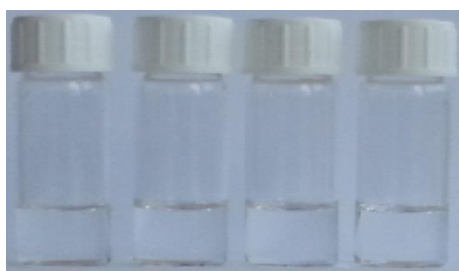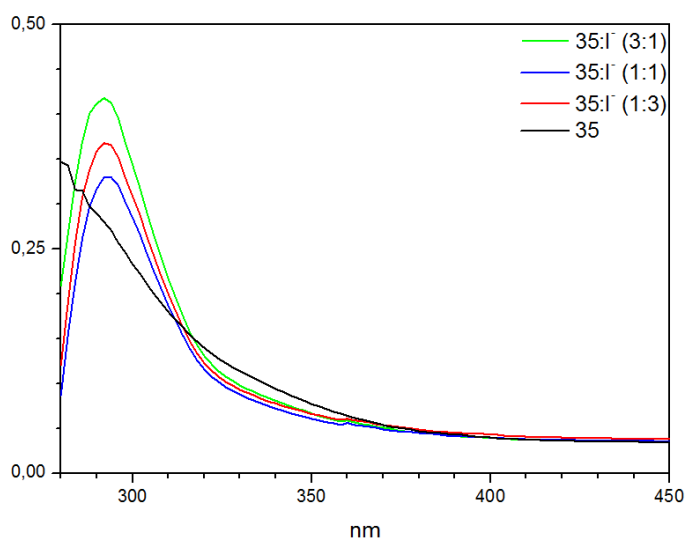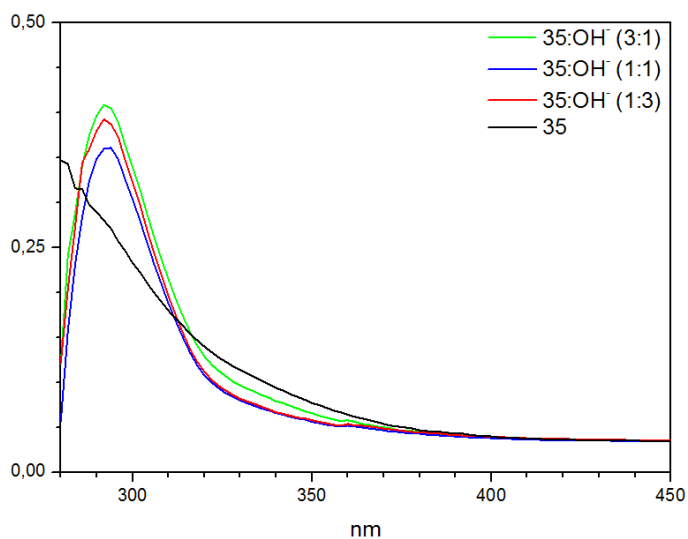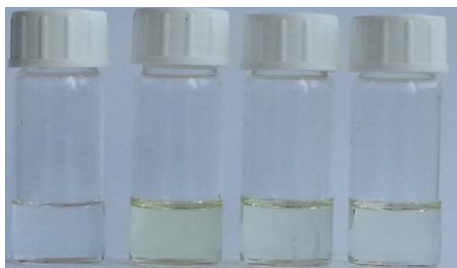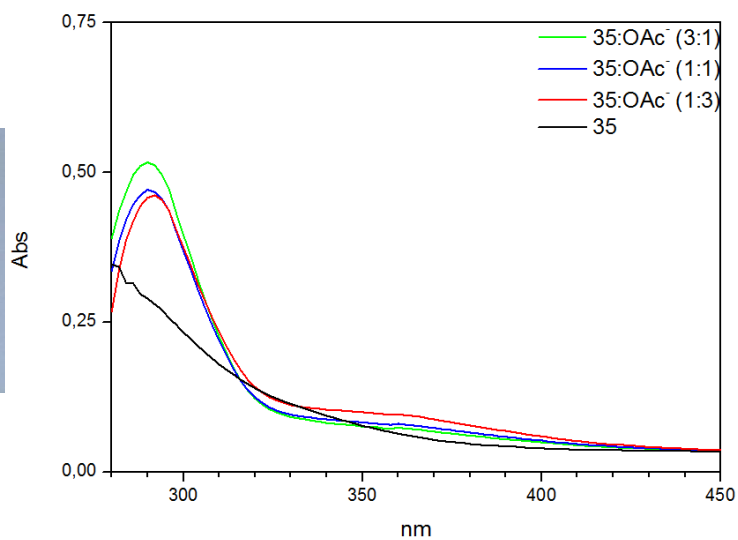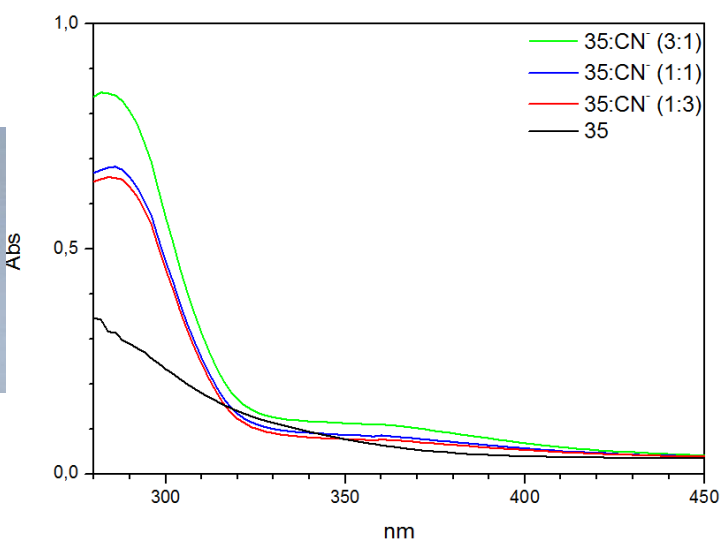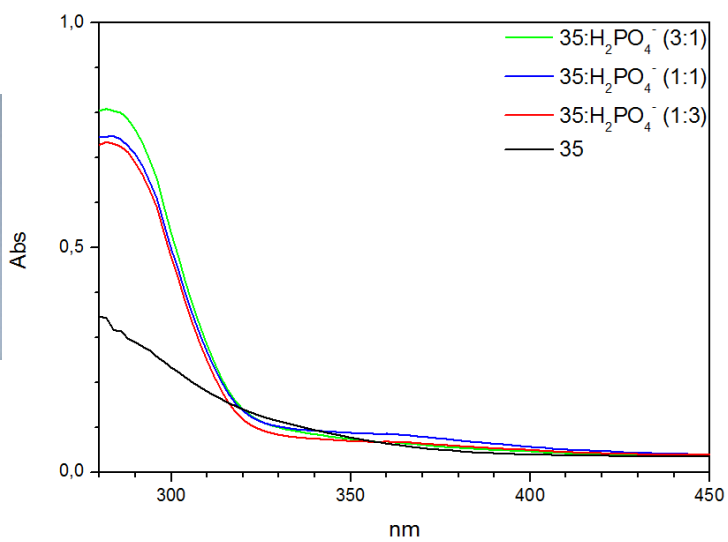
35 + Br⁻

Figure 52: Colors of DMSO solutions of pure **35** and upon addition of 3:1, 1:1 and 1:3 mole ratios of I⁻ from left to right

35 + I⁻

Figure 53: Colors of DMSO solutions of pure **35** and upon addition of 3:1, 1:1 and 1:3 mole ratios of OH⁻ from left to right

35 + OH⁻

Figure 54: Colors of DMSO solutions of pure **35** and upon addition of 3:1, 1:1 and 1:3 mole ratios of OAc⁻ from left to right

35 + OAc⁻

Figure 55: Colors of DMSO solutions of pure **35** and upon addition of 3:1, 1:1 and 1:3 mole ratios of CN⁻ from left to right
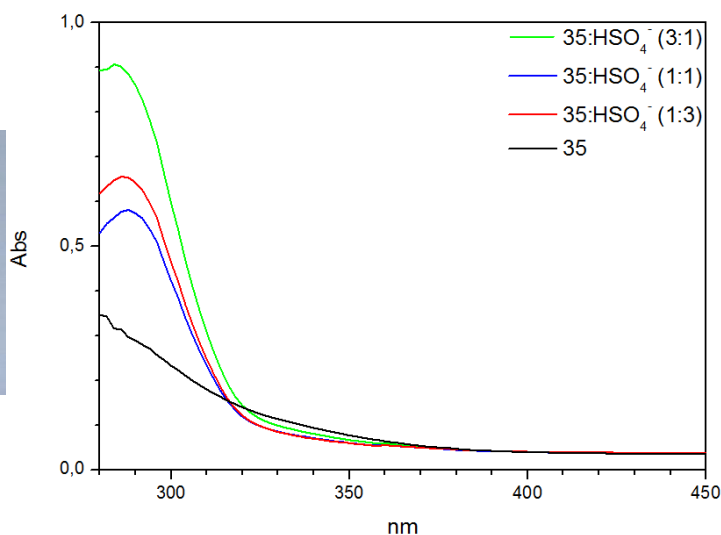
35 + CN⁻

Figure 56: Colors of DMSO solutions of pure **35** and upon addition of 3:1, 1:1 and 1:3 mole ratios of $H_2PO_4^-$ from left to right
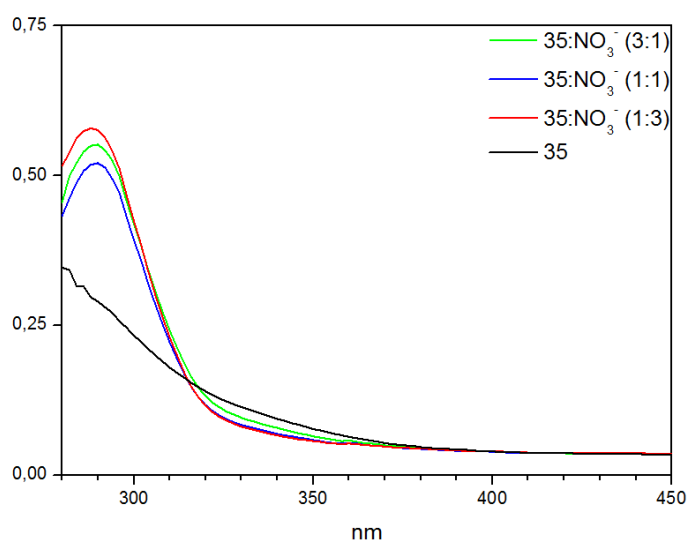
35 + $H_2PO_4^-$

Figure 57: Colors of DMSO solutions of pure **35** and upon addition of 3:1, 1:1 and 1:3 mole ratios of HSO_4^- from left to right

35 + HSO_4^-

Figure 58: Colors of DMSO solutions of pure **35** and upon addition of 3:1, 1:1 and 1:3 mole ratios of NO_3^- from left to right

35 + NO_3^-

The data obtained from ^{1}H NMR analysis confirmed the observances made by comparing the colors of the solutions and UV-Vis spectra. Addition of 1:1 mole ratios of F^-, OAc^-, CN^- and $H_2PO_4^-$ caused both NH peaks of **35** to broaden and their intensities to decrease in their ^{1}H NMR spectra. Both NH peaks disappeared upon the addition of OH^-, which proves that both NH protons were fully deprotonated by the strongly basic hydroxyl anion. The rest of the anions; Cl^-, Br^-, I^-, HSO_4^- and NO_3^- didn't cause any change in the ^{1}H NMR spectrum of **35**, possibly because of low charge density and/or mismatching geometry.

To sum up, addition of any anion seemed to cause hydrogen bonds with varying strengths, which was proven by the bathochromic shifts of the main absorption band in the UV-Vis spectra and slight downfield shifts of NH peaks of the sensor. Addition of F^-, OAc^-, CN^-

and $H_2PO_4^-$ on the other hand caused the formation of detectable complexes by ^1H NMR and UV-Vis spectroscopy without any specific sensitivity to one. The color analysis was ineffective because all the colored complexes were similar to each other and it was not possible to distinguish which anion was present in the solution by looking at the color.
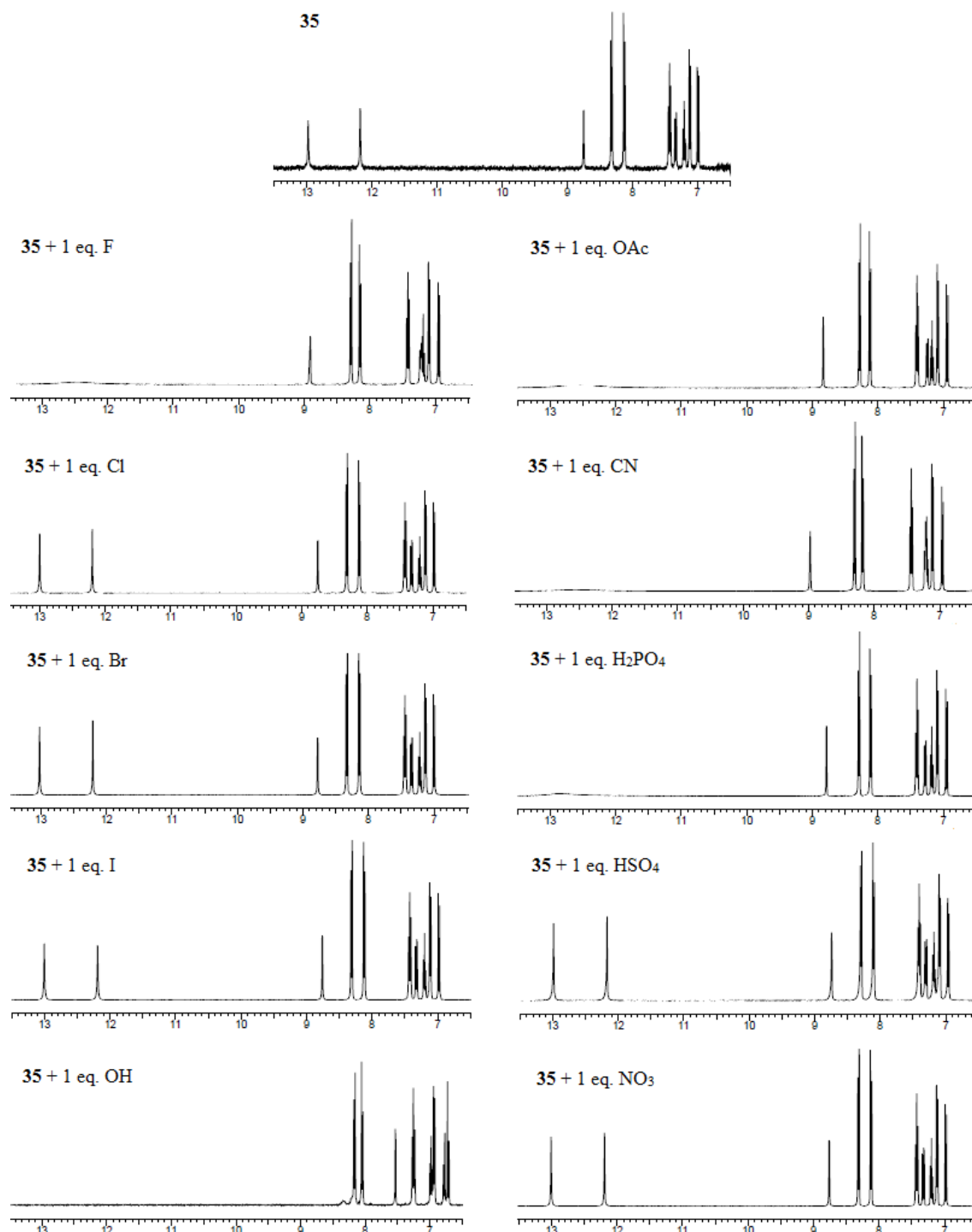
Scheme 3: Partial ^1H NMR spectra of **35** upon interaction with 1:1 ratios of anions

3.2.4. *N*-(5-Chloro-2-phenoxyphenyl)-*N'*-(3,5-dinitrobenzoyl)thiourea (36)

DMSO solution of compound **36** turned from very light yellow to dark yellow upon addition of 3:1 ratios of F⁻. The color of the 1:1 complex was somewhat lighter, but after adding 1:3 ratios of F⁻, the color of the solution turned dark purple. UV-Vis titrations of **36**+F⁻ showed that a bathochromic shift upon addition of F⁻. Addition of OH⁻ caused a similar change in the color of solutions of **36**, but with a lighter shade of purple. The color of the solution turned to a darker yellow when acetate anion was added. Both OH⁻ and OAc⁻ additions caused the same bathochromic shift to appear in UV-Vis titrations, but for those two anions, the band appeared after reaching 1:1 host-anion ratio. The addition of CN⁻ caused a striking color change immediately first to orange, and then to dark purple for 1:1 complexation. After 15 minutes, the purple solutions turned to red and did not change further, which indicates that an equilibrium was reached. UV-Vis analysis of these solutions showed that a new band at around 540 nm had appeared in addition to the one at around 410 nm. Addition of $H_2PO_4^-$ also showed a color change from very light yellow to dark yellow, but no change was observed in UV-Vis titrations with hydrogen phosphate anion, which might be caused by the dependance of the forming complex to concentration. The remaining anions Cl⁻, Br⁻, I⁻, HSO_4^- and NO_3^- didn't cause any changes in the color of the host solutions or in its UV-Vis spectra.
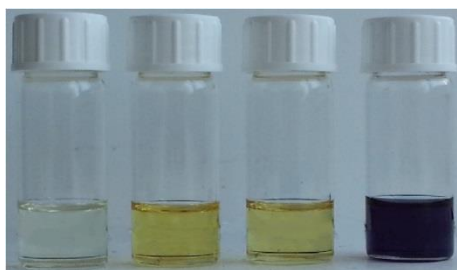

Figure 59: Colors of DMSO solutions of pure **36** and upon addition of 3:1, 1:1 and 1:3 mole ratios of F⁻ from left to right
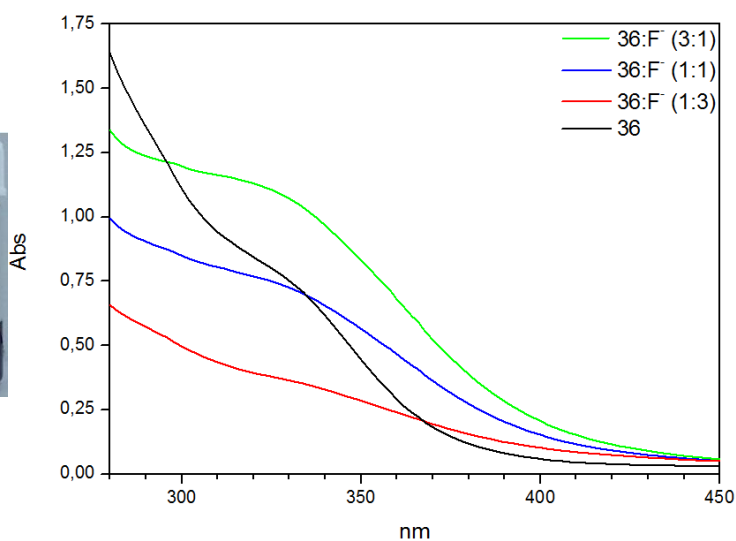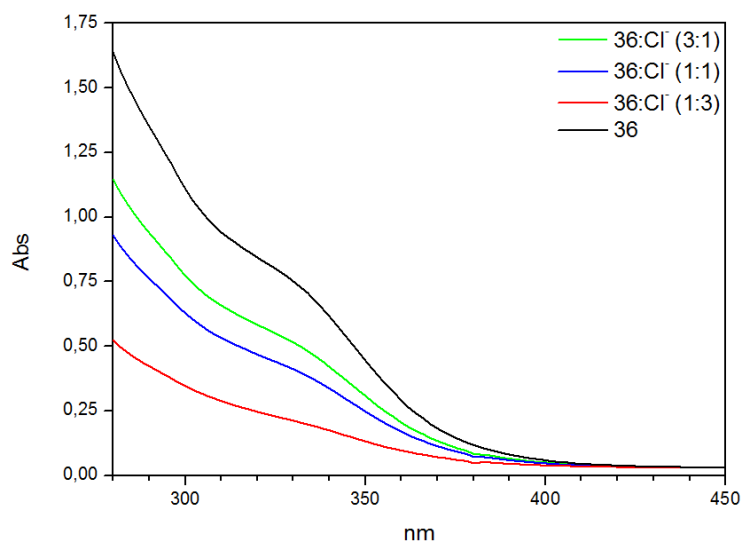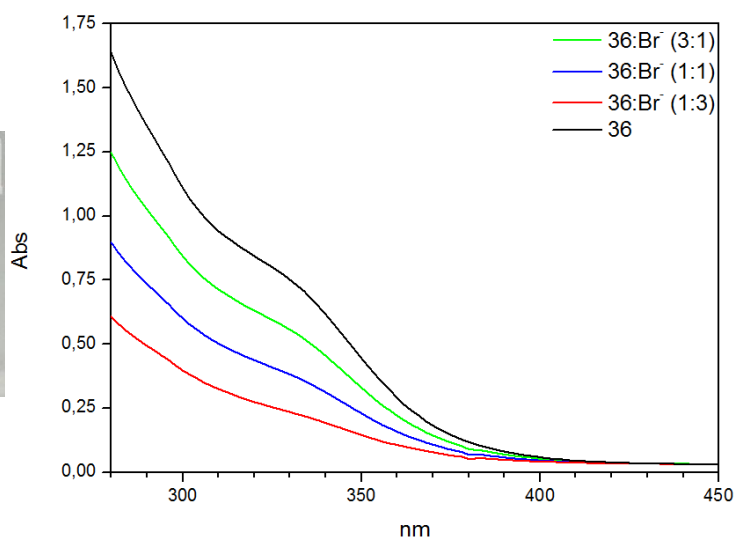
36 + F⁻

Figure 60: Colors of DMSO solutions of pure **36** and upon addition of 3:1, 1:1 and 1:3 mole ratios of Cl⁻ from left to right
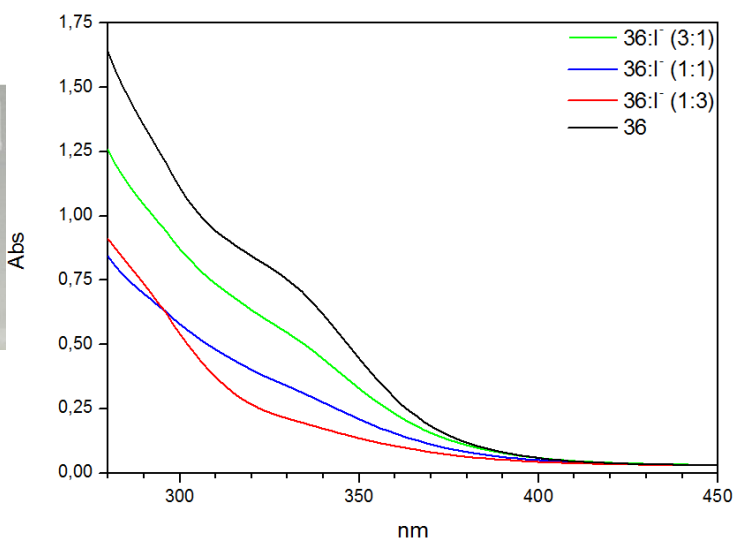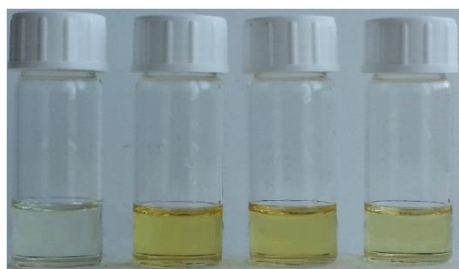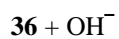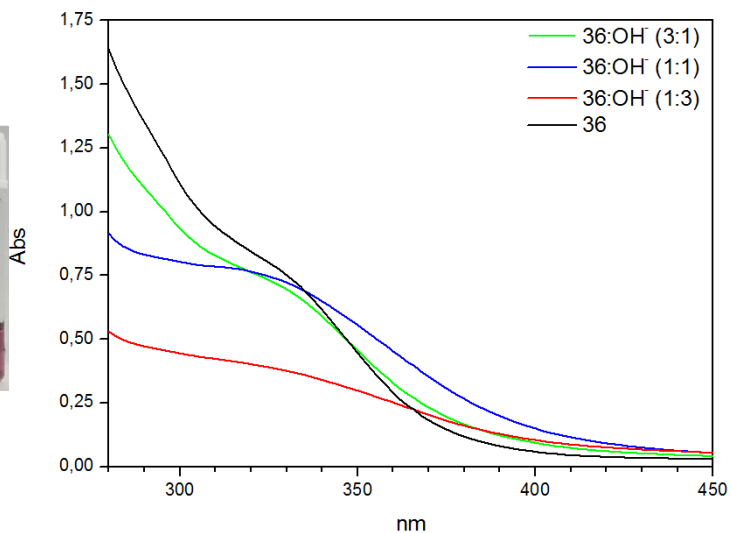
36 + Cl⁻

Figure 61: Colors of DMSO solutions of pure **36** and upon addition of 3+1 eq., 1+1 eq.,1+3 eq. of Br⁻ from left to right

36 + Br⁻

Figure 62: Colors of DMSO solutions of pure **36** and upon addition of 3:1, 1:1 and 1:3 mole ratios of I⁻ from left to right

36 + I⁻

Figure 63: Colors of DMSO solutions of pure **36** and upon addition of 3:1, 1:1 and 1:3 mole ratios of OH⁻ from left to right

36 + OH⁻

Figure 64: Colors of DMSO solutions of pure **36** and upon addition of 3:1, 1:1 and 1:3 mole ratios of OAc⁻ from left to right
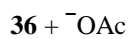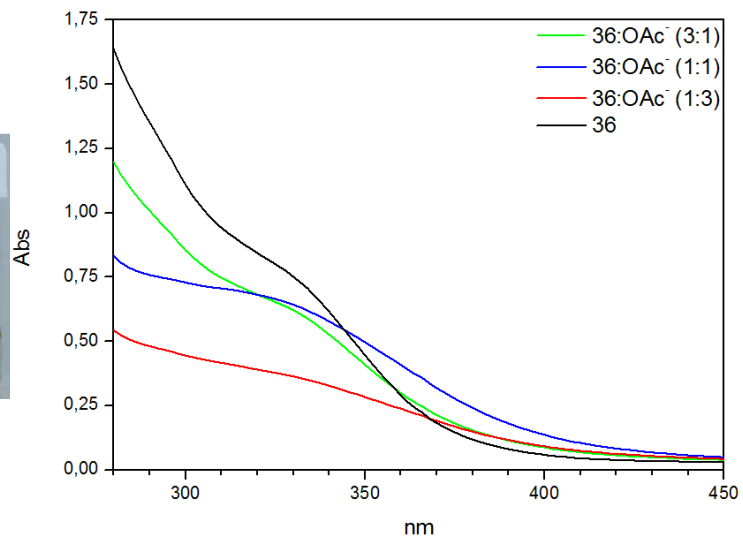

36 + ⁻OAc

Figure 65: Colors of DMSO solutions of pure **36** and upon addition of 3:1, 1:1 and 1:3 mole ratios of CN⁻ right after the addition from left to right
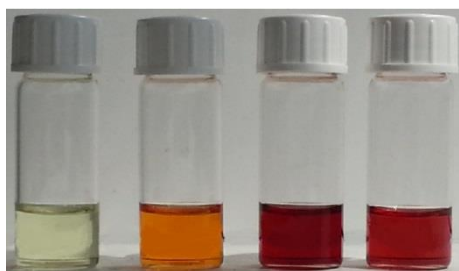

Figure 66: Colors of DMSO solutions of pure **36** and upon addition of 3+1 eq., 1+1 eq., 1+3 eq. of CN⁻ 15 min after the addition from left to right
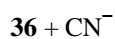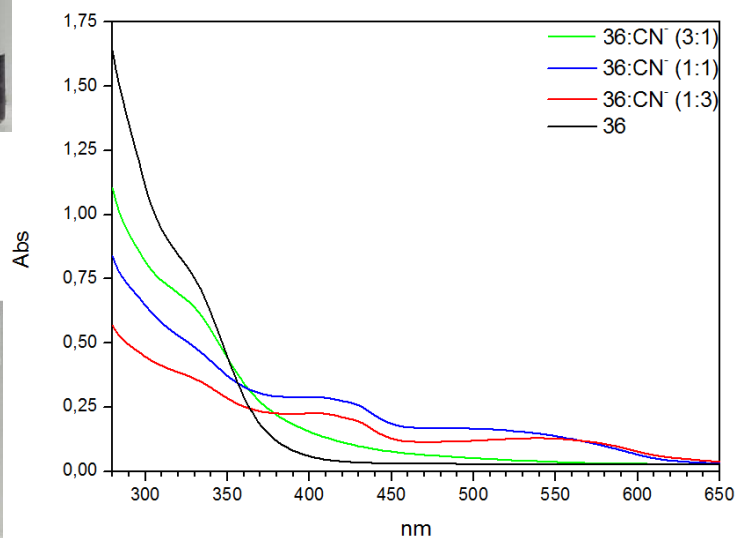

36 + CN⁻

Figure 67: Colors of DMSO solutions of pure **36** and upon addition of 3:1, 1:1 and 1:3 mole ratios of $H_2PO_4^-$ from left to right from left to right
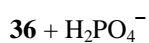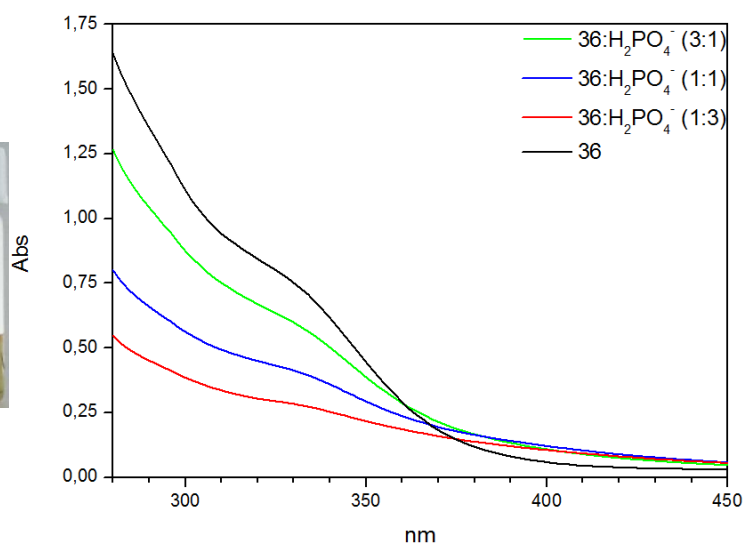

36 + $H_2PO_4^-$

Figure 68: Colors of DMSO solutions of pure **36** and upon addition of 3:1, 1:1 and 1:3 mole ratios of HSO_4^- from left to right
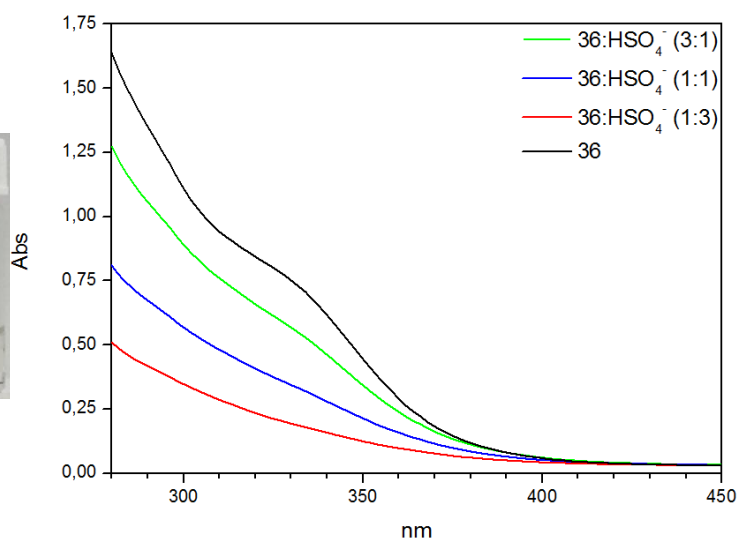
36 + HSO_4^-
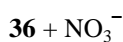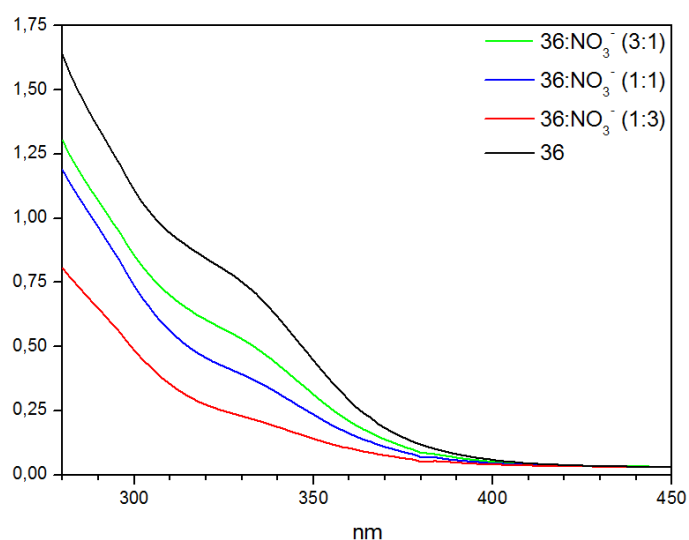

Figure 69: Colors of DMSO solutions of pure **36** and upon addition of 3:1, 1:1 and 1:3 mole ratios of NO_3^- from left to right

36 + NO_3^-

Results of ^{1}H NMR analyses were parallel to UV-Vis titrations. Upon addition of 1+1 eq. of F^- and $H_2PO_4^-$, the first NH peak disappeared and the second was broadened to almost disappearance for each anion. The strongly basic OH^- deprotonated both NH moieties, which is proved by the disappearance of both NH peaks from the spectrum. Addition of OAc^- caused both NH peaks to significantly broaden, which indicates the hydrogen bonding interaction between **36** and acetate anion. Lastly, in the presence of CN^-, the first NH peak shrank significantly and the second disappeared. The rest of the anions Cl^-, Br^-, I^-, HSO_4^- and NO_3^- didn't cause any changes in compound's ^{1}H NMR spectrum.
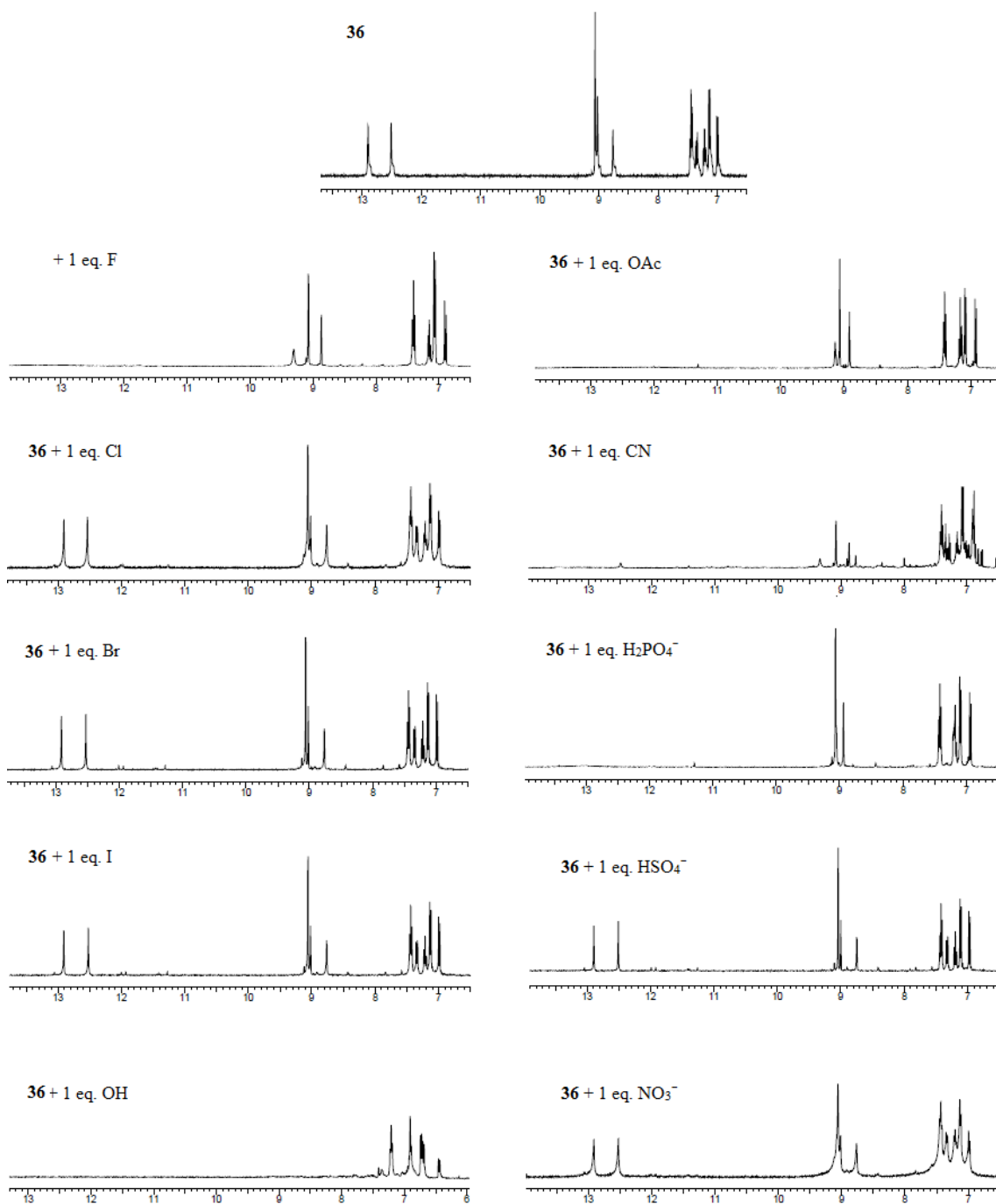
Scheme 4: Partial ^{1}H NMR spectra of **36** upon interaction with 1:1 ratios of anions

Compound **36** displayed a very distinct and intense color change upon addition of F⁻, OH⁻, OAc⁻ and CN⁻. All the colors were somewhat similar, and after the systems had reach equilibrium, some differences in the shade of the colors were observed, which were not very distinct for a good sensor, since every eye can define the color they see differently. The final color of host-CN⁻ complex was red in color, which was significantly different than others. Also the UV-Vis titrations showed that a new unique absorption band appeared upon complexation compared to other anions, which showed that **36** is a selective sensor for CN⁻, for which the recognition can be monitored by UV-Vis spectroscopy or by naked-eye observation of the color changes.

3.2.5. *N*-(Biphenyl-4-ylcarbamothioyl)-3,5-dinitrobenzamide (37)

Color of the DMSO solution of **37** shifted from light yellow to a darker yellow, orange and then to red upon addition of F⁻. A new band at 303 nm accompanied this change at 3:1 host-anion interaction. Addition of 1:3 mole ratios of fluoride caused two new bands to form at 431 nm and in addition to the one at around 600 nm. The addition of OH⁻ turned the solution of **37** to orange, light orange, and then yellow at the end. When an excess of anion was added, the solution turned to dark purple. The UV-Vis spectra showed no change up to the addition of 1:3 mole ratio of, at which the absorption band of **37** flattens. Addition of $H_2PO_4^-$ results in the same behavior both in their UV-Vis spectra and colorwise. Upon the addition of OAc⁻, the color of the solution turns to orange, light orange and then to dark yellow at the end. UV-Vis titrations showed the appearance of a new band at 305 nm. Addition of CN⁻ also resulted in a color change to red, dark orange and then orange. However, no changes were observed in their UV-Vis spectra, apart from a slight flattening, which may be a result of the distruption of hydrogen bonds upon dilution while preparing the UV-Vis analytes. Addition of Cl⁻ caused a slight color change for 1:3 complex, but no changes were observed during UV-Vis titrations. The rest of the anions Cl⁻, Br⁻, I⁻, HSO_4^- and NO_3^- didn't cause any changes in the color of the host solutions or in its UV-Vis spectra.

Figure 70: Colors of DMSO solutions of pure **37** and upon addition of 3:1, 1:1 and 1:3 mole ratios of F⁻ from left to right
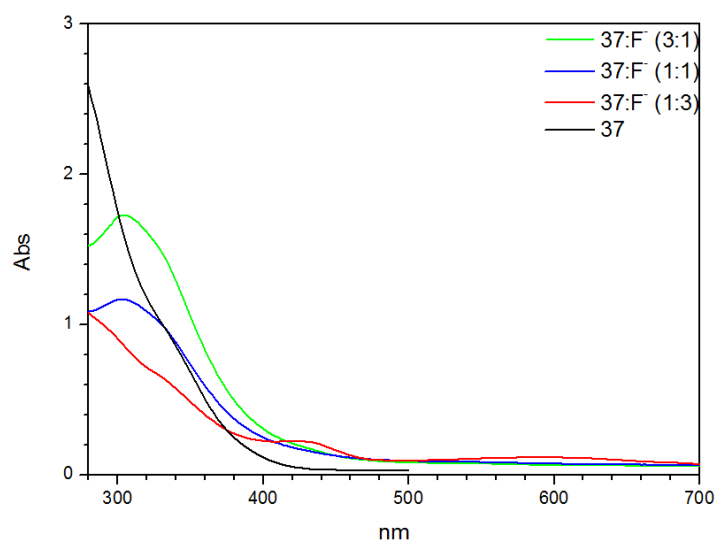
37 + F⁻

Figure 71: Colors of DMSO solutions of pure **37** and upon addition of 3:1, 1:1 and 1:3 mole ratios of Cl⁻ from left to right
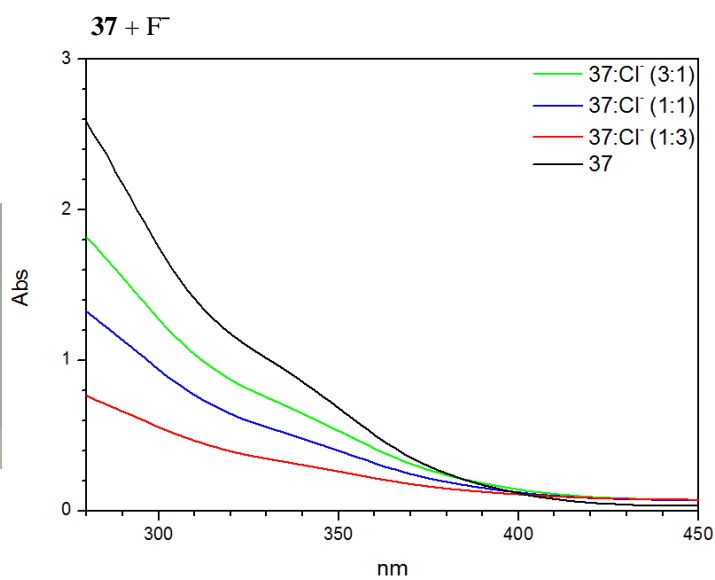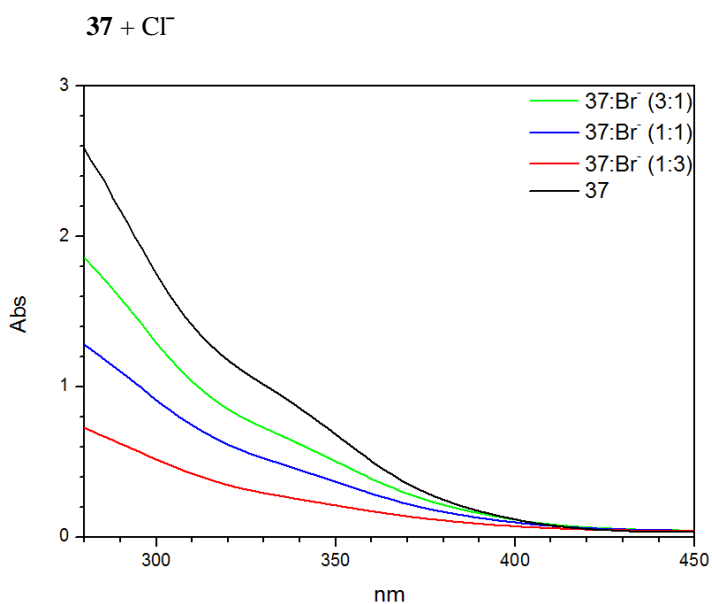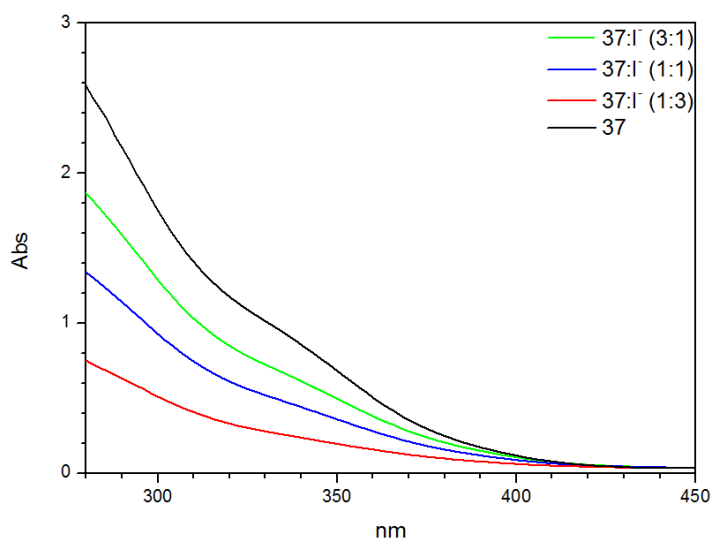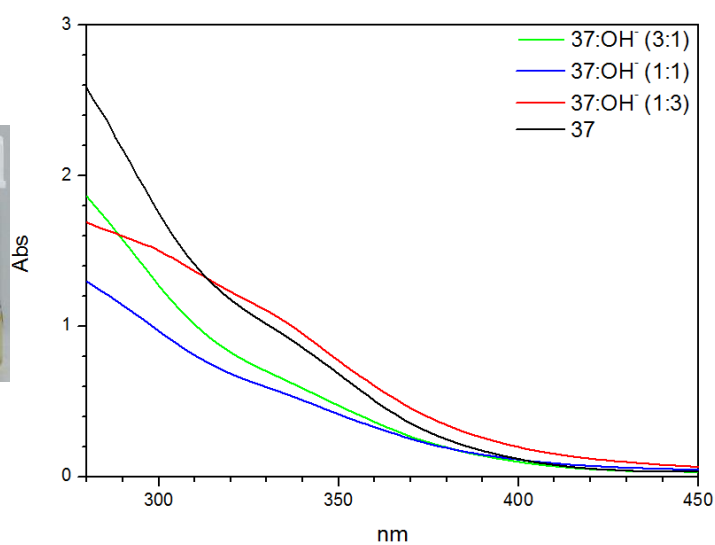
37 + Cl⁻

Figure 72: Colors of DMSO solutions of pure **37** and upon addition of 3:1, 1:1 and 1:3 mole ratios of Br⁻ from left to right

37 + Br⁻

Figure 73: Colors of DMSO solutions of pure **37** and upon addition of 3+1 eq., 1+1 eq.,1+3 eq. of I¯ from left to right
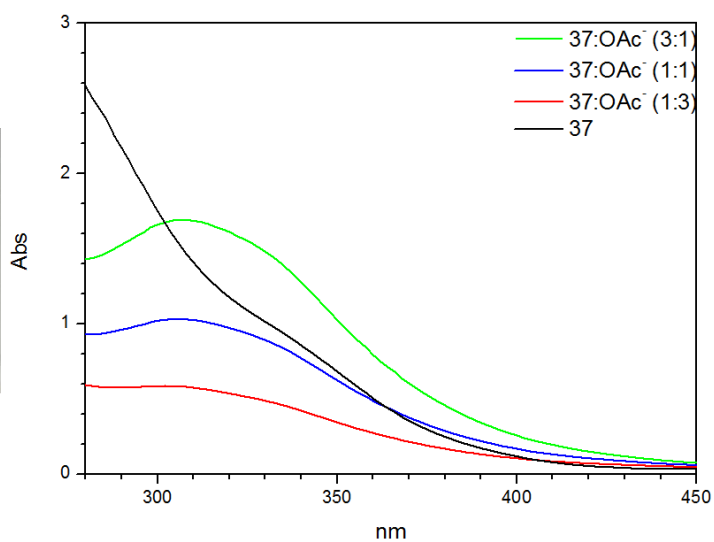
37 + I¯

Figure 74: Colors of DMSO solutions of pure **37** and upon addition of 3:1, 1:1 and 1:3 mole ratios and an excess of OH¯ from left to right
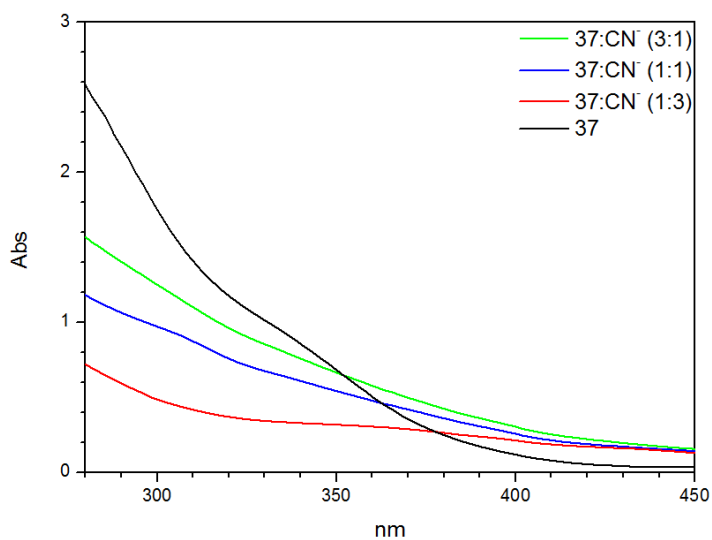
37 + OH¯

Figure 75: Colors of DMSO solutions of pure **37** and upon addition of 3:1, 1:1 and 1:3 mole ratios of OAc¯ from left to right
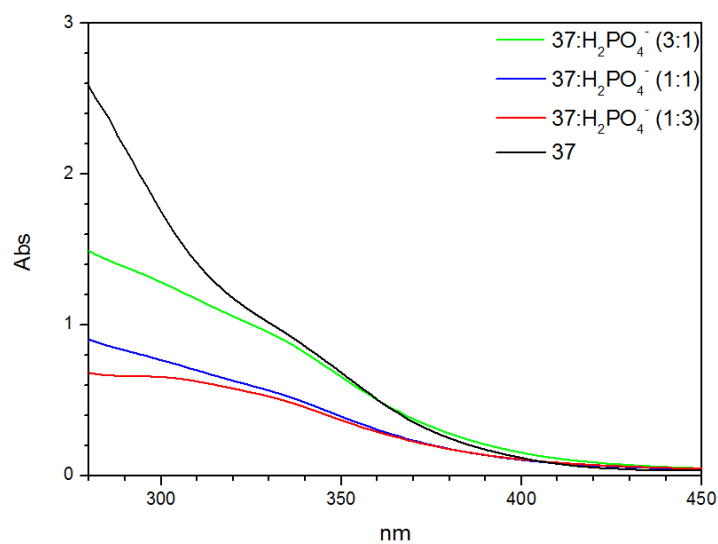
37 + OAc¯

Figure 76: Colors of DMSO solutions of pure **37** and upon addition of 3:1, 1:1 and 1:3 mole ratios of CN^- from left to right
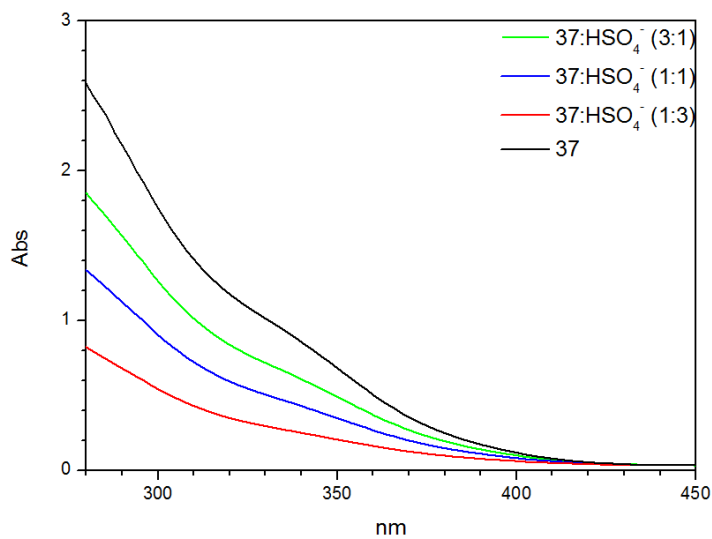
37 + CN^-

Figure 77: Colors of DMSO solutions of pure **37** and upon addition of 3:1, 1:1 and 1:3 mole ratios of $H_2PO_4^-$ from left to right
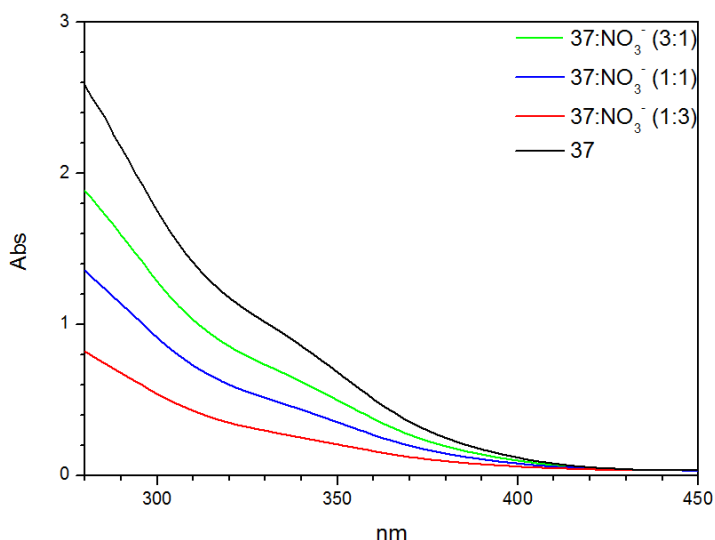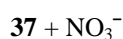
37 + $H_2PO_4^-$

Figure 78: Colors of DMSO solutions of pure **37** and upon addition of 3:1, 1:1 and 1:3 mole ratios of HSO_4^- from left to right

37 + HSO_4^-

Figure 79: Colors of DMSO solutions of pure **37** and upon addition of 3:1, 1:1 and 1:3 mole ratios of NO_3^- from left to right

37 + NO_3^-

The ^{1}H NMR analysis generally support the deductions made by observing the color of the solutions and by UV-Vis titrations. Addition of F^-, OH^-, OAc^-, CN^- and $H_2PO_4^-$ all caused both NH peaks of **37** to disappear, indicating the hydrogen bonding has let to deprotonation. There were two new peaks at about 16 ppm after addition of F^-, which might be related to the formation of H_2F^+ upon deprotonation. Both NH peak intensities slightly decreased upon addition of Cl^- and I^-, due to a weak hydrogen bonding interaction. The remaining anions Br^-, HSO_4^- and NO_3^- didn't cause a change in the ^{1}H NMR spectrum of **37**.
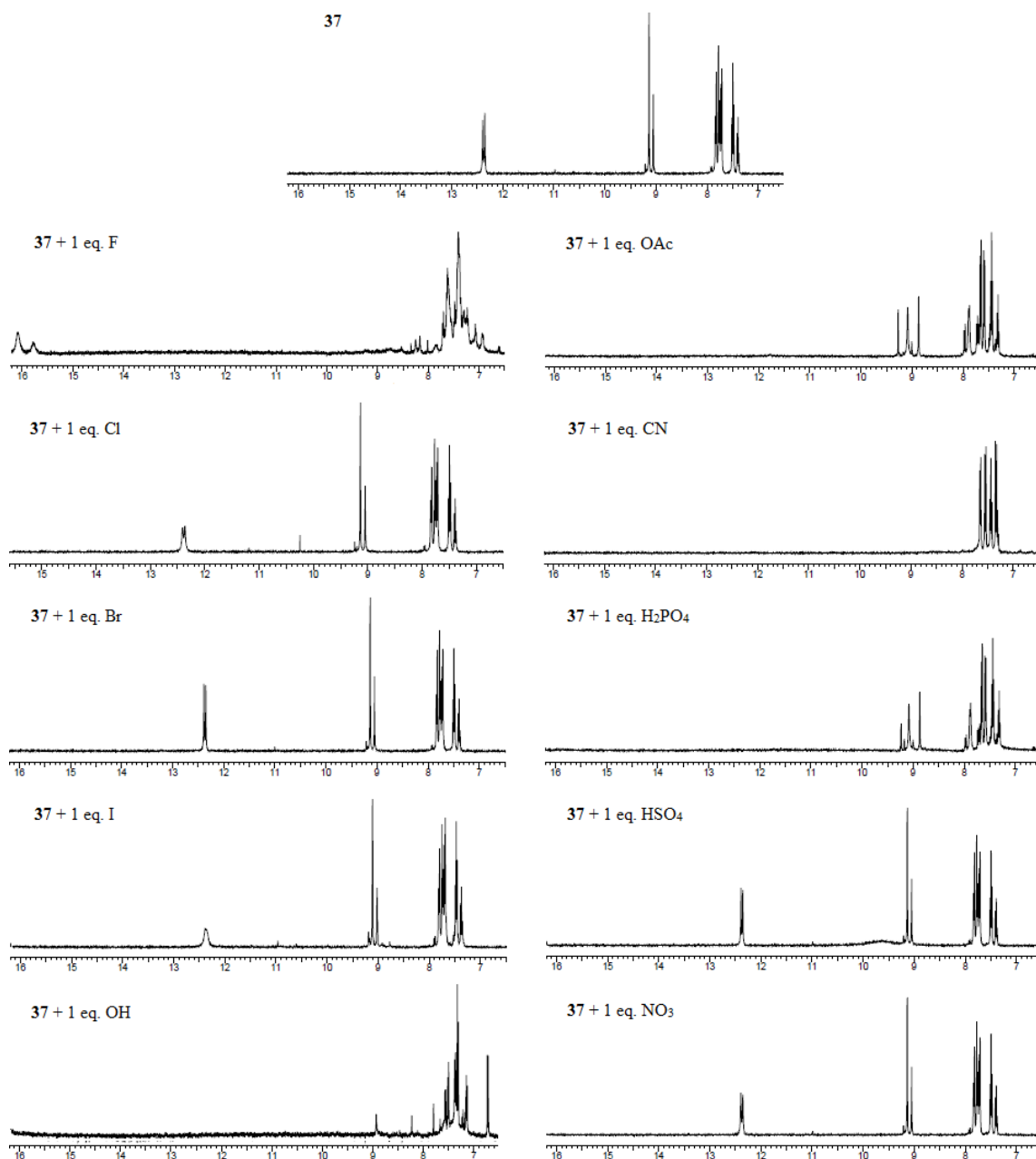
Scheme 5: Partial ^{1}H NMR spectra of **37** upon complexation with 1+1 eq. of anions

37 responded to the addition of F$^-$, OH$^-$, OAc$^-$, CN$^-$and H$_2$PO$_4^-$ by displaying significant color changes to orange, red and even dark purple. The new colors had little specifity except for OH$^-$, which turned to dark purple; but that color change was achieved by addition of an excess of the anion. Since it responds just to higher concentrations, **37** is not a suitable sensor of hydroxyl anion. Detection with ^{1}H NMR titrations didn't give unique responses for each anion either. However, the two newly forming bands in the UV-Vis spectra of **37** can be used to detect the presence F$^-$; thus **37** can be a selective fluoride sensor.

### 3.2.6. *N*-(5-Chloro-2-phenoxyphenyl)-*N'*-[4-(5-chloro-2-phenoxyphenyl)benzamido] thiourea (38)

The host molecule was insoluble in DMSO, so the molecule was not a suitable host for anion studies that are carried out in solution state. The only solvent that the compound was dissolved in was DMF, which participates itself in hydrogen bonding, thus anion studies of this compound were abandoned.

3.2.7. *N*-[5-(4-Methoxyphenyl)-1,3,4-thiadiazol-2-yl]benzamide (39)

DMSO solutions of **39** didn't show any change in their colors upon addition of any of the studied anions. However, UV-Vis titrations gave information about the complexation, or lack, thereof. Upon addition of 1:1 F⁻, a new absorption band at 356 nm which indicates complex formation was observed. Addition of 1:1 mole ratios of OAc⁻ caused a broadening in the UV-Vis spectrum of **39**, which turned into two seperate peaks at 294 nm and 358 nm when anion content was increased to 1:3 mole ratios. Addition of CN⁻ resulted in the formation of same new absorption bands, but in that case, the bands were first appeared with 1:1 complexation. The same bands were also observed upon addition of 1+3 eq. of $H_2PO_4^-$. Lastly, the addition of I⁻ resulted in a slight decrease in the absorption of **39**. The rest of the anions Cl⁻, Br⁻, OH⁻, HSO_4^- and NO_3^- didn't yield in any change in the color or the UV-Vis spectrum of compound **39**.

Figure 80: Colors of DMSO solutions of pure **39** and upon addition of 3:1, 1:1 and 1:3 mole ratios of F⁻ from left to right
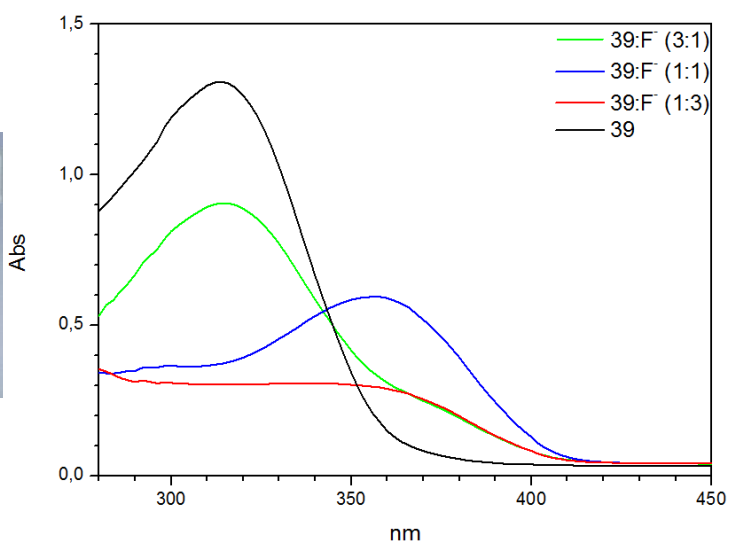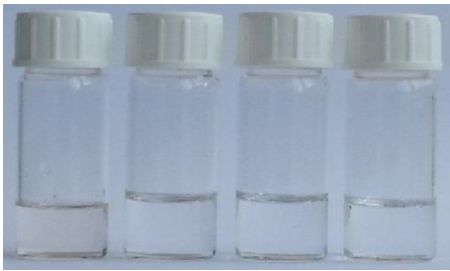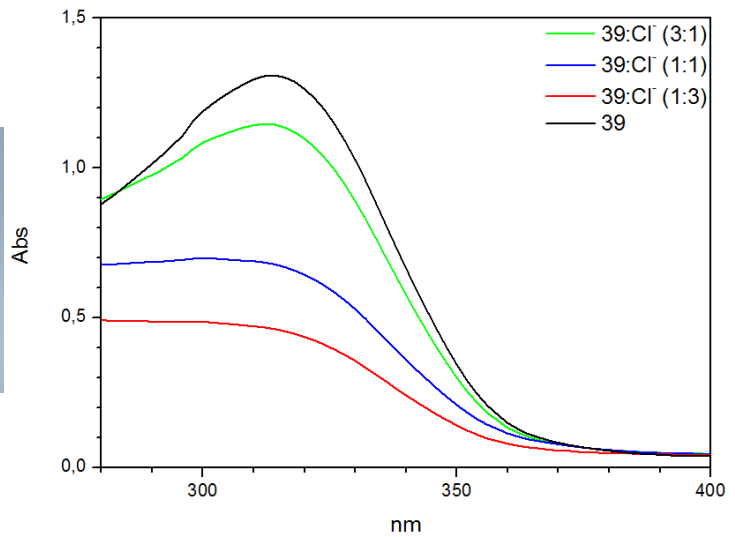
39 + F⁻

Figure 81: Colors of DMSO solutions of pure **39** and upon addition of 3:1, 1:1 and 1:3 mole ratios of Cl⁻ from left to right
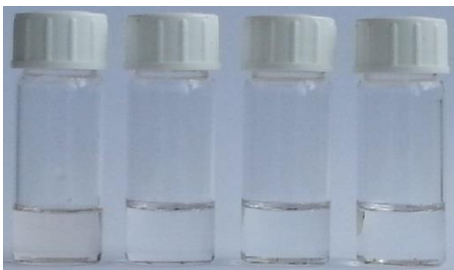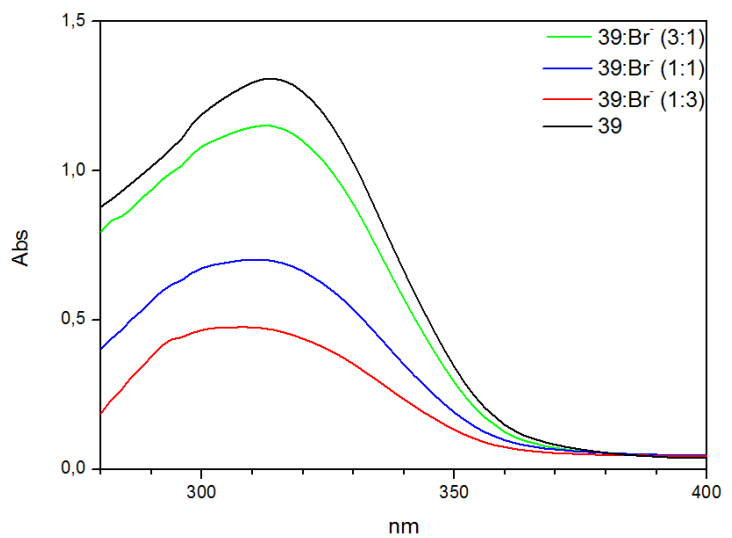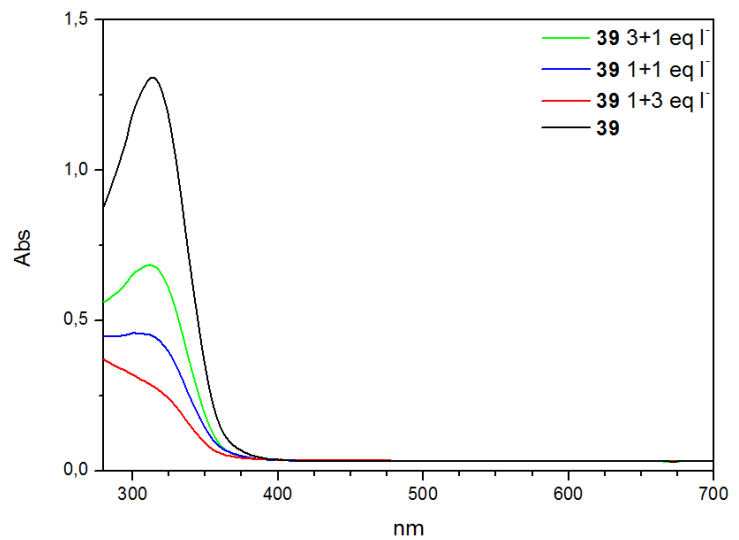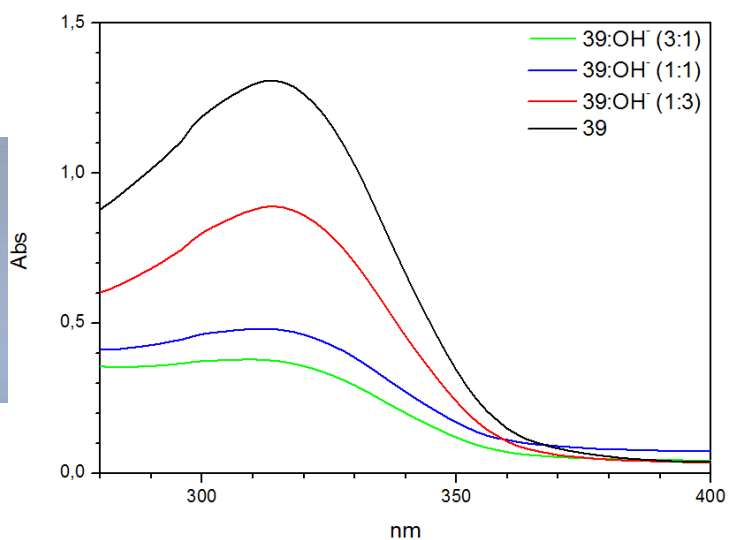
39 + Cl⁻

Figure 82: Colors of DMSO solutions of pure **39** and upon addition of 3:1, 1:1 and 1:3 mole ratios of Br⁻ from left to right
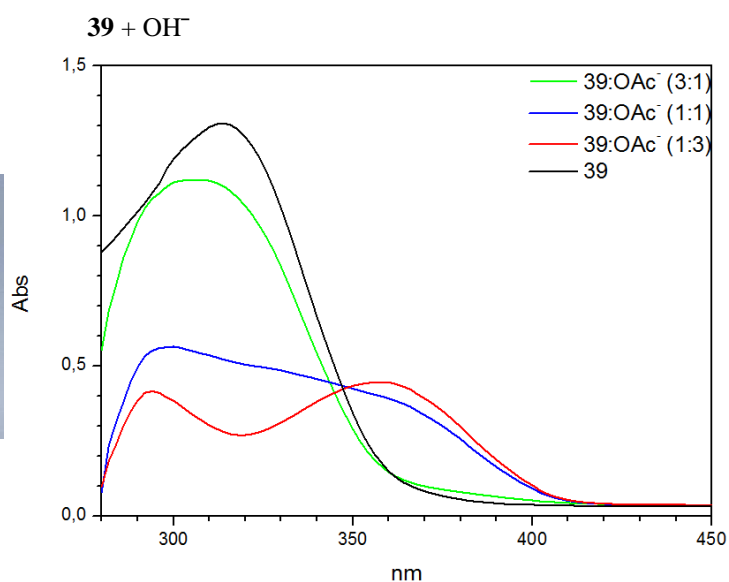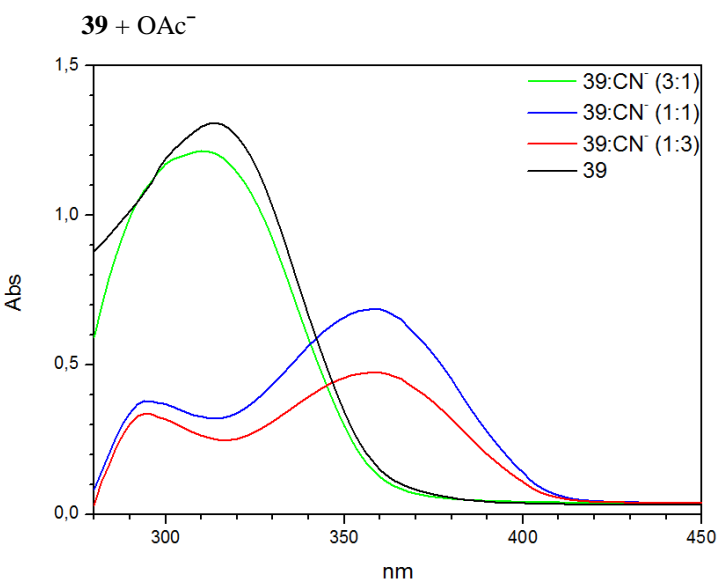
39 + Br⁻

Figure 83: Colors of DMSO solutions of pure **39** and upon addition of 3:1, 1:1 and 1:3 mole ratios of I⁻ from left to right

39 + I⁻

Figure 84: Colors of DMSO solutions of pure **39** and upon addition of 3:1, 1:1 and 1:3 mole ratios of OH⁻ from left to right
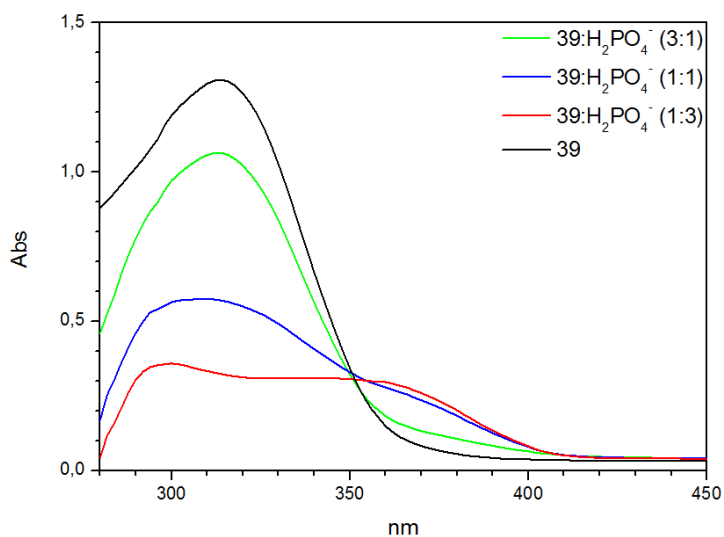
39 + OH⁻

Figure 85: Colors of DMSO solutions of pure **39** and upon addition of 3:1, 1:1 and 1:3 mole ratios of OAc⁻ from left to right

39 + OAc⁻

Figure 86: Colors of DMSO solutions of pure **39** and upon addition of 3:1, 1:1 and 1:3 mole ratios of CN⁻ from left to right

39 + CN⁻

Figure 87: Colors of DMSO solutions of pure **39** and upon addition of 3:1, 1:1 and 1:3 mole ratios of $H_2PO_4^-$ from left to right
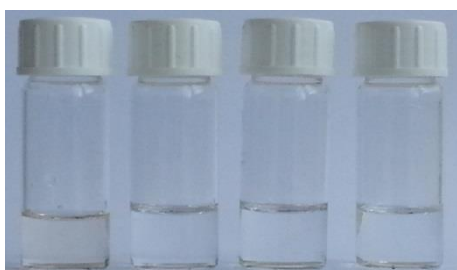
39 + $H_2PO_4^-$

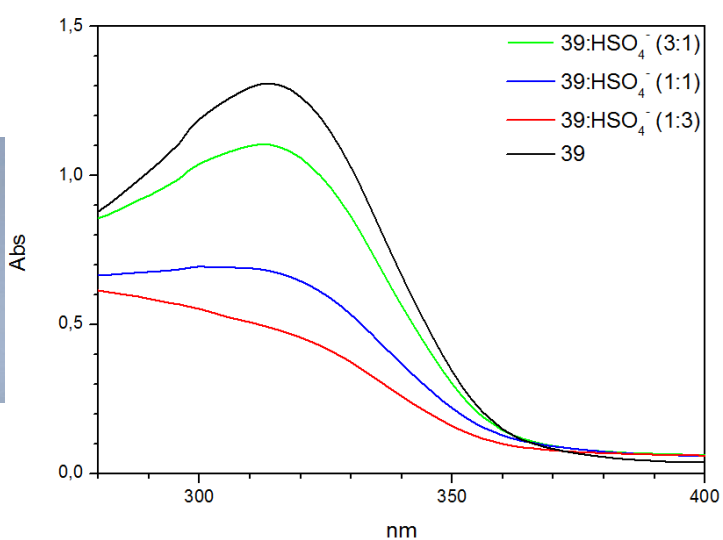
Figure 88: Colors of DMSO solutions of pure **39** and upon addition of 3:1, 1:1 and 1:3 mole ratios of HSO_4^- from left to right
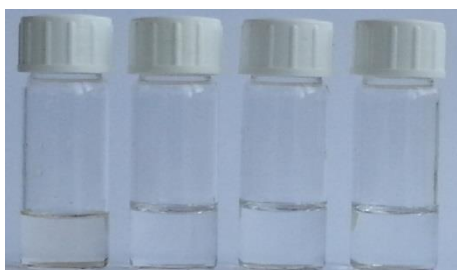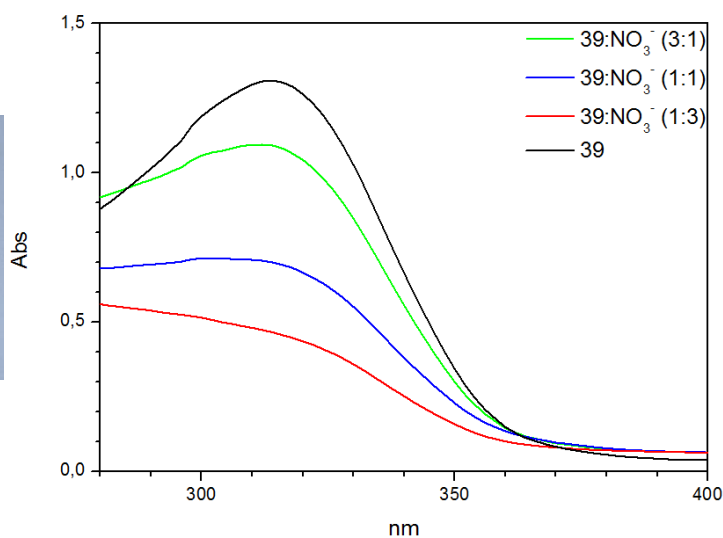
39 + HSO_4^-

Figure 89: Colors of DMSO solutions of pure **39** and upon addition of 3+1 eq., 1+1 eq.,1+3 eq. of NO_3^- from left to right

39 + NO_3^-

The results obtained by ^{1}H NMR studies were somewhat different than the ones obtained by color observations and UV-Vis titrations. Despite the compounds didn't show any color change, the addition of F⁻, OH⁻, CN⁻ and $H_2PO_4^-$ caused complete deprotonation of the NH moiety of the sensor molecule **39**. Additions of I⁻, Cl⁻ and Br⁻ caused the intensities of NH peaks to decrease, and OAc⁻ caused the peak to broaden, which indicate weak hydrogen bonding interactions with the sensor. Upon addition of HSO_4^-, the peak broadened to almost disappearance, meaning the anion was strongly bonded to the sensor. The remaining NO_3^- didn't cause any change in the ^{1}H NMR spectrum of **39**.
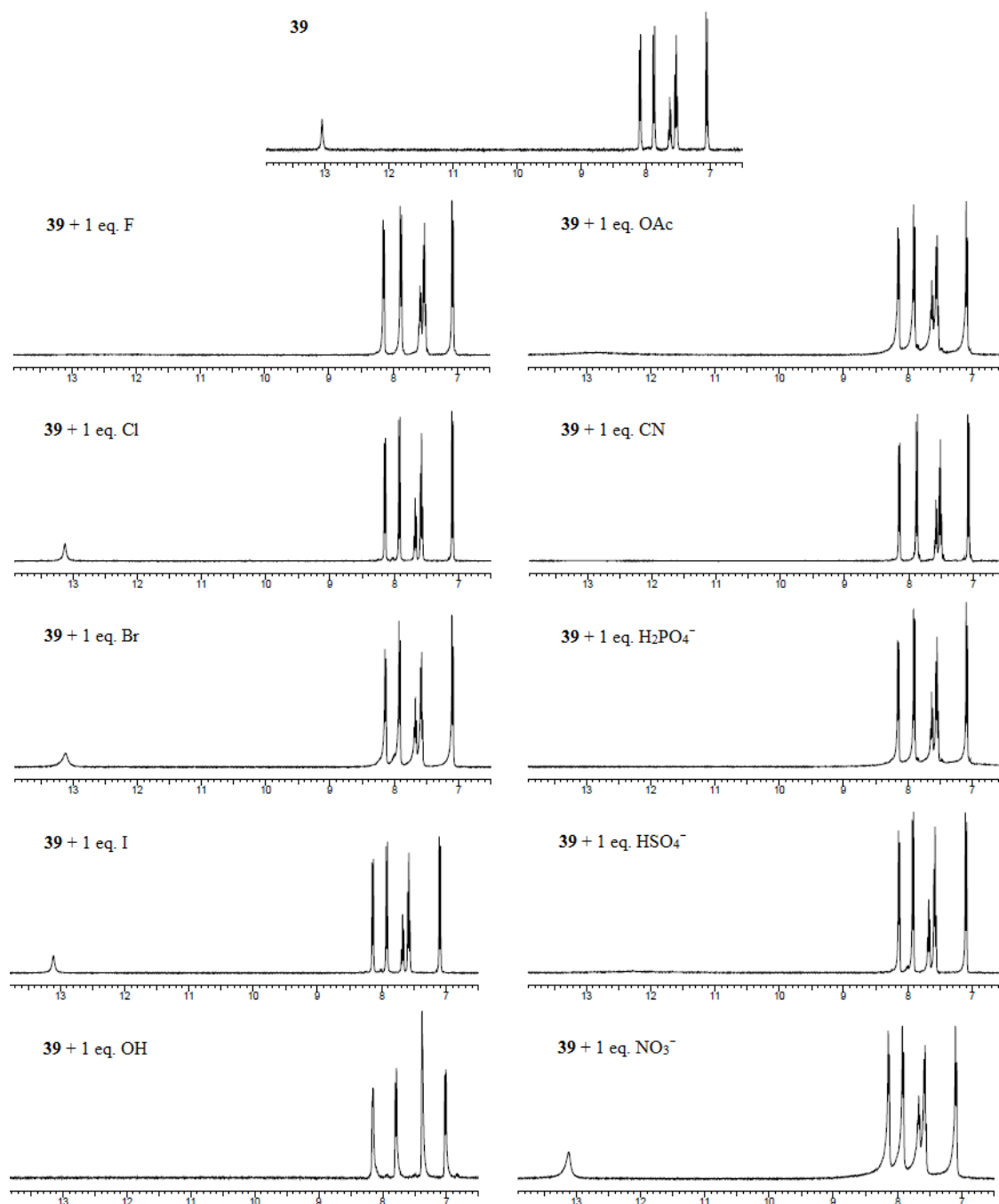
Scheme 6: Partial ^{1}H NMR spectra of **39** upon interaction with 1:1 ratios of anions

Overall, compound **39** formed a complex which gave a unique response to UV-Vis titrations, therefore can be proposed as a selective sensor of fluorine. Also, it was the only sensor who responded to hydrogen sulfate anion, which might be a result of an aggregate formation via intermolecular formation that has a tetrahedral cavity for the anion to be attached. The presence of heteroatoms also suggests that **39** might as well be a potential cation sensor.

3.2.8. *N,N'*-bis(5-Chloro-2-phenoxyphenyl)benzene-1,4-dicarboxamide (40)

Addition of F⁻, OH⁻ and CN⁻ caused the color of DMSO solutions of **40** to change to a light yellow. The color change was the most prominent in the 3:1 mixture of **40** and F⁻. However, the UV-Vis titration shows the appearance of a new absorption band (at 360 nm) was observed for 1:3 complex. Despite the slight color change when OH⁻ and CN⁻ was added, no changes were observed in UV-Vis titrations using those two anions.
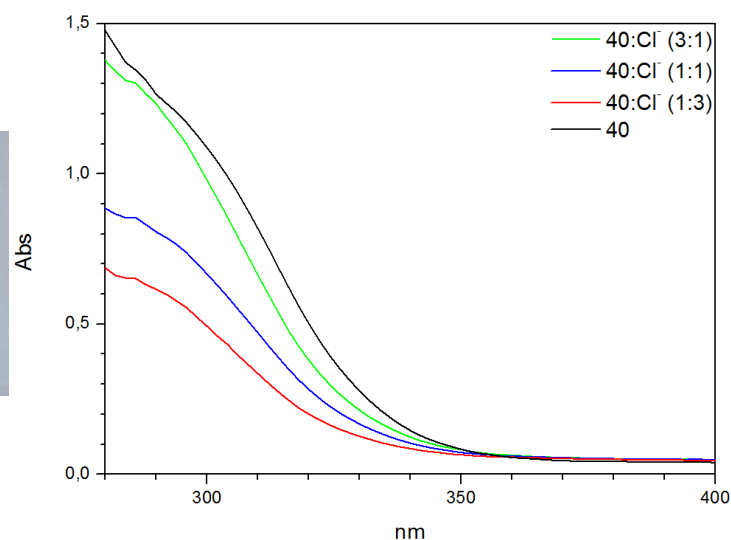

Figure 90: Colors of DMSO solutions of pure **40** and upon addition of 3:1, 1:1 and 1:3 mole ratios of F⁻ from left to right
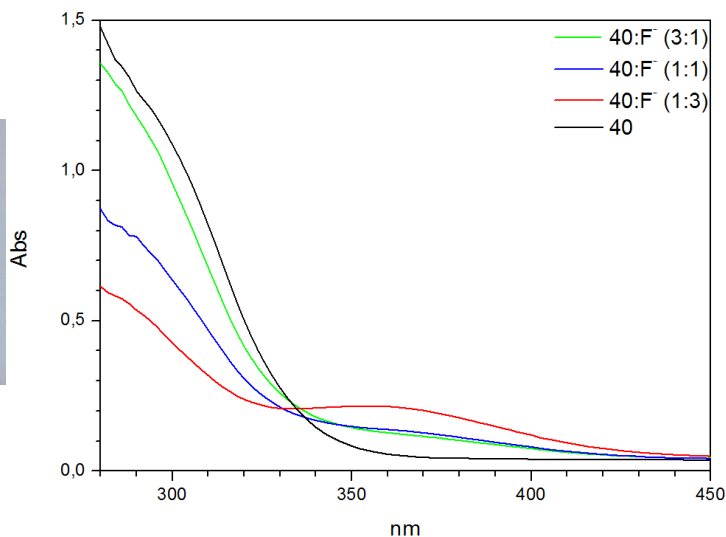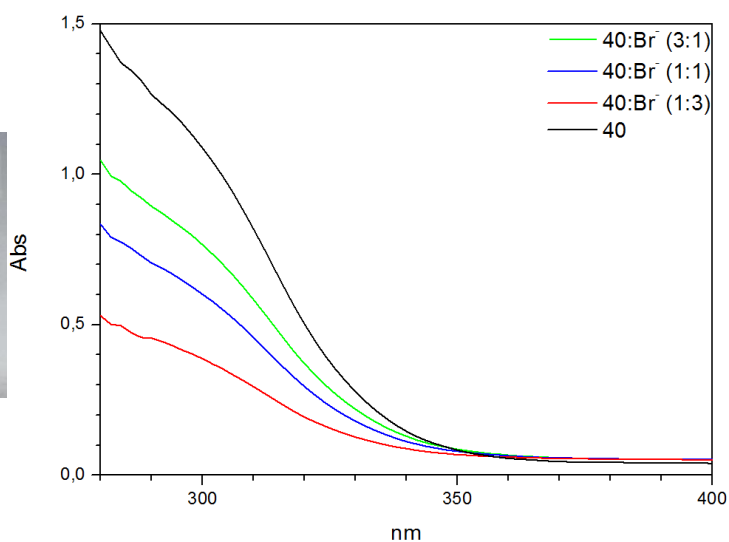

40 + F⁻

Figure 91: Colors of DMSO solutions of pure **40** and upon addition of 3:1, 1:1 and 1:3 mole ratios of Cl⁻ from left to right
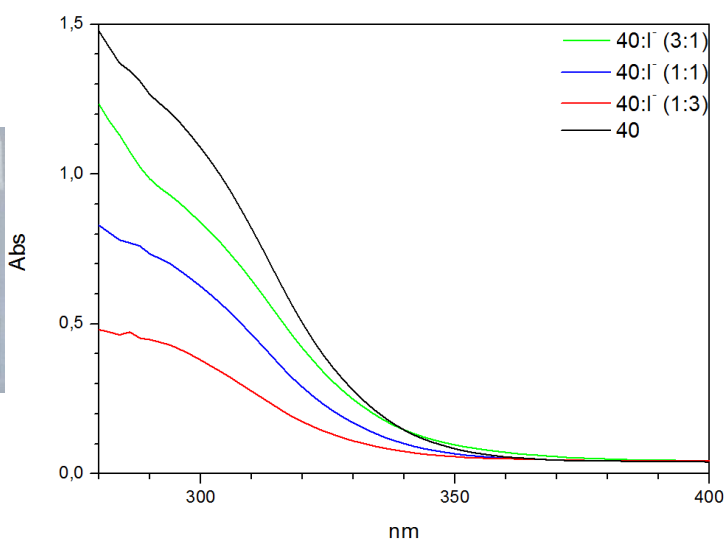

40 + Cl⁻

Figure 92: Colors of DMSO solutions of pure **40** and upon addition of 3:1, 1:1 and 1:3 mole ratios of Br⁻ from left to right
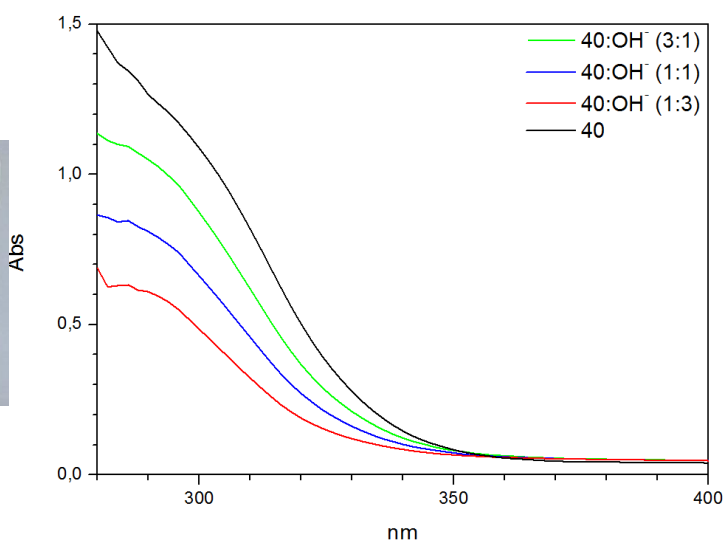
40 + Br⁻

Figure 93: Colors of DMSO solutions of pure **40** and upon addition of 3:1, 1:1 and 1:3 mole ratios of I⁻ from left to right

40 + I⁻

Figure 94: Colors of DMSO solutions of pure **40** and upon addition of 3:1, 1:1 and 1:3 mole ratios of OH⁻ from left to right
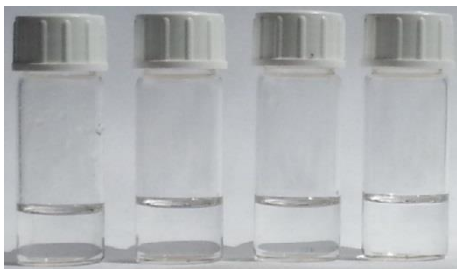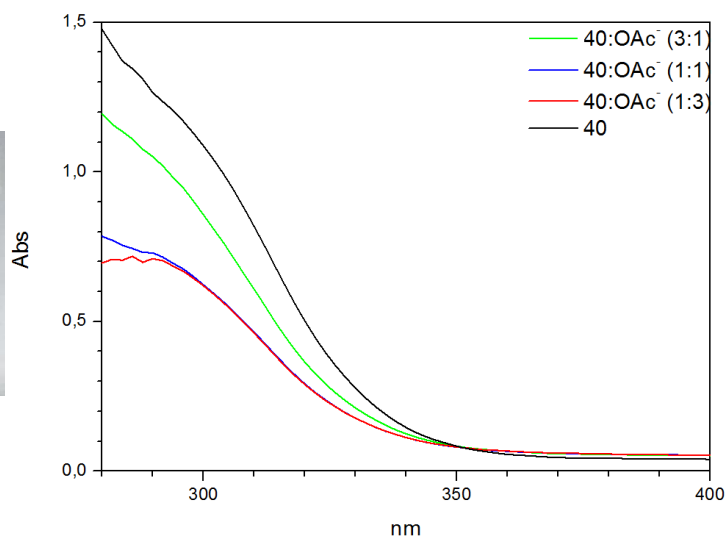
40 + OH⁻

Figure 95: Colors of DMSO solutions of pure **40** and upon addition of 3:1, 1:1 and 1:3 mole ratios of OAc⁻ from left to right
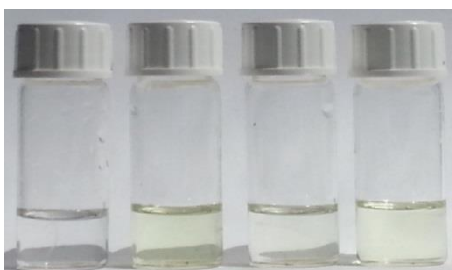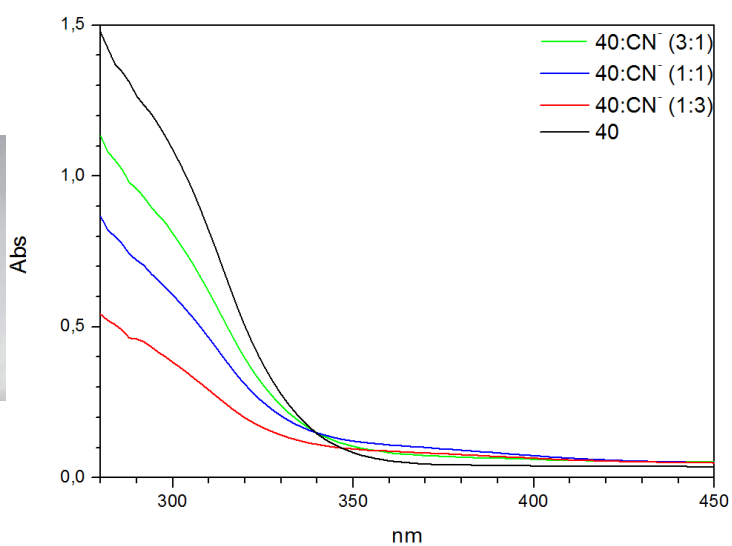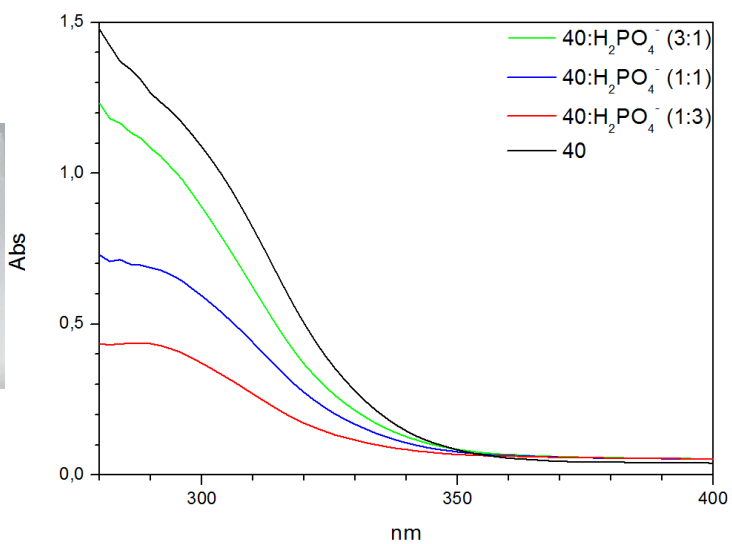
40 + OAc⁻

Figure 96: Colors of DMSO solutions of pure **40** and upon addition of 3:1, 1:1 and 1:3 mole ratios of CN⁻ from left to right
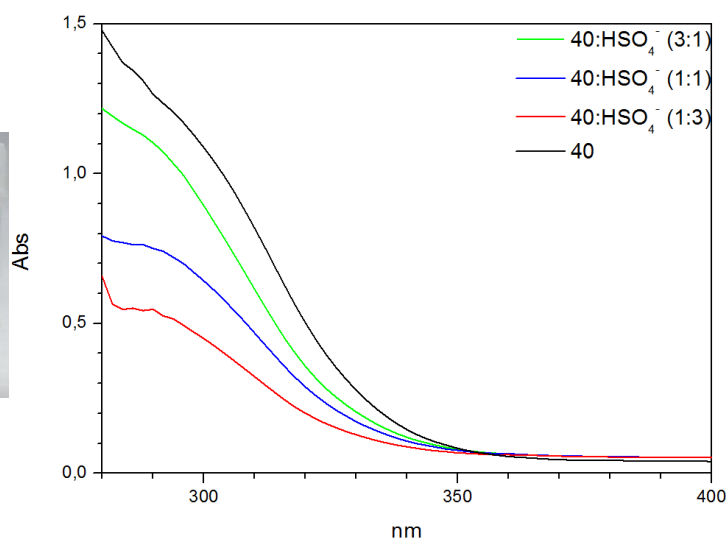
40 + CN⁻

Figure 97: Colors of DMSO solutions of pure **40** and upon addition of 3:1, 1:1 and 1:3 mole ratios of $H_2PO_4^-$ from left to right
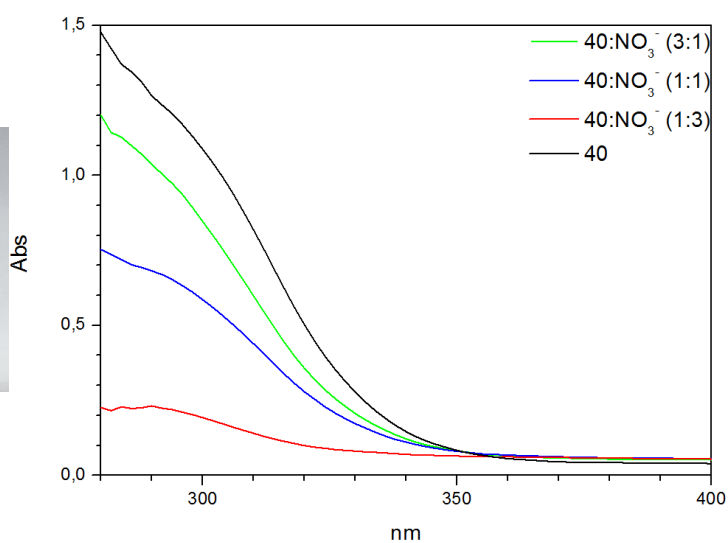
40 + $H_2PO_4^-$

Figure 98: Colors of DMSO solutions of pure **40** and upon addition of 3:1, 1:1 and 1:3 mole ratios of HSO_4^- from left to right
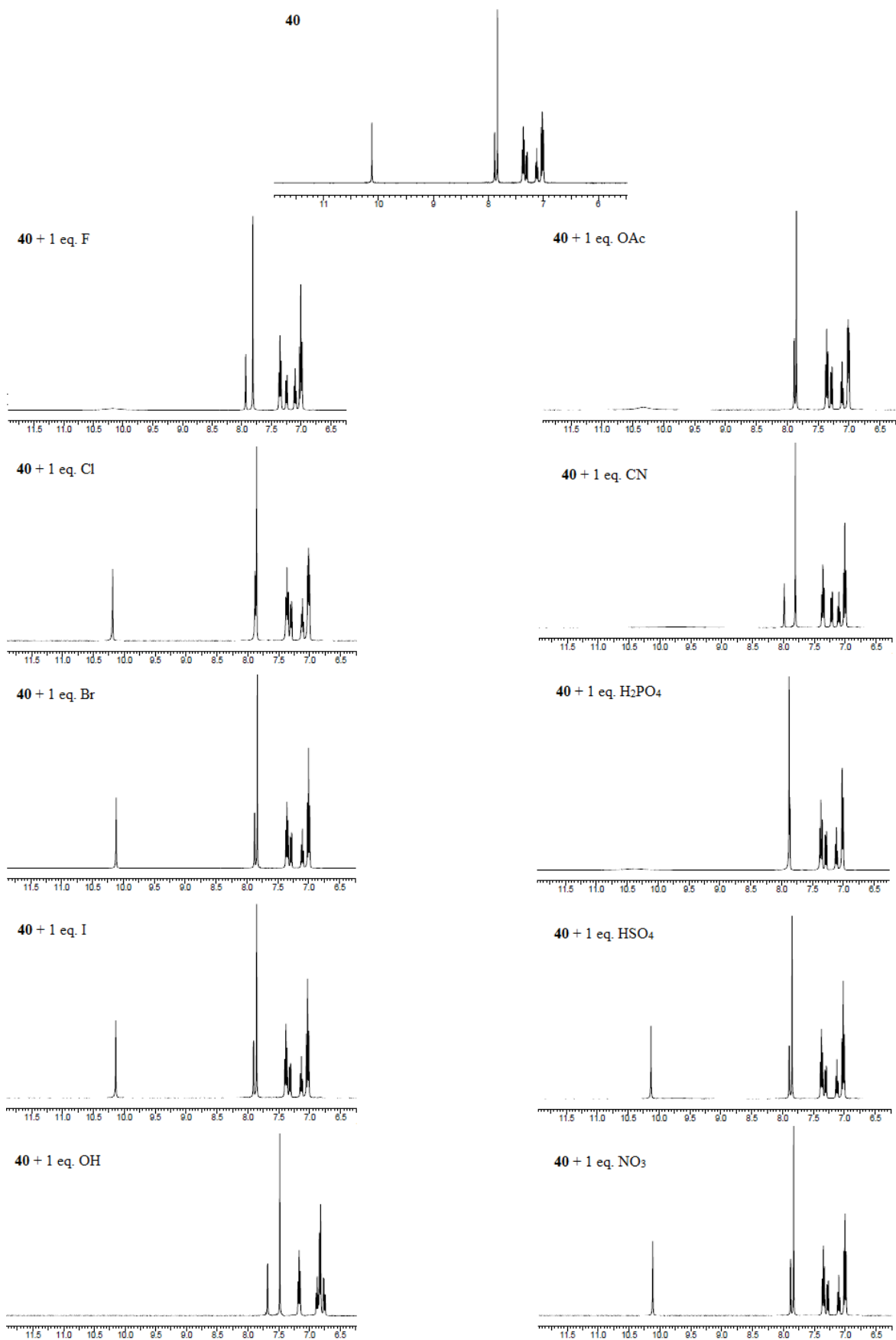
40 + HSO_4^-

Figure 99: Colors of DMSO solutions of pure **40** and upon addition of 3:1, 1:1 and 1:3 mole ratios of NO_3^- from left to right

40 + NO_3^-

[^1]H NMR studies of compound **40** gave more or less similar results with UV-Vis titrations. Addition of F^-, OAc^- and $H_2PO_4^-$ caused the NH peak of the anion to broaden, which is an indication of weak hydrogen bonding with **40**. This broadening was more significant for CN^-, for which the peak was almost disappeared, which might be a result of a matching geometry with the sensor. Addition of strongly basic OH^- caused deprotonation, indicated by the disappearance of the NH peak. The remaining anions; Cl^-, Br^-, I^-, HSO_4^- and NO_3^- didn't cause any changes in the [^1]H NMR spectrum of **40** because of relatively low basicities.

40

40 + 1 eq. F

40 + 1 eq. OAc

40 + 1 eq. Cl

40 + 1 eq. CN

40 + 1 eq. Br

40 + 1 eq. H_2PO_4

40 + 1 eq. I

40 + 1 eq. HSO_4

40 + 1 eq. OH

40 + 1 eq. NO_3

Scheme 7: Partial ^{1}H NMR spectra of **40** upon interaction with 1:1 ratios of anions

Although, compound **40** showed color changes with the addition of several anions, none of them were specific. The same observations stand for ^{1}H NMR studies. However, addition of F⁻ caused the formation of a new absorption band at 360 nm, which was specific for fluoride anion. Thus, compound **40** might be a selective sensor for fluoride anion by UV-Vis spectroscopic recognition.

4. CONCLUSION

In this thesis, six thiourea derivatives (five being novel) and two amide derivatives (one being novel) were synthesized by reacting the corresponding acyl chlorides and amines (in the presence of ammonium thiocyanate for thioureas). After characterization, all the products except **38** were brought in contact with anions (F^-, Cl^-, Br^-, I^-, OH^-, OAc^-, CN^-, $H_2PO_4^-$, HSO_4^- and NO_3^-). The presence or lack of a host-anion complex were detected by observing the color changes of host solutions by naked eye, by UV-Vis titrations and by observing the changes in hosts' ^{1}H NMR spectra.

Among the synthesized compounds, **36** found to be a selective colorimetric and UV-Vis sensor of cyanide anion. **37** gave a unique response to fluoride anion in UV-Vis titrations and colorwise, therefore can be proposed as a selective fluoride sensor. Compound **39** was the only sensor that responded to hydrogen sulfate anion, but the response was not specific to the anion. **39** can also be proposed as a selective sensor of fluoride. **40** responded to fluoride anion by forming a new absorption band that is unique to the anion. Thus it can be proposed as a receptor of fluoride anion.

REFERENCES

[1]   G.H. Cassell, J. Mekalanos, *Journal of American Medical Association* 285 601–605, **2001**

[2]   O.F. Huebner, J.L. Marsh, R.H. Mizzoni, R.P. Mull, D.C. Schroeder, H.A. Troxell, C.R. Scholz, *Journal of American Chemical Society*, 75, 2274–2275, **1953**

[3]   Aamer Saeed, Uzma Shaheen, A. Hameed, S.Z. Haider Naqvi, *Journal of Fluorine Chemistry*, 130, 1028–1034, **2009**

[4]   Joachim Müller, Carmen Limban, Britta Stadelmann, Alexandru Vasile Missir, Ileana Cornelia Chirita, Mariana Carmen Chifiriuc, George Mihai Nitulescu, Andrew Hemphill, *Parasitology International* 58, 128–135, **2009**

[5]   Samir Y. Abbas, Marwa A.M.Sh. El-Sharief, Wahid M. Basyouni, Issa M.I. Fakhr, Eman W. El-Gammal, *European Journal of Medicinal Chemistry*, 64, 111-120, **2013**

[6]   K. Ziegler-Skylakakis, S. Rossberger, U. Andrae, *Archives of Toxicology*, 58, 5, **1985**

[7]   Jianwen Yao, Jing Chen, Zuopeng He, Wei Sun, Wenfang Xu, *Bioorganic & Medicinal Chemistry*, 20, 2923–2929, **2012**

[8]   Wukun Liu, Jinpei Zhou, Tong Zhang, Haiyang Zhu, Hai Qian, Huibin Zhang, Wenlong Huang, Ronald Gust, *Bioorganic & Medicinal Chemistry Letters,* 22, 2701–2704, **2012**

[9]   W. Mohammad, H. Barry, G. Martin, P.M. Christoper, C.S.H. Duncan, B. Harold, *Biochemical Journal*, 243, 867–870, **1987**

[10]   Faizul Azam, Ismail A. Alkskas, Musa A. Ahmed, *European Journal of Medicinal Chemistry* 44, 3889–3897, **2009**

[11]   Song Bai, Xueping Liang, Baoan Song, Pinaki S. Bhadury, Deyu Hu, Song Yang, *Tetrahedron: Asymmetry* 22, 518–523, **2011**

[12]   Yuki Nakayama, Takashi Gotanda, Katsuji Ito, *Tetrahedron Letters* 52, 6234–6237, **2011**

[13]   Yasutaka Hoashi, Takaya Yabuta, Pei Yuan, Hideto Miyabe and Yoshiji Takemoto, *Tetrahedron,* 62, 365–374, **2006**

[14]   A Yamaguchi, R.B Penland, S Mizushima, T.J Land, J.V Quagliano, *Journal of American Chemical Society*, 80, 527, **1958**

[15]   Haile G. Berhe, Susan A. Bourne, Martin W. Bredenkamp, Catharine Esterhuysen, Michael M. Habtu, Klaus R. Koch, Robert C. Luckay, *Inorganic Chemistry Communications* 9, 99–102, **2006**

[16]   E. Otazo-Sanchez, P. Ortiz-del-Toro, O. Estevez-Hernandez, L. Perez-Marin, I. Goicoechea, A. Ceron Beltran, J.R. Villagomez-Ibarra, *Spectrochimica Acta,* Part A, 58, 2281–2290, **2002**

[17]   Laura M. Cubillana-Aguilera, José M. Palacios-Santander, Osvaldo L. Estévez-Hernández, Ignacio Naranjo-Rodríguez, José Luis Hidalgo-Hidalgo de Cisneros, *Talanta,* 82, 129–136, **2010**

[18]   K.H. König, M. Schuster, B. Steinbrech, G. Schneeweis, R. Schlodder, Fresenius, Z. *Analytical Chemistry*, 321, 457, **1985**

[19]   Luckay, R.C. , Mebrahtu, F., Esterhuysen, C., Koch, K.R. *Inorganic Chemistry Communications,* 13, 468–470, **2010**

[20]   Sung Min Seo, Eun Jin Cho, Soo Jin Lee, Kye Chun Nam, Seong-Hun Park, Jong Hwa Jung, *Microporous and Mesoporous Materials,* 114, 448–454, **2008**

[21]   Sohail Saeed, Naghmana Rashid, Peter G. Jones, Muhammad Ali, Rizwan Hussain, *European Journal of Medicinal Chemistry*, 45, 1323–1331, **2010**

[22]   Kavitha Sankar, Venugopal Rajendran, *Ultrasonics Sonochemistry,* 20, 329–337, **2013**

[23]   Gui-Chun Yang , Zu-Xing Chen, Zhao-Jun Zhang, *Reactive & Functional Polymers* 51, 1-6, **2002**

[24]   Shao-Yong Ke, Tai-Bao Wei, Si-Jia Xue, Li Ping Duan, Jin-Zhi Li, *Indian Journal of Chemistry*, Vol 44B, 1957-1960, **2005**

[25]   Ulrik Boas, Heidi Gertz, Jørn B. Christensen, Peter M. H. Heegaard, *Tetrahedron Letters*, 45, 269–272, **2004**

[26]   Nguyen Dinh Thanh, Nguyen Thi Thanh Mai, *Carbohydrate Research*, 344, 2399–2405, **2009**

[27]   Paul D. Beer, Philip A. Gale, *Angewandte Chemie International Edition*, 40, 486–516, **2001**

[28]   Jie Shao, Hai Lin, Ming Yu, Zunsheng Cai, Huakuan Lin, *Talanta,* 75, 551–555, **2008**

[29]   D. W. Christianson, W. N. Lipscomb, *Accounts of Chemical Research*, 22, 62, **1989**

[30]   Anna K.H. Hirsch, F.R. Fisher, F. Diederich, *Angewandte Chemie International Edition,* 46, 338–352, **2007**

[31]   S. Ayoob, A.K. Gupta, *Critical Reviews in Environmental Science and Technology,* 36, 433–487, **2006**

[32]   T.-Y. Ho, M.I. Scranton, G.T. Taylor, R. Varela, R.C. Thunell, F. Muller-Karger, *Limnology & Oceanography*, 47, 1119, **2002**

[33]   V. Krail, J.L. Sessler, *Tetrahedron*, 51, 539–554, **1995**

[34]   D.P. Curran, L.H. Kuo, *Tetrahedron Letters,* 36, 6647–6650, **1995**

[35] F.P. Schmidtchen, *Journal of American Chemical Society*, 108, 8249, **1986**

[36] Jose M. Llinares, Douglas Powell, Kristin Bowman-James, Coordination Chemistry Reviews 240, 57-75, **2003**

[37] A. P. Bisson, V. M. Lynch, M. K. C. Monahan, E. V. Anslyn, *Angewandte Chemie*, 109, 2435, **1997**

[38] Huijuan Yan, Haibing Li, *Sensors and Actuators B*, 148, 81–86, **2010**

[39] A. Andrievsky, F. Ahuis, J. L. Sessler, F. Vögtle, D. Gudat, M. Moini, *Journal of American Chemical Society*, 120, 9712, **1998**

[40] Snigdha Panda, Sanjio S. Zade, Arunashree Panda, Harkesh B. Singh, Ray J. Butcher, *Journal of Organometallic Chemistry,* 691, 2793–2809, **2006**

[41] Jie Shao, Hai Lin, Hua-Kuan Lin, *Talanta,* 75, 1015–1020, **2008**

[42] Kumaresh Ghosh, Indrajit Saha, Goutam Masanta, Evan B. Wang, Carol A. Parish, *Tetrahedron Letters,* 51, 343–347, **2010**

[43] Shin-ichi Kondo, Masakazu Sato, *Tetrahedron*, 62, 4844–4850, **2006**

[44] Yeong-Joon Kim, Han Kwak, Se Jin Lee, Je Sin Lee, Hyun Jung Kwon, Sang Ho Nam, Kyoungrim Lee, Cheal Kim, *Tetrahedron*, 62, 9635–9640, **2006**

[45] Shaoji Xiang, Guiqin Yu, Yongmin Liang, Longmin Wu, *Journal of Molecular Structure* 789, 43–51, **2006**

[46] Komala Pandurangan, Jonathan A. Kitchen, Thorfinnur Gunnlaugsson, *Tetrahedron Letters*, 54, 2770–2775, **2013**

[47] Rebecca M. Duke, Thorfinnur Gunnlaugsson, *Tetrahedron Letters,* 51, 5402–5405, **2010**

[48] Xiaoping Bao, Jinhua Yu, Yuhui Zhou, *Sensors and Actuators B,* 140, 467–472, **2009**

[49] Pui-Lam Ng, Chi-Sing Lee, Hoi-Lun Kwong, Albert S.C. Chan, *Inorganic Chemistry Communications,* 8, 769–772, **2005**

[50] Run Zhang, Xiaojing Yu, Yuejiao Yin, Zhiqiang Ye, Guilan Wang, Jingli Yuan, *Analytica Chimica Acta,* 691, 83–88, **2011**

[51] Hanna Lee, Yun Mi Chung, Kyo Han Ahn, *Tetrahedron Letters,* 49, 5544–5547, **2008**

[52] V. Kral, J. L. Sessler, T. V. Shishkanova, P. A. Gale, R. Volf, *Journal of American Chemical Society*, 121, 8771, **1999**

[53] P. D. Beer, M. G. B. Drew, J. Hodacova, S. E. Stokes, *Journal of the Chemical Society, Dalton Transactions*, 3447, **1995**

APPENDIX
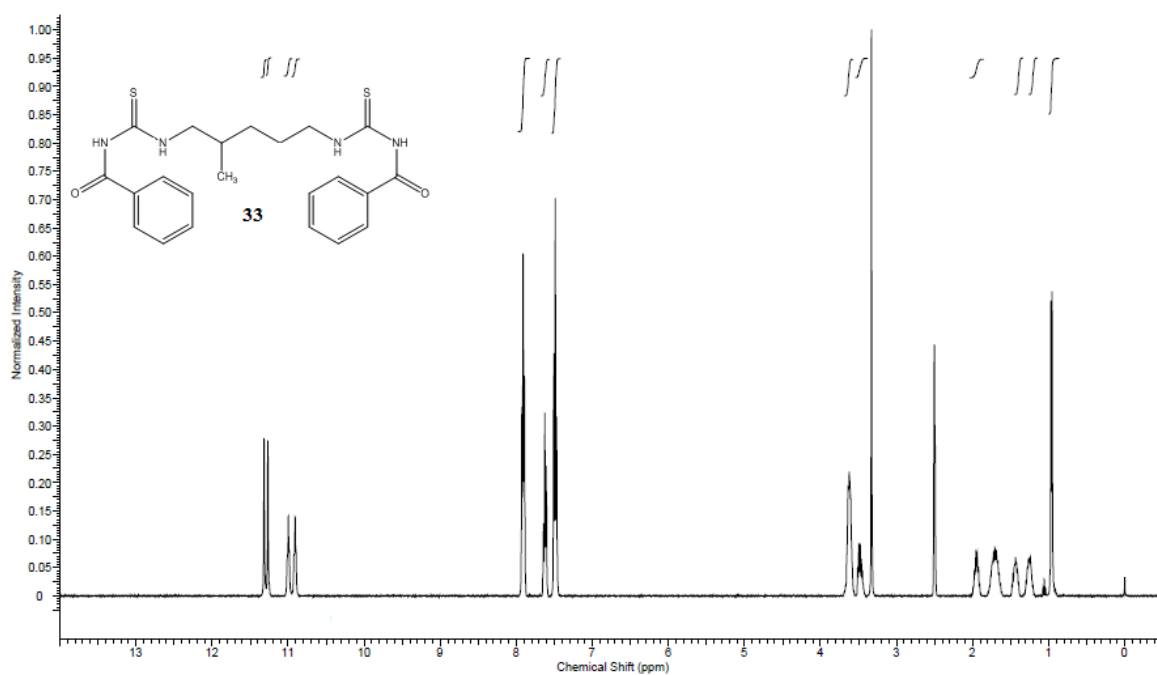
Scheme 8: ^{1}H NMR spectrum of **33**
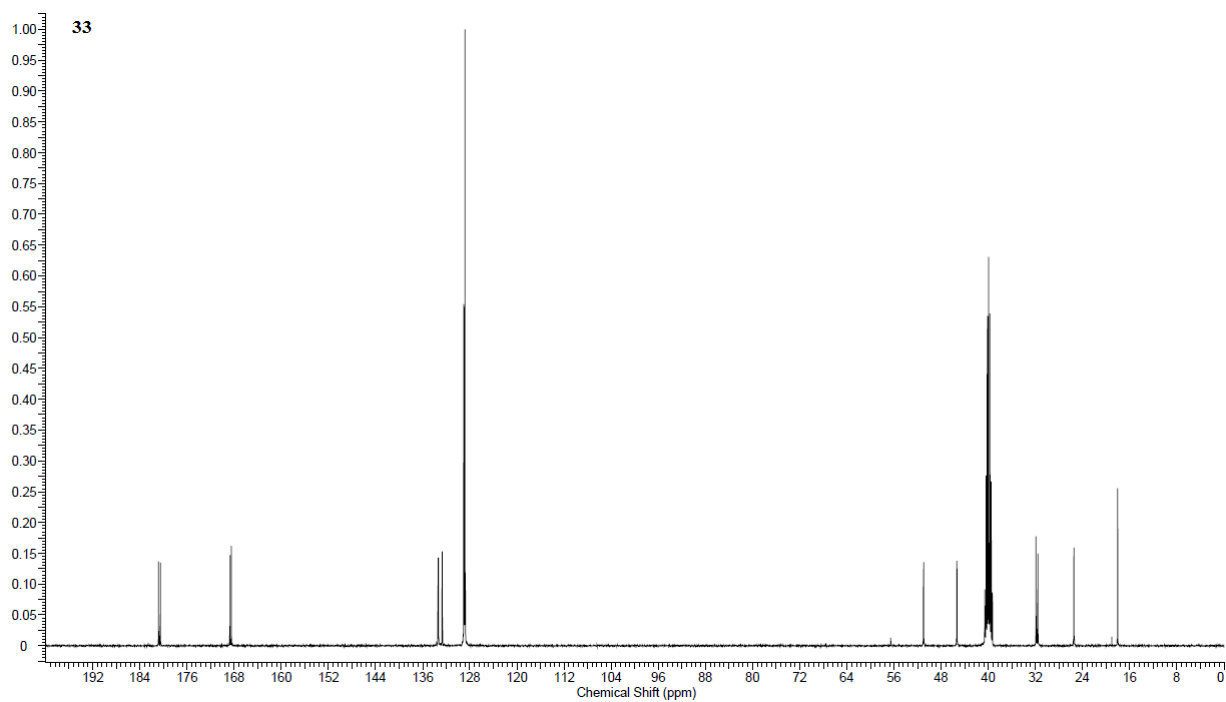
Scheme 9: ^{13}C NMR spectrum of **33**

33
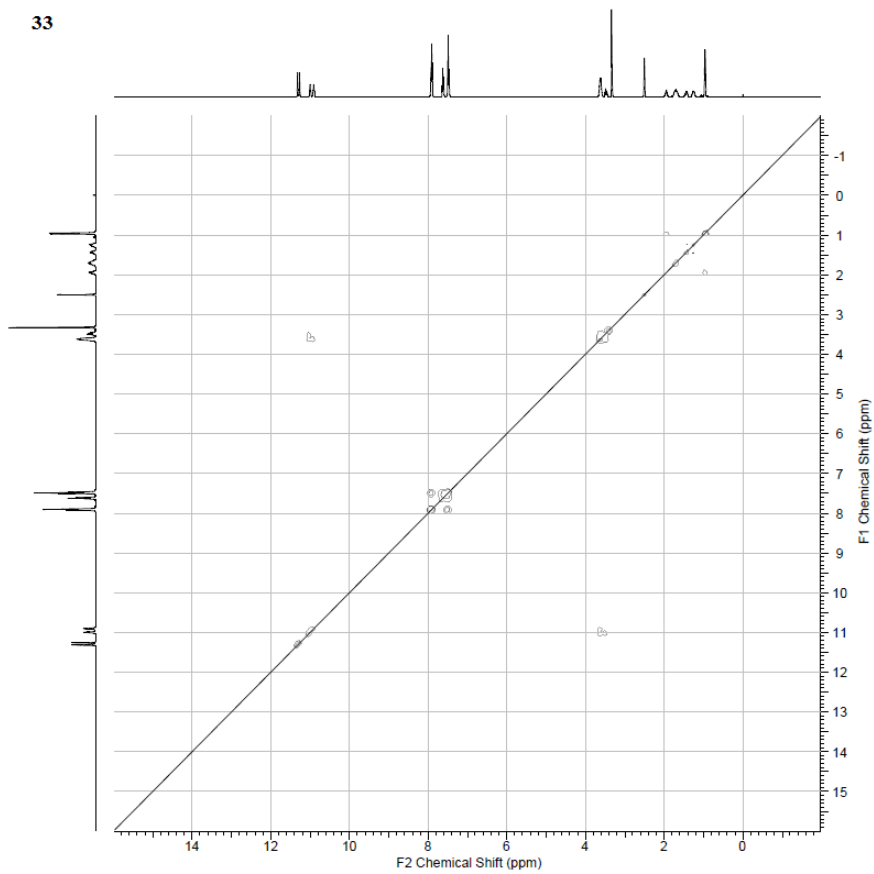
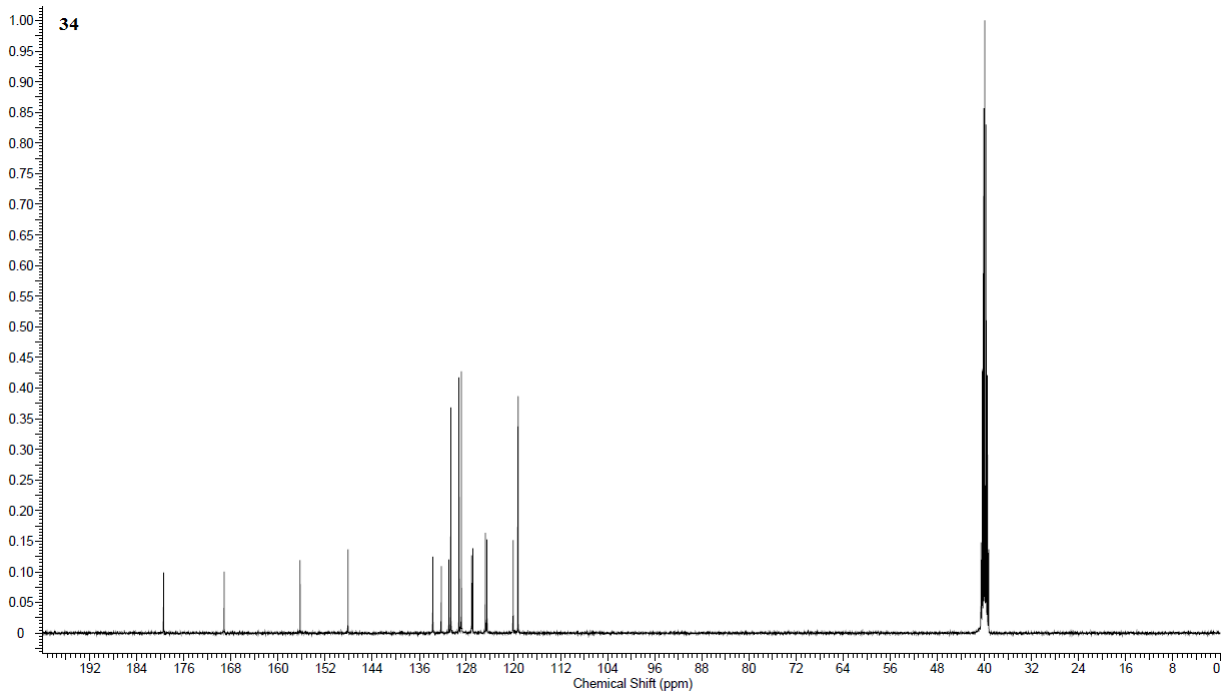Scheme 10: COSY spectrum of **33**

33
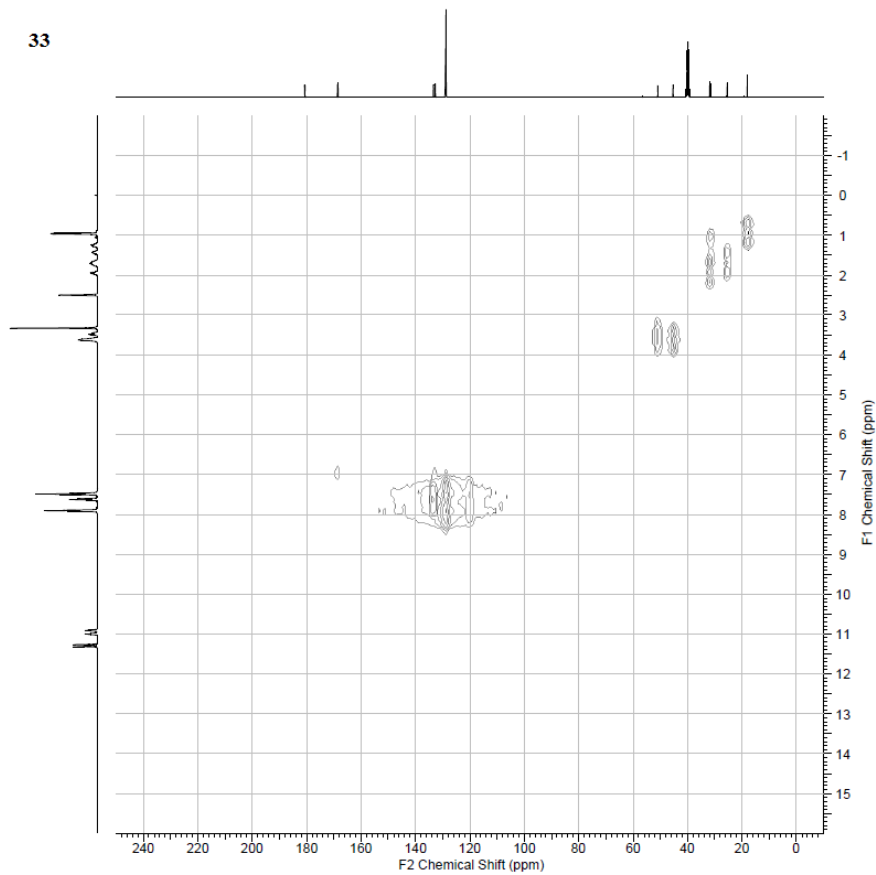
Scheme 11: HETCOR spectrum of **33**
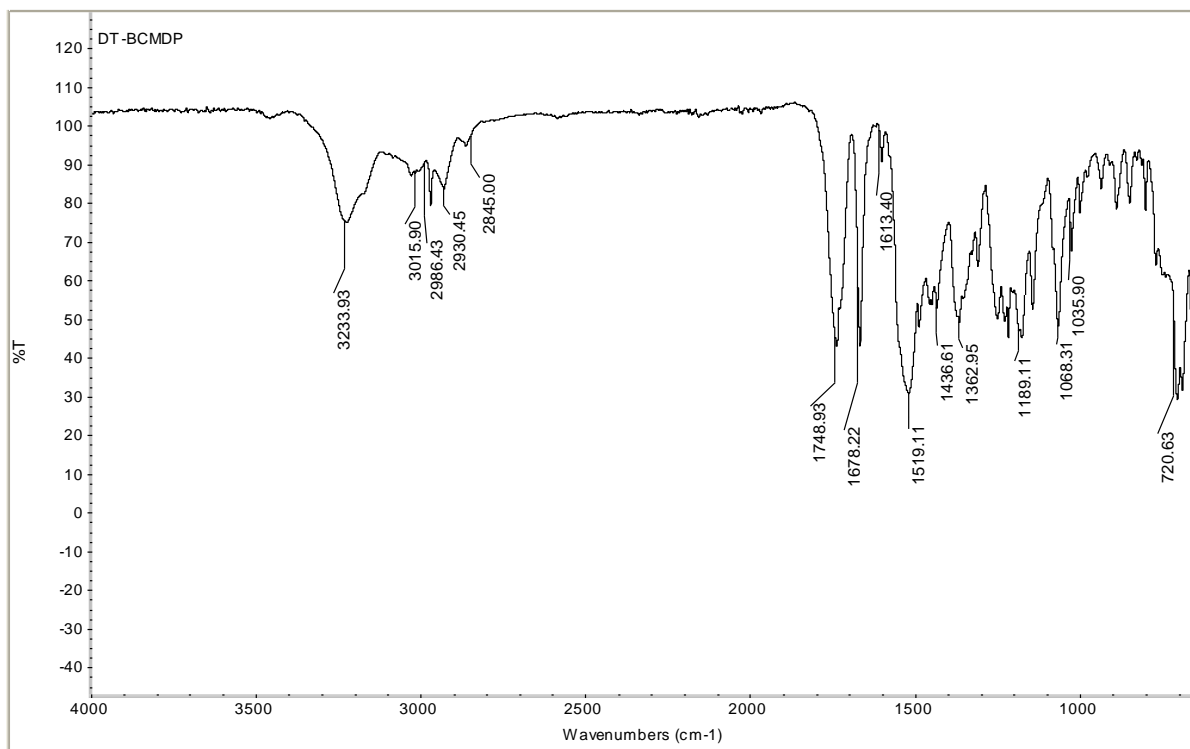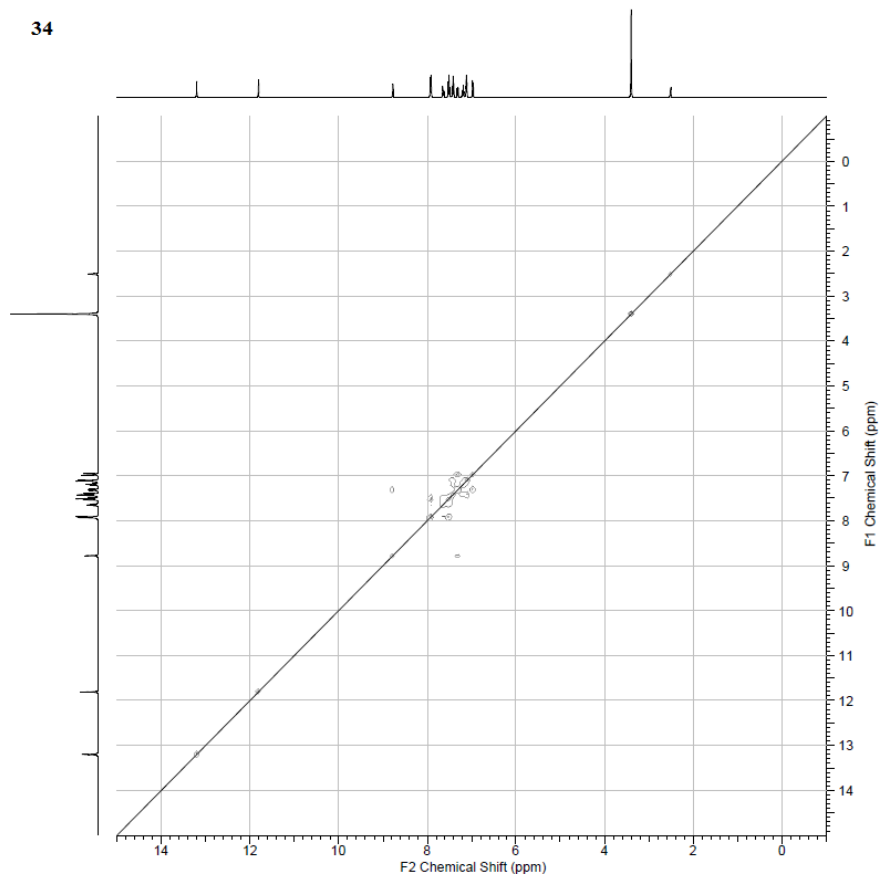
Scheme 12: FT-IR spectrum of **33**
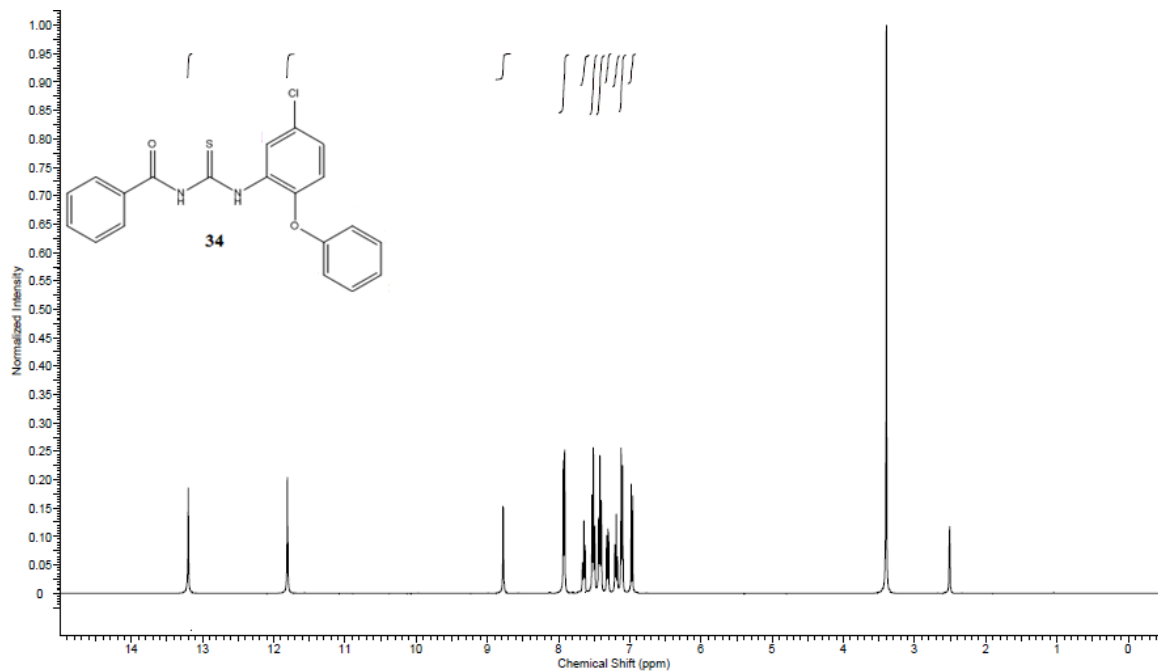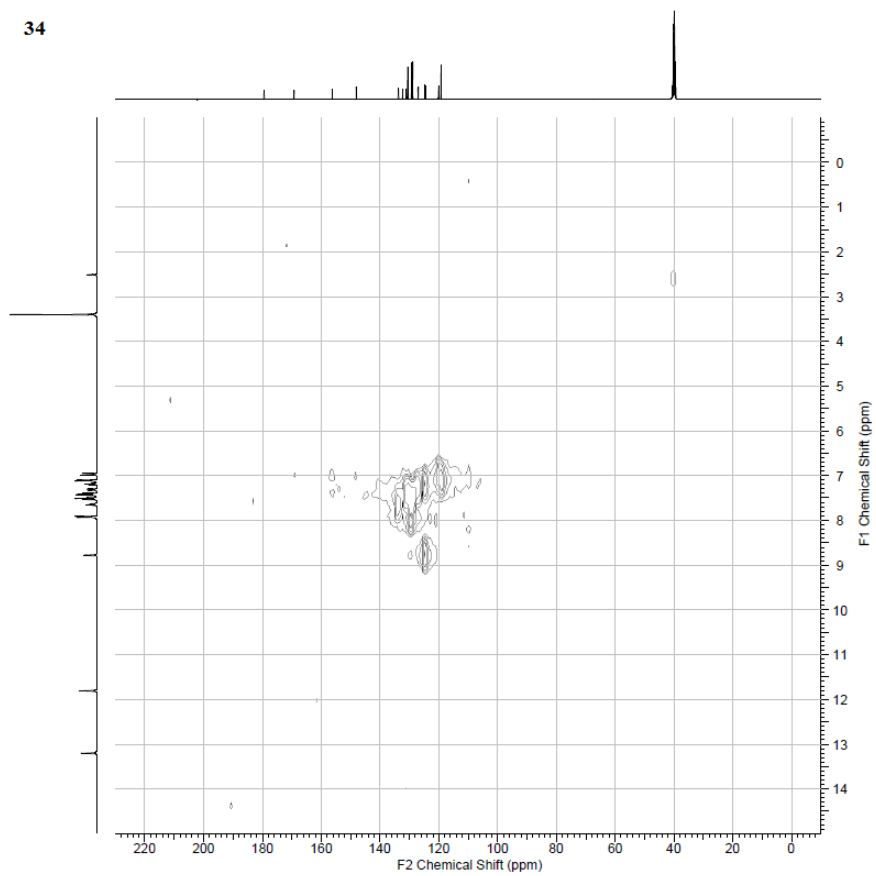
Scheme 13: ^{1}H NMR spectrum of **34**

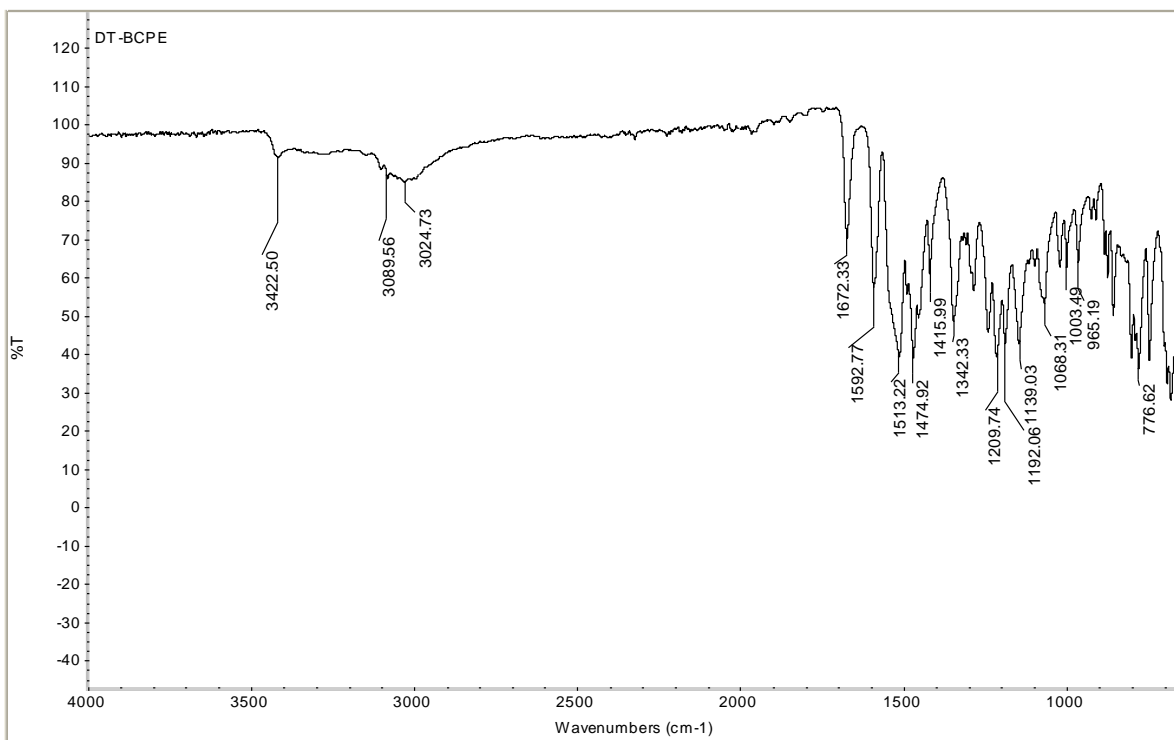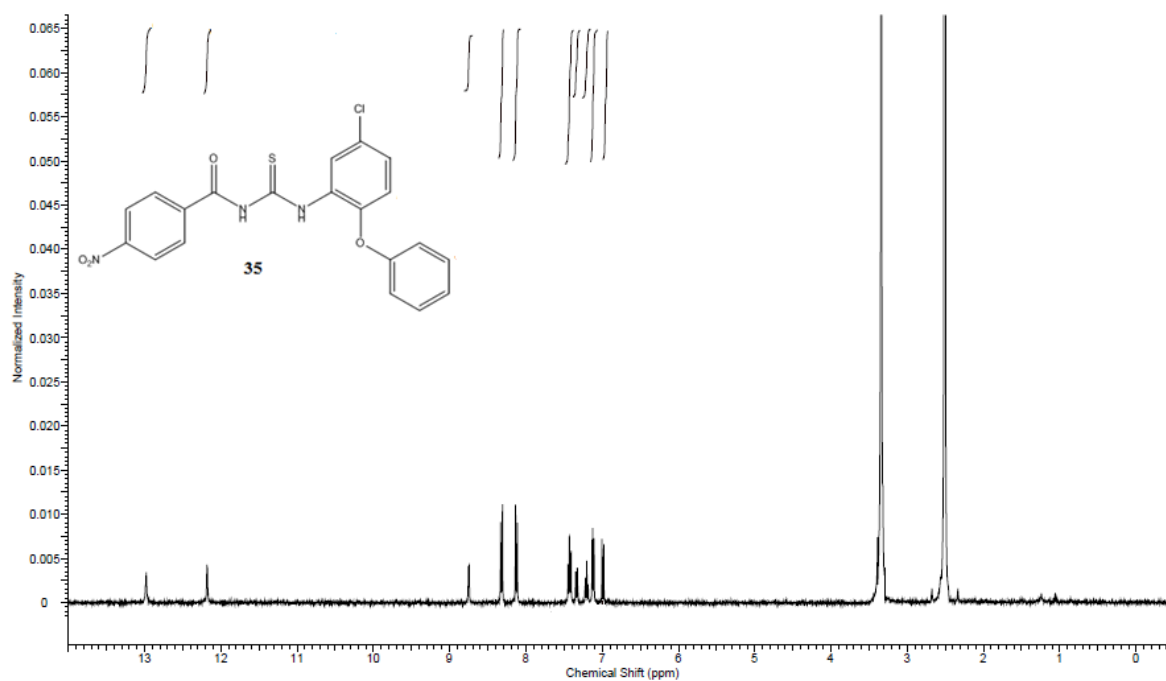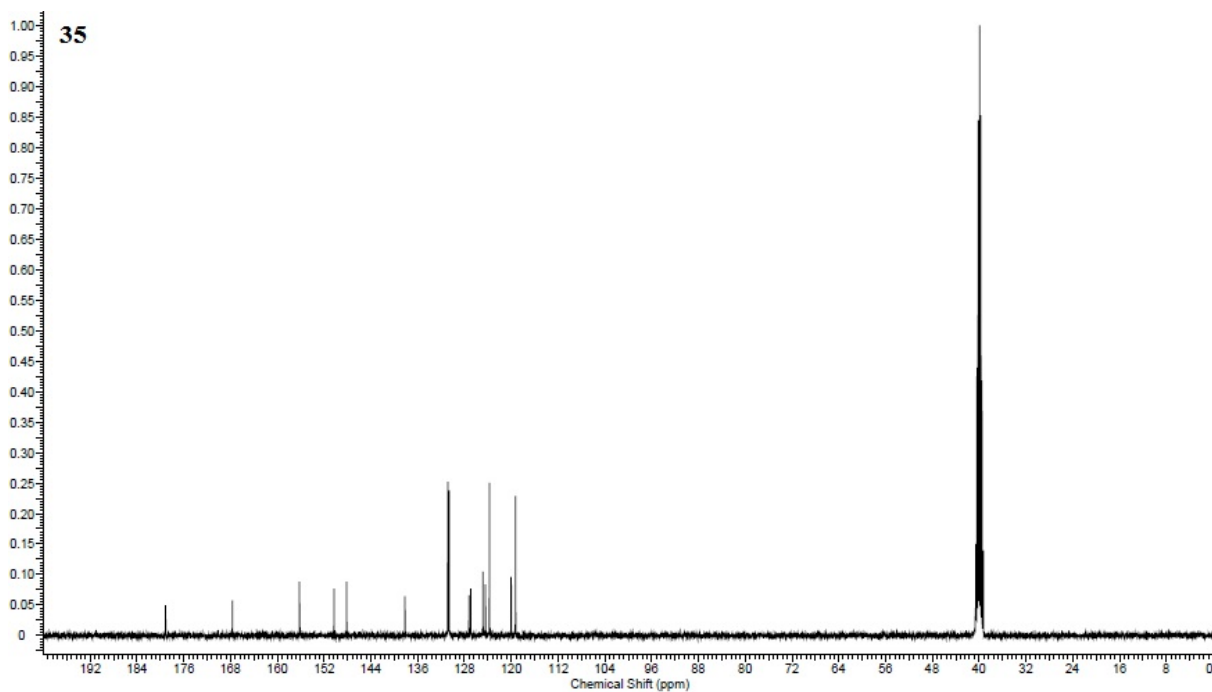Scheme 14: ^{13}C NMR spectrum of **34**

34

Scheme 15: COSY spectrum of **34**
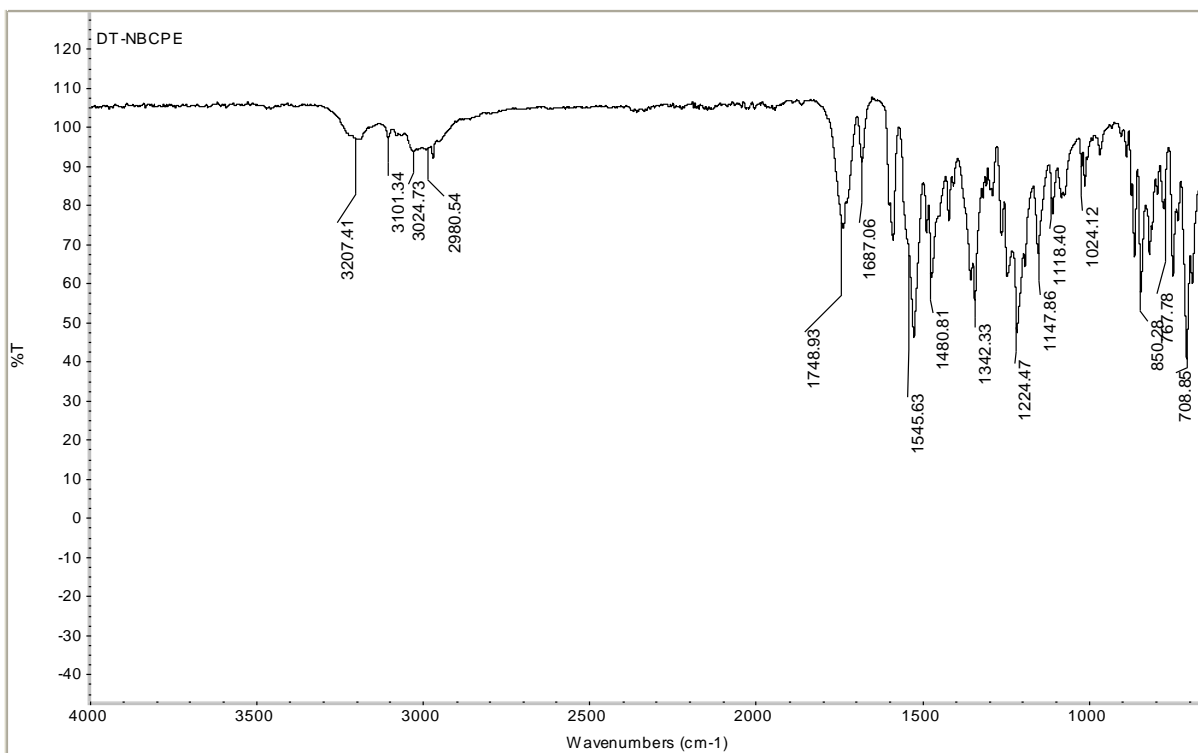
34

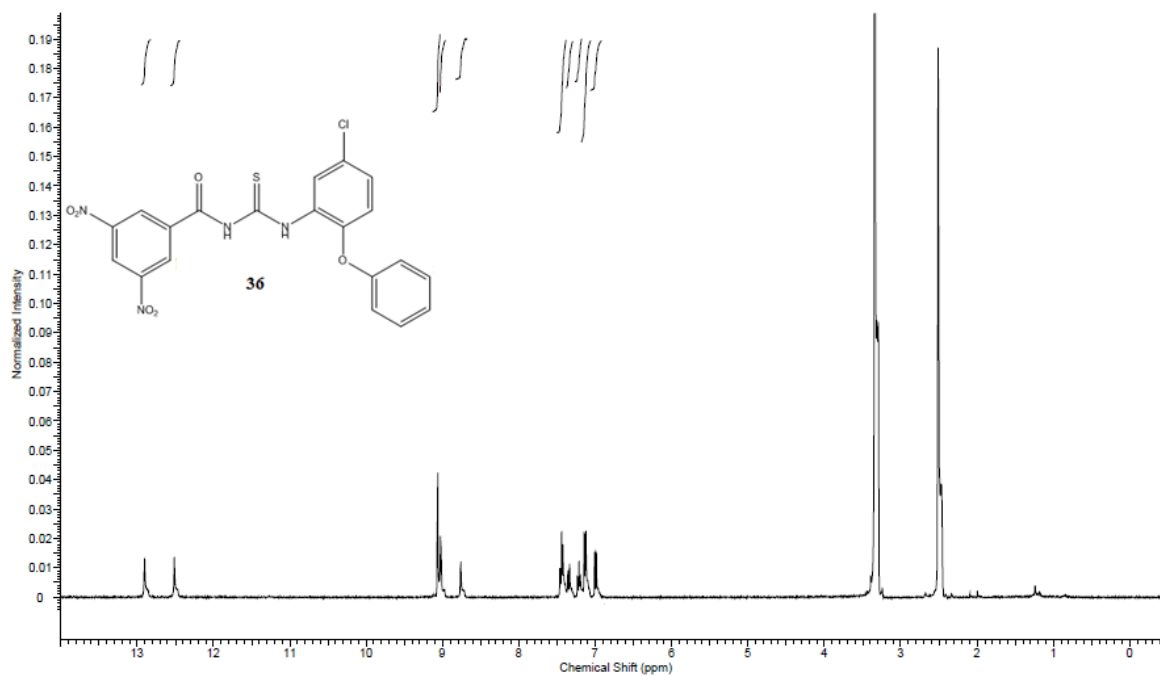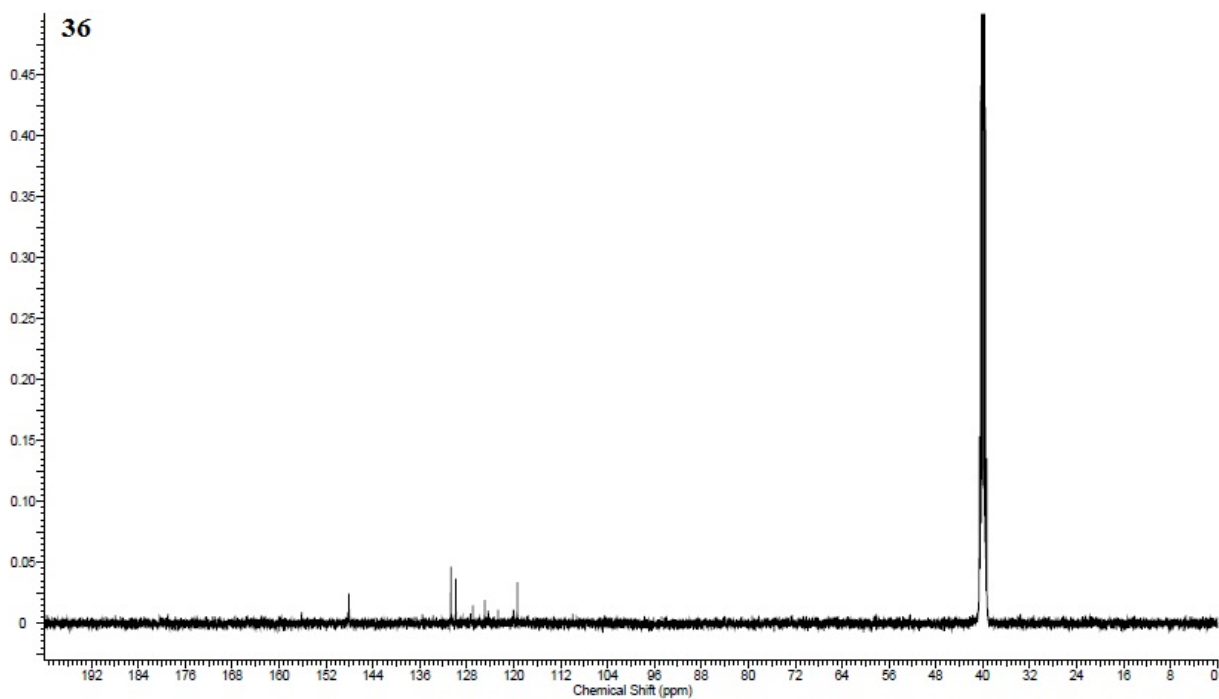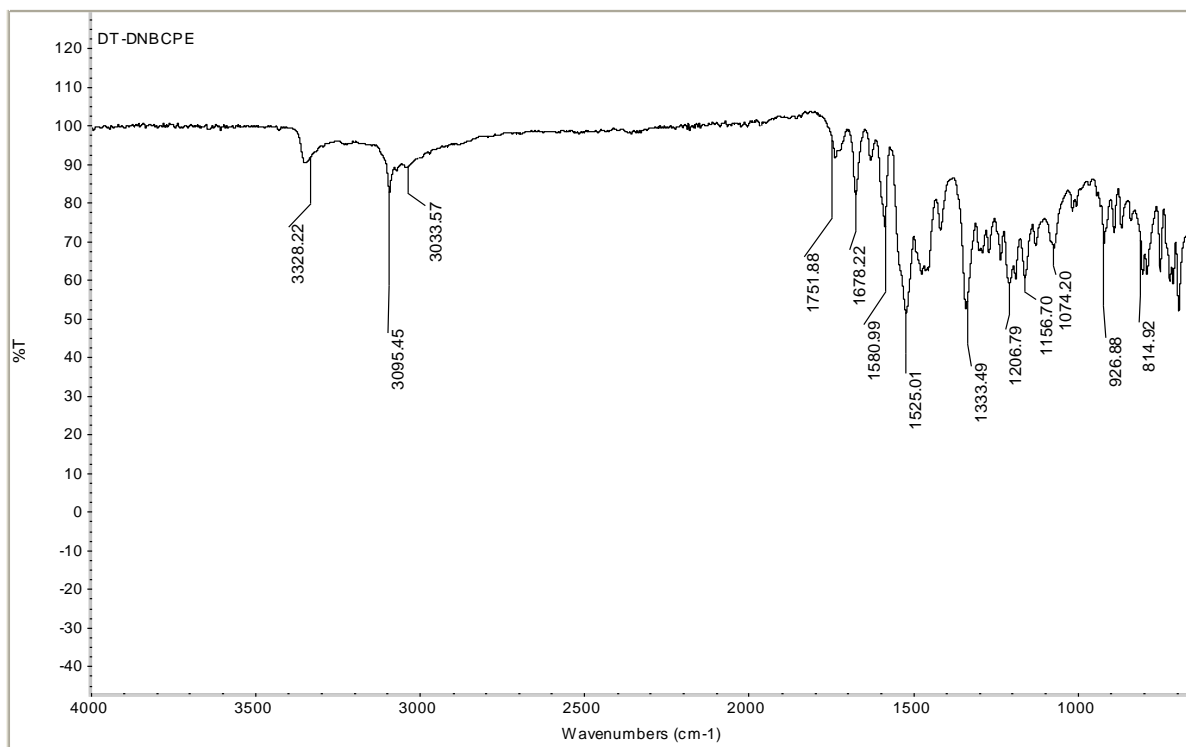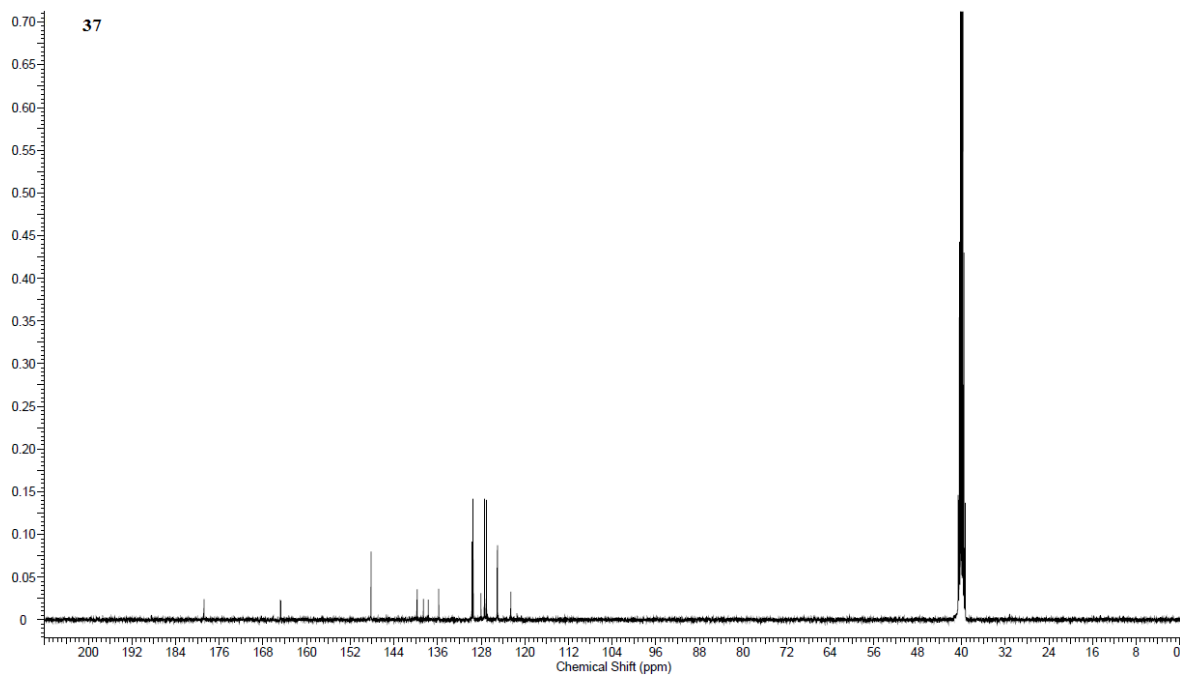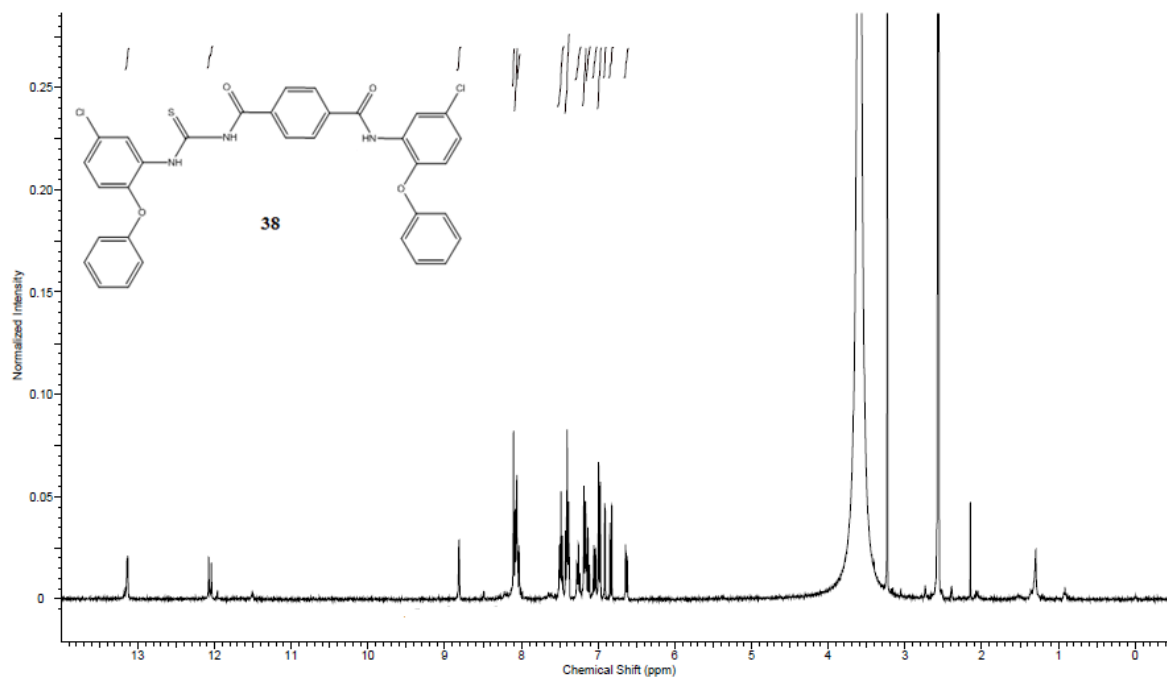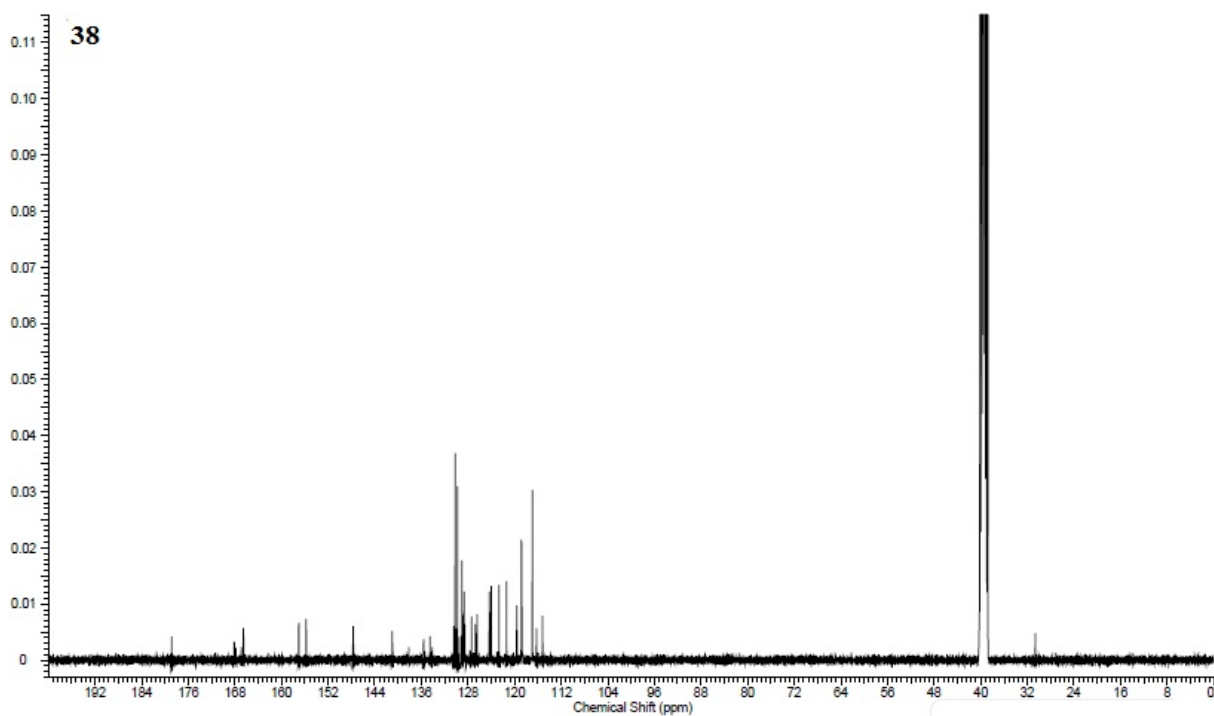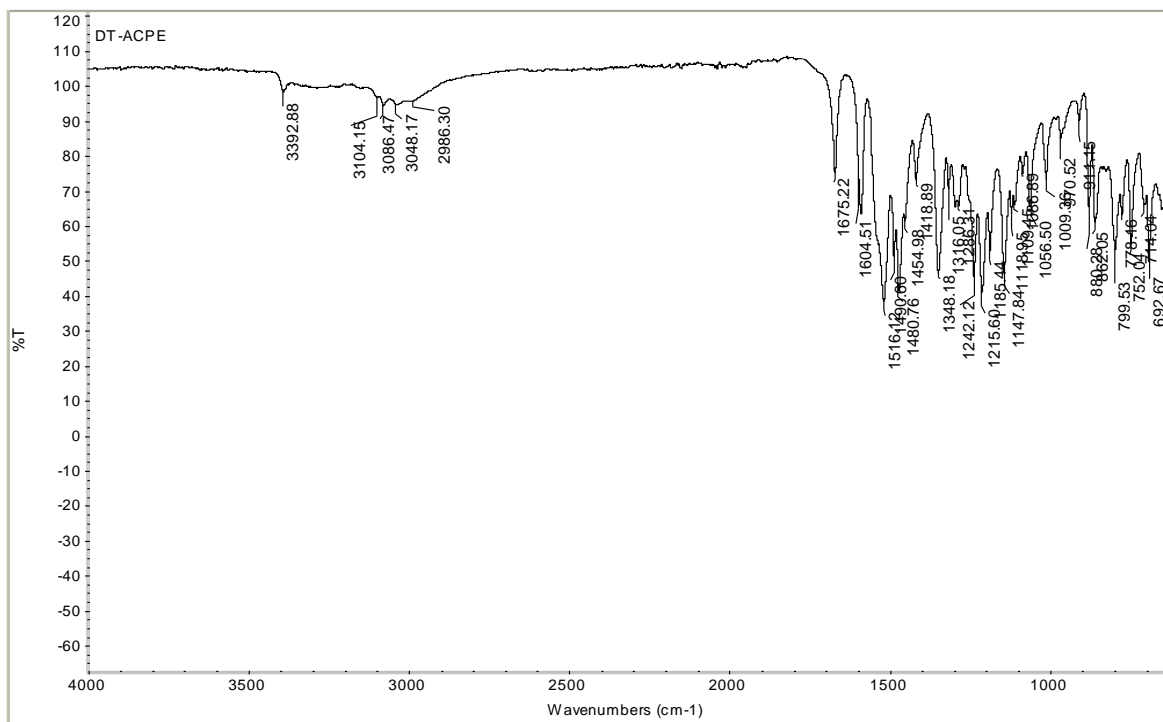Scheme 16: HETCOR spectrum of **34**

Scheme 17: FT-IR spectrum of **34**

Scheme 18: ^{1}H NMR spectrum of **35**

Scheme 19: ^{13}C NMR spectrum of **35**
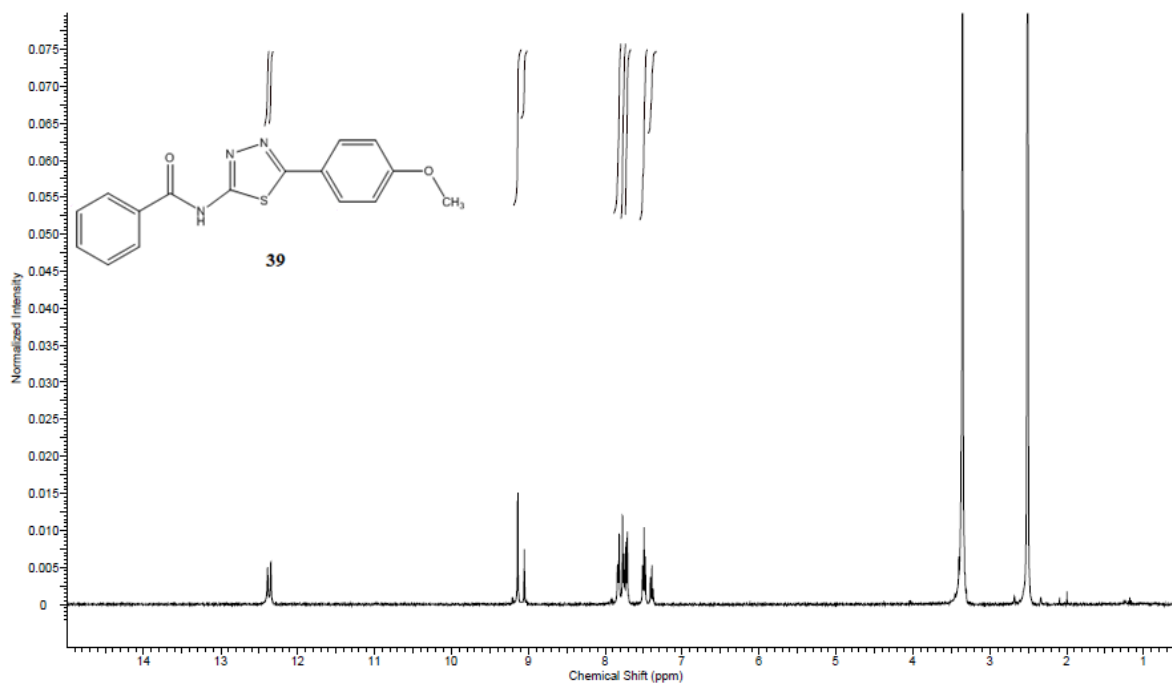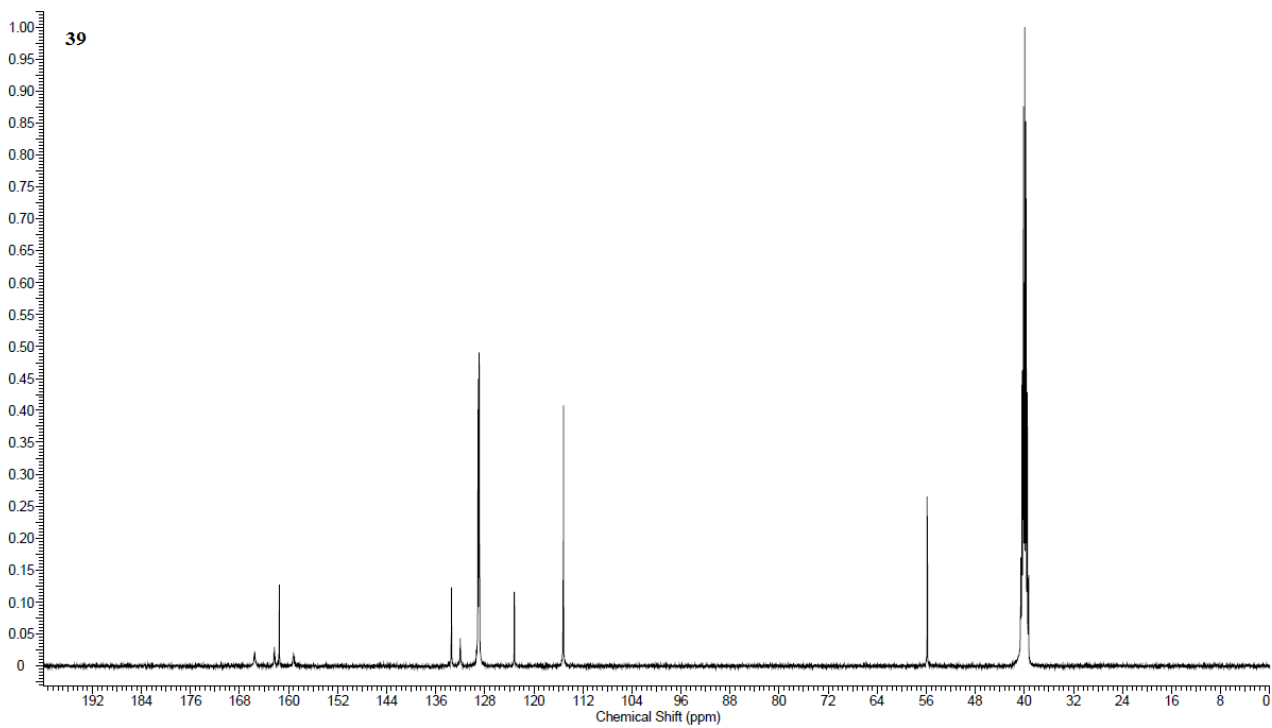
Scheme 20: FT-IR spectrum of **35**

Scheme 21: ^{1}H NMR spectrum of **36**

Scheme 22: ^{13}C NMR spectrum o**f 36**

Scheme 23: FT-IR spectrum of **36**
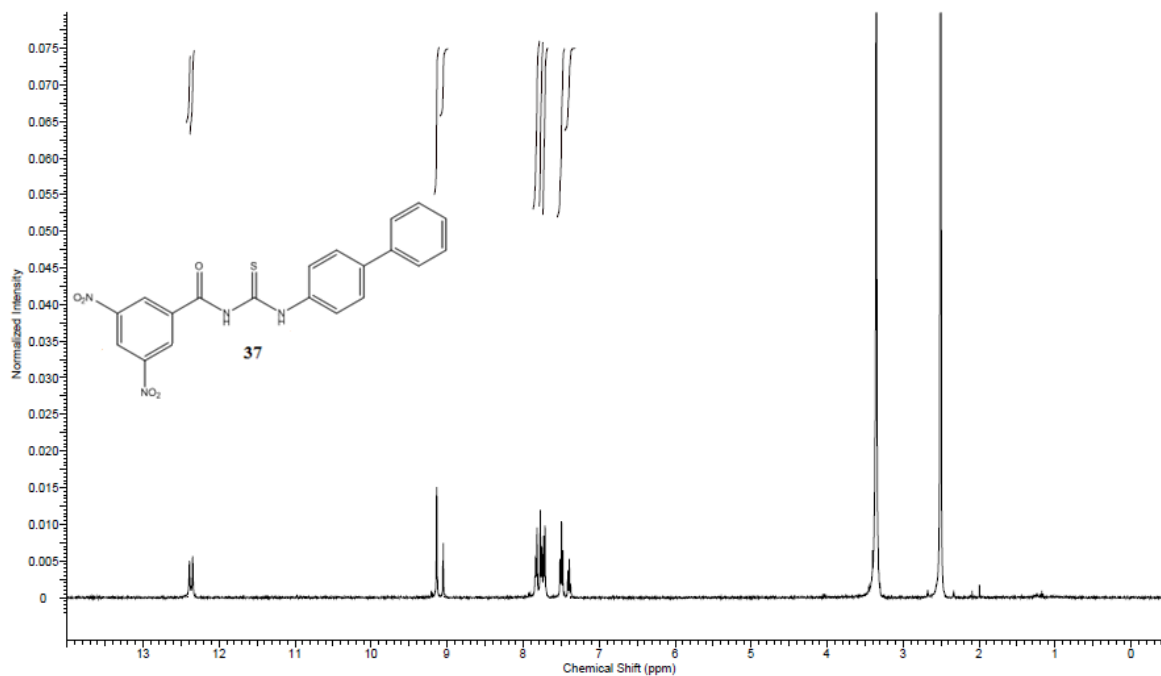
Scheme 24: ^{1}H NMR spectrum of **37**

Scheme 25: ^{13}C NMR spectrum of **37**

37
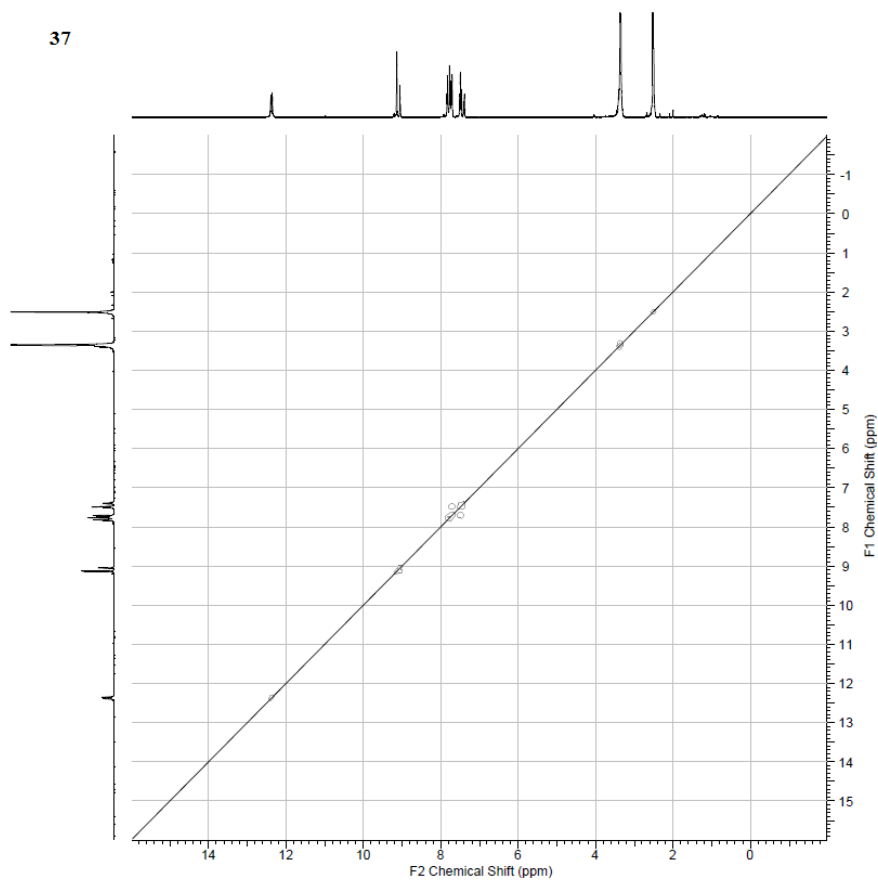
Scheme 26: COSY spectrum of **37**

37
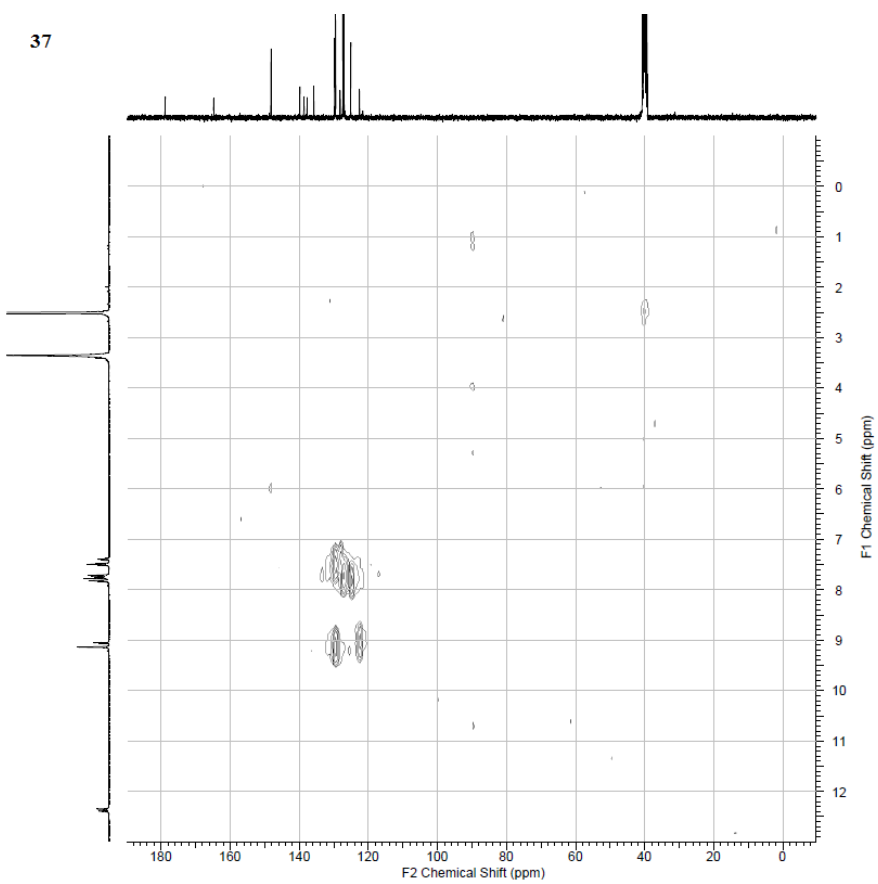
Scheme 27: HETCOR spectrum of **37**
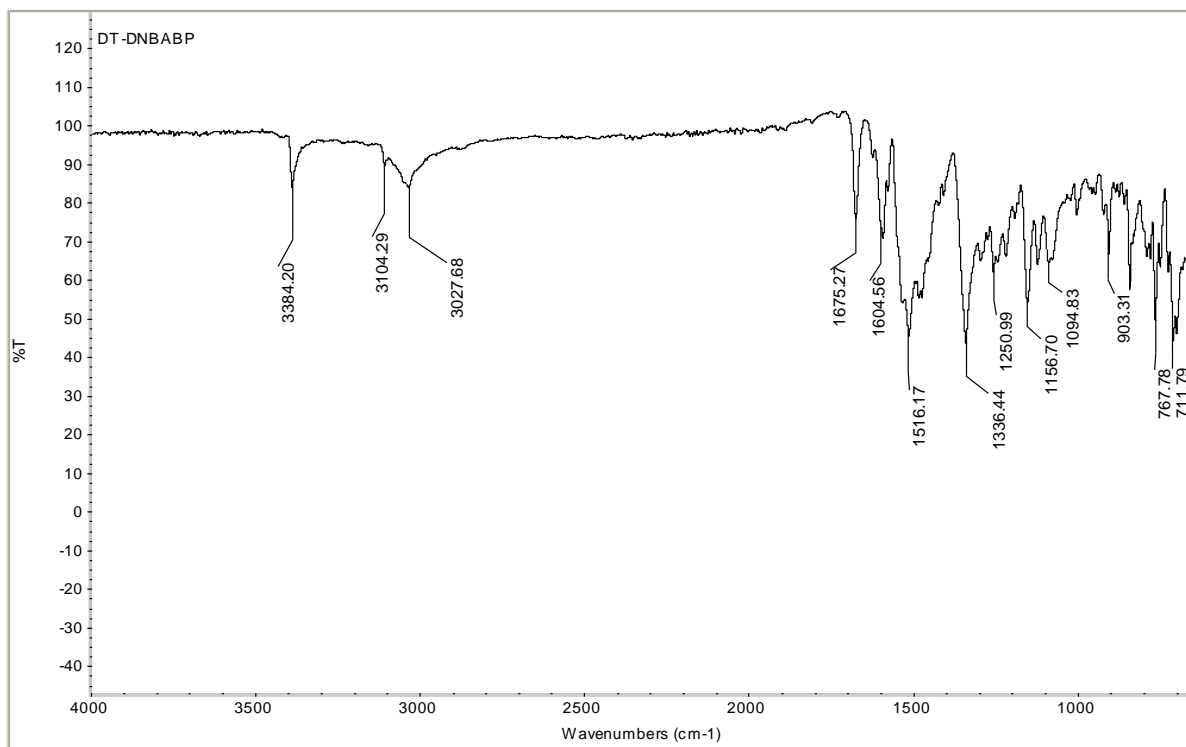
Scheme 28: FT-IR spectrum of **37**

Scheme 29: ^{1}H NMR spectrum of **38**

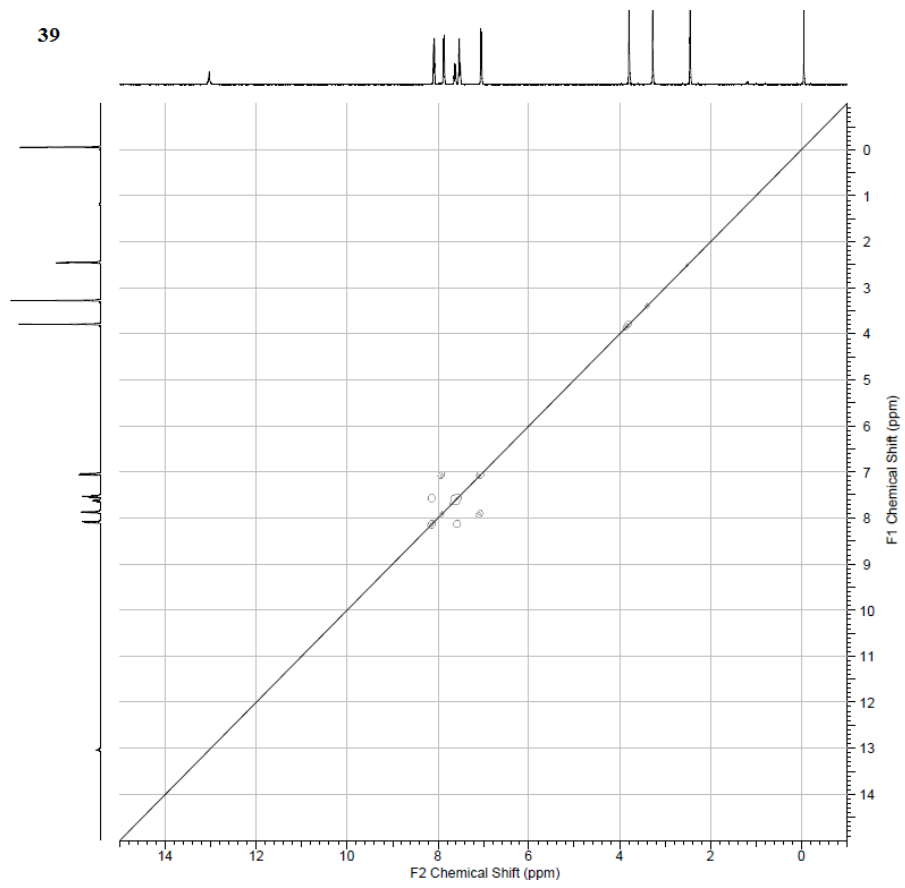Scheme 30: ^{13}C NMR spectrum of **38**
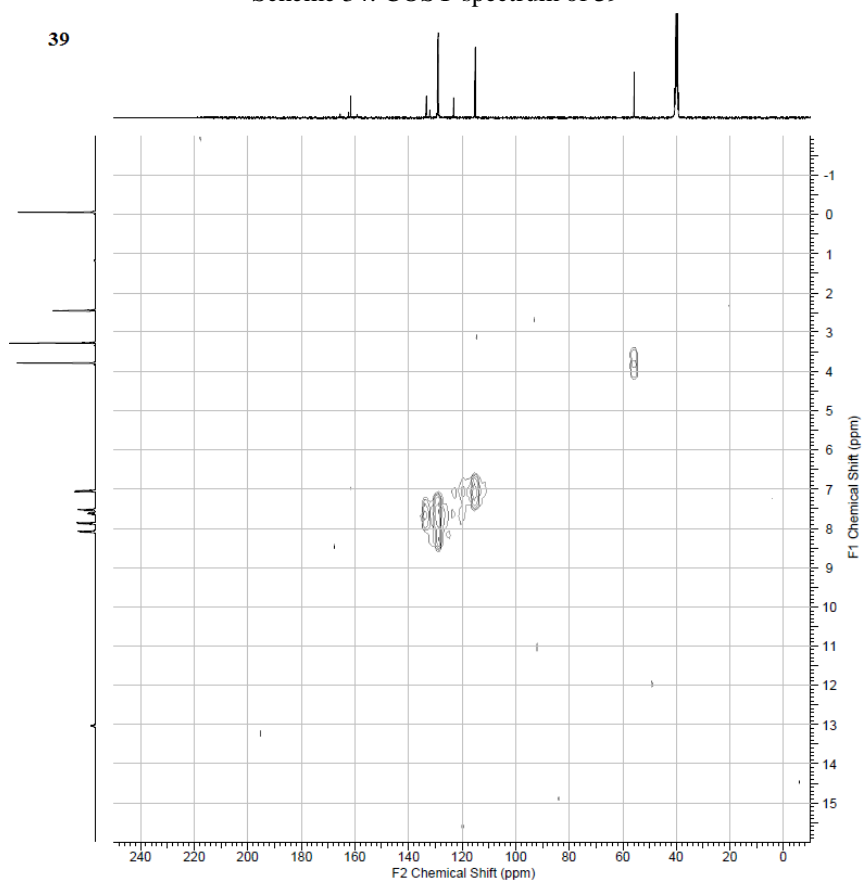
Scheme 31: FT-IR spectrum of **38**
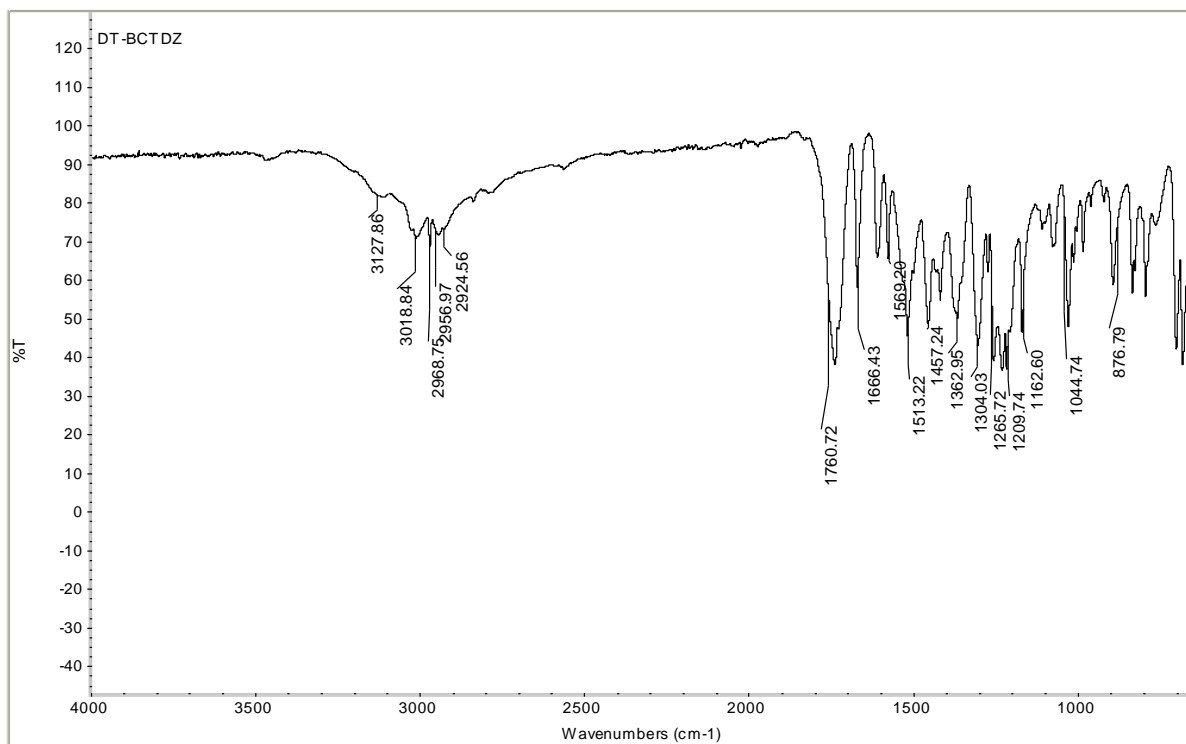
Scheme 32: ^{1}H NMR spectrum of **39**

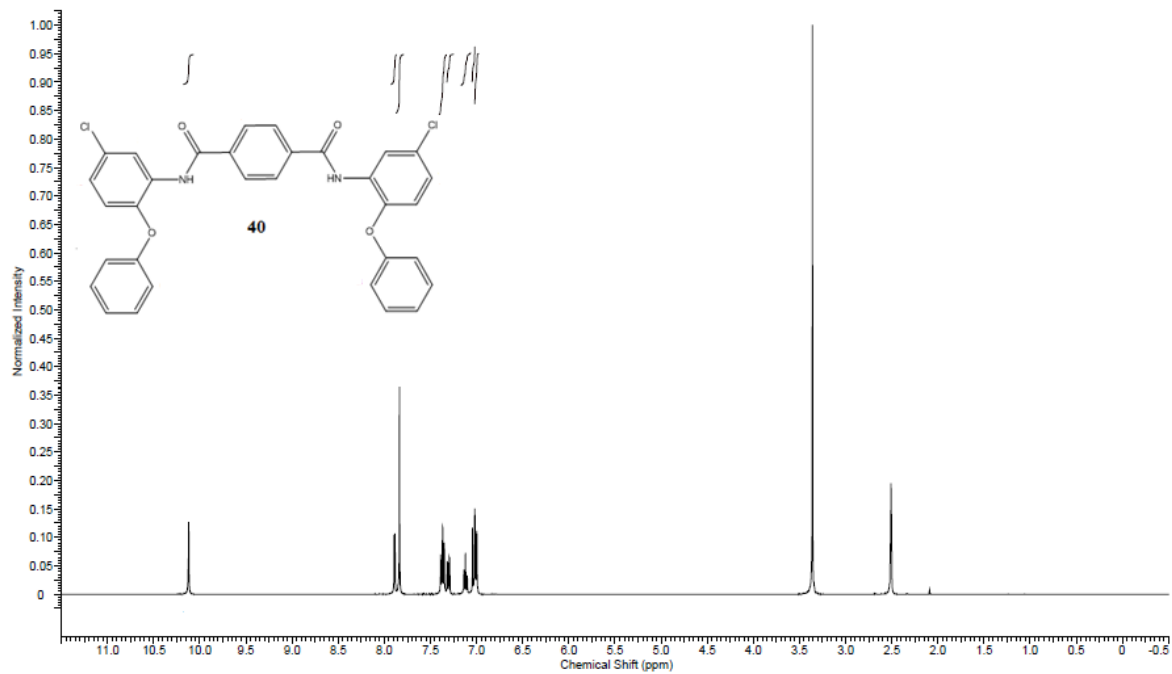Scheme 33: ^{13}C NMR spectrum of **39**
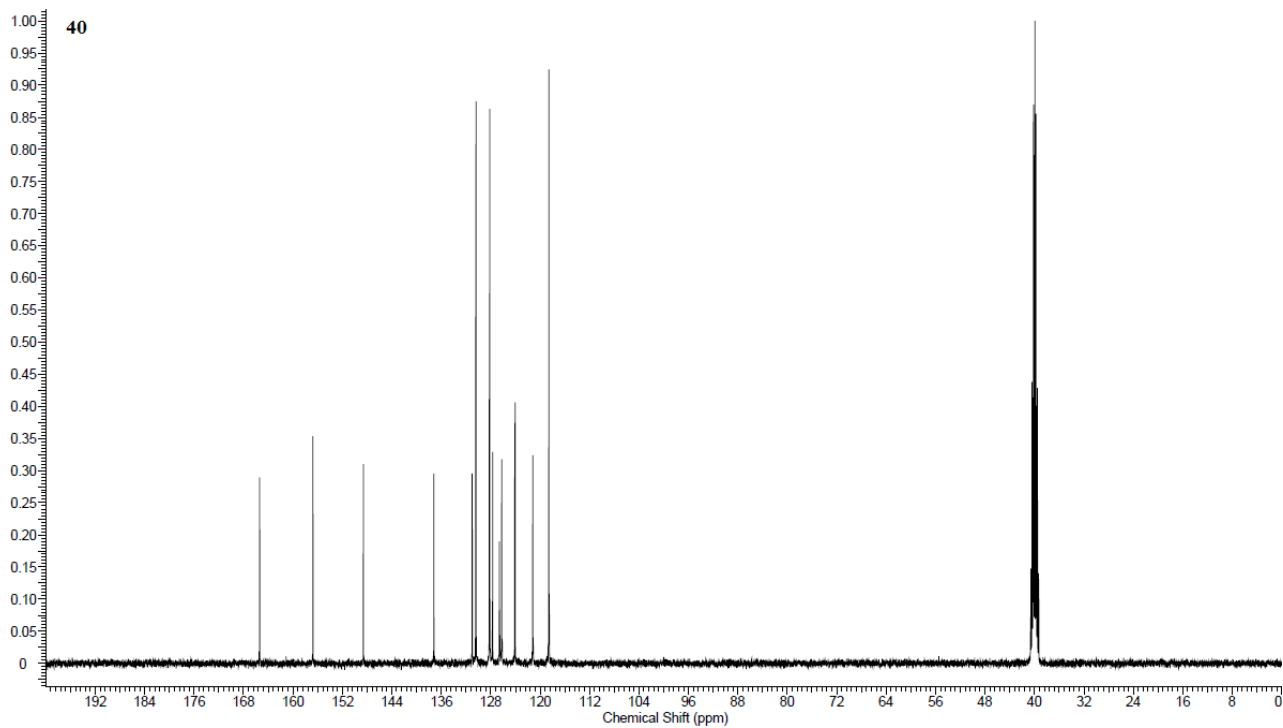
Scheme 34: COSY spectrum of **39**

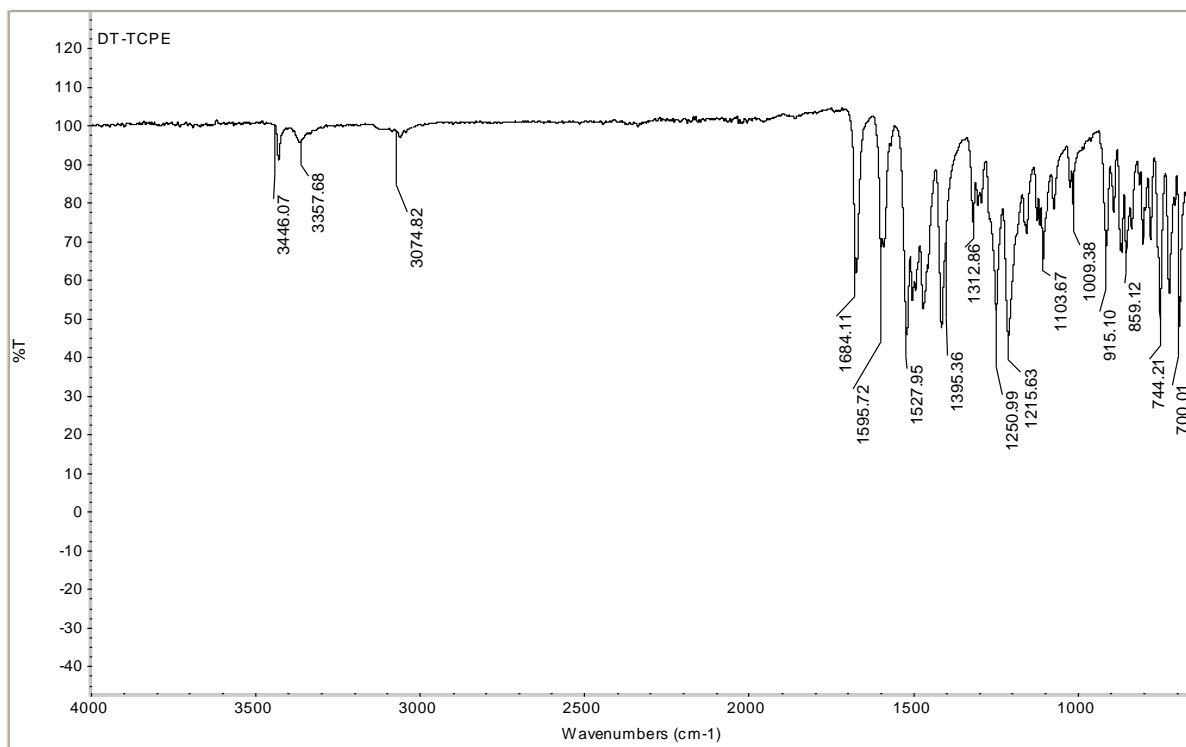Scheme 35: HETCOR spectrum of **39**

Scheme 36: FT-IR spectrum of **39**

Scheme 37: ^{1}H NMR spectrum of **40**

Scheme 38: ^{13}C NMR spectrum of **40**

Scheme 39: FT-IR spectrum of **40**

CURRICULUM VITAE

ID Information

Name & Surname : Deniz Tözendemir

Place of Birth : Ankara

Date of Birth : 16.07.1989

Marial Status : Single

Education and Academic Career

High School : 2006, Ankara Etimesgut Anadolu Lisesi

B.Sc. : 2010, Hacettepe University, Faculty of Science, Department of Chemistry

Foreign Language

English (Advanced)

Work Experience

2011- : Research Assistant, Hacettepe University, Faculty of Science, Department of Chemistry

Fields of Experience

Organic synthesis

Projects Derived from the Thesis

-

Publications Derived from the Thesis

-

Meetings Attended with Poster Presentations Derived from the Thesis

-